Technische Universität München
Lehrstuhl für Anorganische Chemie

Synthesis and characterization of heterogeneous rhenium and molybdenum catalysts. Applications in olefin metathesis and olefin epoxidation

Draganco Veljanovski

Vollständiger Abdruck der von der Fakultät für Chemie der Technischen Universität München zur Erlangung des akademischen Grades eines

Doktors der Naturwissenschaften

genehmigten Dissertation.

Vorsitzender: Univ.-Prof. Dr. Fritz E. Kühn

Prüfer der Dissertation:

1. Univ.-Prof. Dr. Dr. h. c. mult. Wolfgang A. Herrmann
2. Prof. Dr. Jean-Marie Basset (em.),
Université Claude Bernard Lyon / Frankreich

Die Dissertation wurde am 14.01.2009 bei der Technischen Universität München eingereicht und durch die Fakultät für Chemie am 10.03.2009 angenommen.

To My Family

If A is success in life, then A equals X plus Y plus Z. Work is X; Y is play; and Z is keeping your mouth shut.

Albert Einstein (1879 - 1955)

Die vorliegende Arbeit entstand in der Zeit vom April 2005 bis January 2009 am
Anorganisch-chemischen Institut der Technischen Universität München

I would like to express my deep gratitude to my academic supervisor

Prof. Dr. Dr. h. c. mult. Wolfgang A. Herrmann

for his trust, advice, interesting discussions and
the continuous support of my work.

Acknowledgment

I am very grateful to **Prof. Fritz E. Kühn** for his support during these years. His continuous encouragement, constructive comments and trust in me and my projects made this work possible.

The most intensive and rewarding cooperation during my Ph. D. has without doubt been with **Dr. Christophe Copéret**. His enthusiasm, patients and working ethic were essential for the success of our metathesis project. Despite the chalange posed by the distance between Lyon and Munich, he was always only a phone call away when I was in a need of advice or a trusted opinion.

I am deeply grateful to **Dr. Klaus Ruhland** who strongly influenced my work with many helpful suggestions and fruitfull discussions. He didn't only improved my scientific work but also accompanied me as a friend as well.

I am also very grateful to **Prof. Peter Härter** who offered me the chance to pursue the research in heterogeneous catalysis by arranging for me to go to Lyon in Laboratoire de Chimie Organométallique de Surface for my metathesis project. All the thanks to **Gabriele Raudaschl-Sieber** for her patience while recording my solid-state NMR spectra. Also many thanks to **Dr. Sven Schneider** who helped me a lot with my deuterium spectra in solution which are also part of this work. I am sending many thanks to **Dr. Ahmad Al-Ajlouni** from the Jordan University of Science and Technology for his constant support during our kinetic studies of the oxidation of $CpMo(CO)_3CH_3$.

All the thanks to **Dr. Eberhardt Herdtweck** for the X-ray structural determination included in this thesis. I am also thankful to the elemental analysis laboratory of the Technische Universität München for their contribution to this work. To **Mrs. Georgeta Krutsch** for the NMR measurement and the TG-MS measurements, and **Thomas Schröfel** for his kind assistance in the GC laboratory.

Many thanks to my laboratory colleague **Dr. Eckhart Louis** for keeping the perfect working atmosphere in our laboratory. His various theoretical as well as practical suggestions revolutionize my preparative work. I also thank to **Alejandro Capape Miralles** and **Evangeline Tosh** for reading and correcting parts of this thesis, as well as for our creative discussions in between the working hours.

Mrs. Grötsch, Mrs. Kaufmann, and **Mrs. Schuhbauer** from the secretary's office are acknowledged for their help with the organizations of all kinds and various burocratic matters during this period.

And finally all the thanks to all my colleagues in Prof. Herrmann's and Prof. Kühn's group for the nice working atmosphere in the university, their cooperation and help. Also many thanks to my colleagues in Laboratoire de Chimie Organométallique de Surface in Lyon, especially **David Gajan**, for helping me to adapt to the new laboratory environment. Also many thanks to **Raphael Wischert** who continued with the practical work after I left.

Contents

Abbreviations

cod	1,5-cyclooctadiene
PCy	tris-cyclohexylphosphine
py	pyridine
Et	ethyl
Me	methyl
MTO	methyltrioxorhenium
TMDO	trimethyldioxorhenium
HPPO	hydrogen peroxide to propylene oxide
PO	propylene oxide
TS-I	titanium(IV)-silicate
Cp	cyclopentadienyl
Cp*	pentamethylcyclopentadienyl
CpMe	methylcyclopentadienyl
Bypy	2,2'-bypiridine
AN	acetonitrile
THF	tetrahydrofurane
TMEDA	tetramethylethylenediamine

UHP	urea hydrogen peroxide
Mes	mesitylene
BINOL	1,1'-bi-2-naphthol
DCM	dichlormethane
acac	acetylacetonate
ROP	ring opening polymerization
ROMP	ring opening metathesis polymerization
SOMC	surface organometallic chemistry
POSS	polyoligomeric silsesquioxanes
DFT	density functional theory
MCM	mobil crystalline of materials
MAS	magic angle spinning
SAB	santa barbara amorphous

1. Introduction

"Sustainable Development should meet the needs of the present without compromising the ability of future generations to meet their own needs."

The Brundtland report, Our Common Future, 1987

Chemistry is defined as a central science, that describes phenomena on a molecular level. As a central science it opens possibilities of understanding our environment better, beginning with small and fast biological systems up to macromolecular and inertly visible processes. Being able to control these occurrences and impair them through a directed synthesis is the ultimate goal of every chemist.

A key step of a synthetic reaction is its efficiency. Efficiency is defined as the ability to convert readily available building blocks into the target molecule in relatively few synthetic operations that require minimal quantities of raw materials and produce minimal waste.[1] Thereby high efficiency achievement can be done through improving the selectivity and the atom economy of a given synthetic procedure.

The selectivity is defined as the ratio of products obtained from given reactants. It is quantitatively expressed as a ratio of rate constants for the alternative reactions, or their decadic logarithms.[2] The generic term of selectivity can be divided in several subgroups as outlined in Figure 1.1:

- **Chemoselectivity** Chemoselectivity is the preferential reaction of a chemical reagent with one of two or more different functional groups. A reagent has a high chemoselectivity if reaction occurs with only a limited number of different functional groups.[3]

- **Regioselectivity** A regioselective reaction is one in which one direction of bond making

or breaking occurs preferentially above all other possible directions. Reactions are termed completely (100 %) regioselective if the discrimination is complete, or partially (x %), if the product of reaction at one site predominates over the product of reaction at other sites.[3]

- **Stereoselectivity** The preferential formation in a chemical reaction of one stereoisomer over another. When the stereoisomers are enantiomers, the phenomenon is called enantioselectivity and is quantitatively expressed by the enantiomer excess; when they are diastereoisomers, it is called diastereoselectivity and is quantitatively expressed by the diastereoisomer excess.[4]

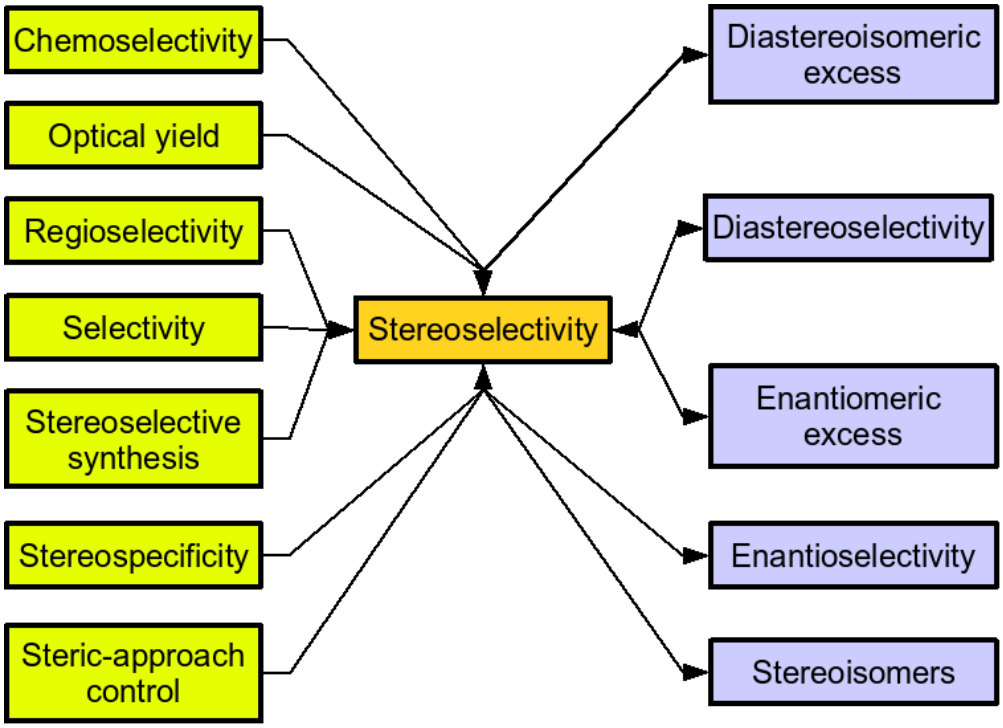

Figure 1.1. An outline of the selectivity reactions[5]

Classical example of improving the synthesis by enhancing the selectivity of the reaction procedures is the ammoxidation of propylene to acrylonitrile. The first trials in the laboratory resulted only in a marginal yield of 6 % . Afterwards, the first power plant built in 1959 using Bismuth phosphomolybdate as catalyst raised the yield to 65 %. Later catalysts followed in 1990 reduced the production of the byproduct acetonitrile to the point that even the required quantities were left unsatisfied.[6] Another achievement in the field of selective synthesis is the

preparation of palytoxin, an highly complex marine neutral product containing 71 stereochemical elements. This feat, reported by Prof. Kishi group of Harvard University in 1994, is due to its complexity in structure still considered today to be one of the greatest synthetic accomplishment ever.[7]

Unfortunately, in this conquest for achieving higher selectivity the second most important feature of an effective synthesis - the atom economy, is often neglected. The atom economy describes the conversion efficiency of a chemical process in terms of all atoms involved. In an ideal chemical process the amount of starting materials or reactants equals the amount of all products generated (see stoichiometry) and no atom is wasted.[8]

Table 1.1: The E factor[9]

Industry segment	Product tonnage[a]	kg waste[b]/kg product
Oil refining	10^6 - 10^8	< 0.1
Bulk chemicals	10^4 - 10^6	$<$ 1-5
Fine chemicals	10^2 - 10^4	5 -> 50
Pharmaceuticals	10 - 10^3	25 - > 100

[a] Typically represents annual production volume of a product at one site (lower end of range) or world-wide (upper end of range

[b] Defined as everything produced except the desired product (including all inorganic salts, solvent losses etc.)

The market situation in 2007 is depicted in Table 1.1 with the help of the E-Factor (byproduct to product ratio) in various industrial sectors.[9] The alarming situation in the pharmacy and the fine chemicals industry can also be seen in Figure 1.2 where the cost of waste is shown.[10] Performing a synthetic reaction on a large scale involving multi-step procedures, could lead to almost 40 % increase of the production costs if the atom economy is not taken into the consideration.

The waste generated during the manufacturing of organic compounds consists mostly of inorganic salts, produced in the reaction, or in the subsequent neutralization steps. Representative examples for this waste generating processes are the stoichiometric reductions with metals and metal hydride reagents and oxidations with permanganate and chromium(VI) reagents.[9] The

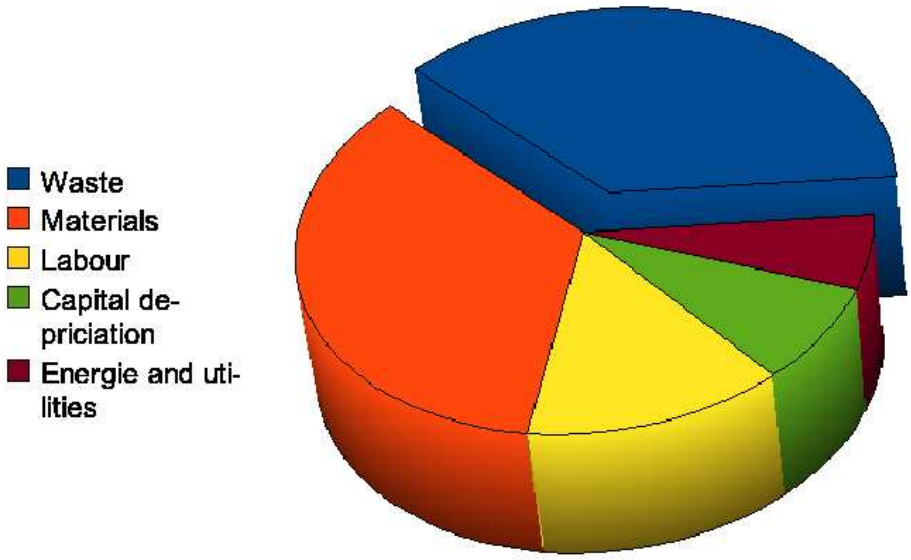

Figure 1.2. The cost of waste as percentage of manufacturing expenses for specialty chemicals[10]

solution of this problems is obvious: Stoiciometric reactions should be displaced by new, clean catalytic reactions using only environmentally compliant reagents like H_2, O_2, H_2O_2, CO, CO_2.

1.1. Industrial catalysis

In a general sense, anything that increases the rate of any process is often called "catalyst", a term derived from Greek $\kappa\alpha\tau\alpha\lambda\vartheta\epsilon\iota\upsilon$, meaning "to annul", or "to untie", or "to pick up". The phrase "catalysed process" was coined by Jakob Berzelius in his work "Consideration respecting a New Power which acts in the Formation of Organic Bodies" in 1836.[11] Nowadays, almost 200 years later, no chemistry plant can be operated without this "catalysed process". The numbers are indeed impressive:[6]

- 90 % of all industrial processes involve catalysts
- In 1999 catalysis was used for manufacturing of goods worth $3 trillion
- 30 % of the US gross national product is generated with the help of catalysis

The global catalyst market can be divided almost evenly in four main areas: petroleum refining, chemical processing, polymerization and environmental applications. The size of the worldwide catalyst market, and its development between 1999 and 2005 are given in Figure 1.3.

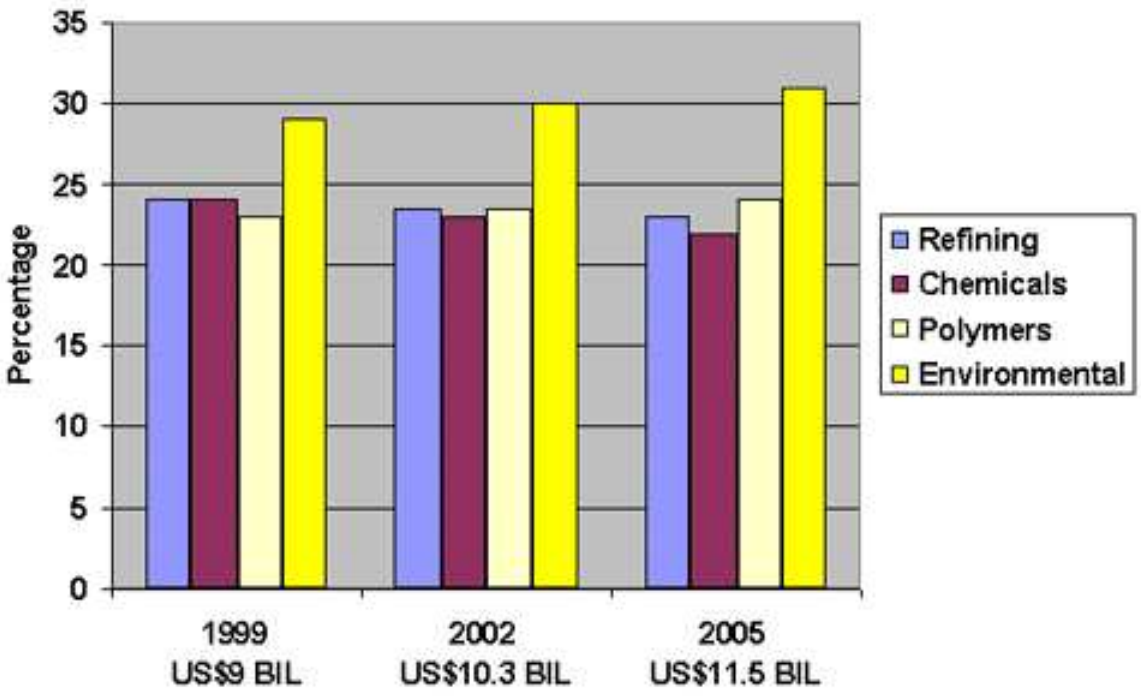

Figure 1.3. The size of the worldwide catalyst markets[12]

Important industrial processes involving catalysis are summarized in Table 1.2. Obviously, the enormous importance of catalysts in the modern chemical industry lies not only in "increasing the rate of a reaction without modifying the overall standard Gibbs energy change in the reaction".[5] However catalysts nowadays are doing a lot more than that. One of their specialties is increasing the selectivity of a reaction by making only one reaction path possible (some examples are given in these Chapter). They can also provide access to unusual "nonequilibrium" products. Prominent example for this feature is the disproportionation of toluene where zeolite catalysts increase the yield of p-xylene - the thermodynamically less stable product. Finally, the catalyst must have exceptionally high activity and needs to be reusable, which are main predicates for cost-effective and environment friendly processes.

1.2. Heterogeneous and homogeneous catalyst

Catalytic processes that take place in a uniform gas or liquid phase are classified as homogeneous catalysis. Homogeneous catalysts are usually well defined compounds, mostly metal complexes that are dispersed in the same medium as the reactants. The homogeneous catalysts have

Table 1.2: A summary of catalytic reactions

Catalytic Reaction	Industrial Application	Used Catalyst
Hydrogenation	Asymetric hydrogenation (L-dopa)	
	Benzene to cyclohexane	$[Ir(cod)(PCy_3)(py)]PF_6$,
	Aldehyde and Ketons to Alcohols	Pd on carbon, Pt on carbon
Oxidation	Hoechst-Wacker Process	$PdCl_2/CuCl_2$, RuO_4
	(oxidation of ethylene to acetaldehyde)	Ag, Mo
	epoxidation (BASF-Dow-HPPO-Process)	
	production of carboxylic acids	
Polymerization	Polymerization of olefins	$TiCl_4$, on $MgCl_2$
	(Zigler-Nata Polymerization)	and $AlEt_3$ as cocatalyst
Metathesis	Ring opening metathesis	Grubbs catalyst (I, II and
	Ring-closing Metathesis	III generation)
	Ring opening metathesis polymerization	Schrock catalyst
Isomerisation	Synthesis of citral (BASF)	$Rh(PPh_3)_3Cl$
	Tagasago menthol process	

high activities with respect to the metal atoms present in the reaction. On the contrary, heterogeneous catalysis is a catalytic process in which the reaction occurs at, or near the interface between two phases. Mostly, the catalyst is distributed on a solid phase that is kept in contact with the reactands in gas or fluid media. Only the atoms on the surface, that are in direct contact with the reaction medium, can take part in the catalysis. The reactivity with respect to the present metal atoms is low.

The well distributed homogeneous systems minimize the diffusion problems, an important issue in some heterogeneous systems where the active centers lie in narrow pores. Typically for zeolite-like materials, the diffusion through the narrow channels can considerably influence the speed of the reaction.

A good mechanistic understanding of the homogeneous systems, provides information for a specific ligand - design for to a given reaction. This results in very high product selectivity under mild conditions. In contrast, the heterogeneous systems are not very well understood. These

Table 1.3: Comparison of homogeneous and heterogeneous catalysts[13]

	Homogeneous	Heterogeneous
Effectivity		
Active centers	all metal atoms	only surface atoms
Catalyst Concentration	low	high
Selectivity	high	lower
Diffusion problems	practically absent	present (mass-transfer-controlled reaction)
Reaction conditions	mild (50 - 200 °C)	severe (often 250°C)
Applicability	limited	wide
Activity loss	irreversible reaction with products (e.g. cluster formation); poisoning	sintering of the metal crystalites; poisoning
Catalyst properties		
Structure/stoichiometrie	defined	undefined
Modification possibilities	high	low
Thermal stability	low	high
Catalyst Separation	sometimes laborious (chemical decomposition, distillation, extraction)	fixed-bed: unnecessary suspension: filtration
Catalyst recycling	possible	unnecessary (fixed bed or easy suspension)
Cost of catalyst losses	high	low

catalysts are used under harsh conditions and usually in many different reactions simultaneously. The best examples of how complex a heterogeneous system can be, and some aspects for better understanding of its complexity, are given in the Nobel lecture of Gerhard Ertl in 2008 on the Mittasch catalyst for Ammonia synthesis and a common car catalyst for CO oxidation.[14]

The major advantage of the heterogeneous catalysts is the simplicity of catalyst separation from reaction media. The catalyst is either automatically removed in the process (e.g., gas-phase reactions in fixed-bed reactors), or separated by simple methods such as filtration or centrifugation. On the other hand, the separation of the homogeneous transition metal catalysts is difficult and often almost not feasible. Therefore, complicated processes such as distillation, liquid-liquid extraction, and ion exchange must often be used. This has been improved by using organometallic complexes soluble both in organic media and water, ionic liquids or super-critical CO_2.[15] By the end of the reaction the media containing the homogeneous catalyst is easily separated from the organic phase using similar procedures as in the case of the heterogeneous catalysts. The pros and cons of both methods are presented in Table 1.3.

In the industrial use, both homogeneous and heterogeneous catalysts have issues with deactivation caused by chemicals or physical processes. However, the ease of the separation of the heterogeneous systems plays the most important role in the industrial processes and despite the disadvantages there are still by far the most important catalysts. The market share of the homogeneous catalysts is estimated to be only 10 - 15 %.[16]

1.3. Outlook

This work stands on the interface between the homogeneous and heterogeneous catalysis. The major task was to find ways for immobilization of the already known η^5 - cyclopentadienylmethyl-molybdenumtricarbonyl [$CpMo(CO)_3CH_3$] and trimethyldioxorhenium (TMDO) [$(CH_3)_3ReO_2$] on alumina, and acetylperrhenate on silica surfaces. After the successfully performed immobilization the novel heterogeneous catalyst were applied as catalysts for epoxidation of olefins (acethylperrhenate on silica) and in the olefin metathesis ($CpMo(CO)_3Me$ and TMDO on alumina). First attempts to understand their catalytic functionality were also performed. In the case of $CpMo(CO)_3Me$ on alumina this endeavor induced further investigations of the still unknown mechanism of the homogeneously performed epoxidation of olefins.

Part I.

Epoxidation

2. Introduction

Epoxides are highly important raw materials in the chemical industry. The production of the simplest epoxide - ethylenoxide was around $5.34 \cdot 10^6$ t in 2007 with an enormous annual increase in Europe of 52.3 % between 2006 and 2007 Table 2.1.[17] The production of propylene oxide was in a similar range, with 1.84 $\cdot 10^6$ t in Europe in 2007, with a slight annual decrease of 0.8 %. In 2002 about 61 % of the ethylenoxide was hydrolyzed to ethylene glycol. Other products are non ionic surfactants, ethanol amine, and glycol ethers. Propylene oxide is the key starting up material in the production of polymers (polyurethane in particular), propylene glycol, glycerin and glycol ether.[18]

Table 2.1: Production of ethylene and propylene oxide[17]

Thousands of metric tons	Country	2006	2007	Annual Change 2006-07 / %
Ethylene Oxide	USA	3445	3415	- 0.9
	Europe	635	967	52.3
	Japan	974	966	- 0.8
Propylene Oxide	Europe	2012	1846	- 8.3

A catalytic oxidation of olefins represents the most desirable route for synthesis of these industrial highly important chemicals. Unfortunately, the oxidation of the hydrocarbons, that are thermodynamically favored, is often difficult. All partial oxidation reactions are kinetically limited processes and the nature of the products is mechanistically determined. Another important issue is the sustainability of the reactions. Typical used oxidants are various alkyl hydroperoxides, hypochlorite or iodosylbenzene. The drawbacks of these oxidants are clearly their low active oxygen content and the production of an immense amount of waste products.

This caused intensive research in the field of catalysis with environmentally friendly oxidants, e.g. oxygen or hydrogen peroxide, where the active oxygen content is around 50 % (reductor is always needed, when pure oxygen is used) producing no- or only water as a byproduct. In the production of ethylene oxide, the silver catalyst is unique in its catalytic properties, fulfilling all these requirements.[19]

The French chemist Theodore Lefort was the first who used silver as a catalyst for the ethylene oxid synthesis from oxygen and ethylene in 1931.[20] Since 1940 almost all ethylene oxide produced industrially has been made using this method. Practically ethylene and oxygen are passed over a solid catalyst containing large silver nanoparticles dispersed on α-Al_2O_3. About 1 ppm of chlorine compound is needed for achieving selectivities higher than 70 %. Chlorine suppresses the formation of O^{2-}, which reacts with ethylene too, forming acetaldehyde - the first step of total combustion to CO_2 and H_2O. The only drawback of this reaction is that the silver catalyst only gives good yields with ethylene. Epoxides from higher olefins can not be synthesized with this method.

Therefor, the chlorhydrine route Scheme 2.1 is still used for oxidizing higher alkenes. Another important reason was the availability of the ethylene chlorhydrine plants, in the early sixties, which were not used due to the new silver-catalyzed procedure. The chlorhydrine reaction is done at 30 - 35 °C and 2 - 3 bar of pressure using a water solution of chlorine as an oxidation reagent (hypochlorous acid). The resulting chlorhydrine is *in situ* dehydrochlorinated to propylene oxide using basic solution of sodium- or calcium-hydroxide. The propylene oxide is than distilled out of the reaction mixture to avoid direct hydration. At present this process is producing 2.01 t NaCl and 0.102 t 1,2-diclorpropane as byproducts per ton of propylene oxide.[21] Huge research efforts were put into discovering a direct oxidation route, for minimizing the waste of chlorine and electricity.

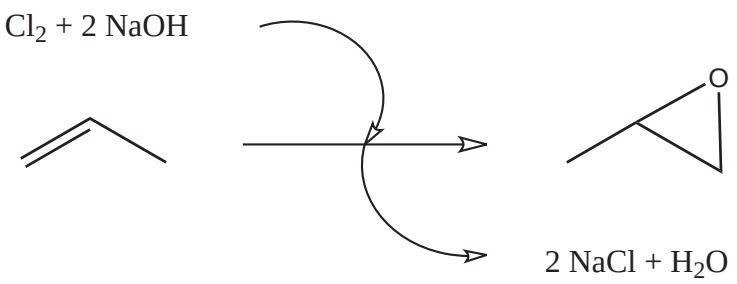

Scheme 2.1. Chlorhydrin process for synthesis of propylene oxide

In 1967 Halcon came up with an improved method for epoxidation of propylene and other unsaturated olefin compounds, employing organic hydro peroxides as the epoxidation agents.[22] It was a homogeneous catalytic process using soluble vanadium naphthenate as catalyst. The alcohols that were formed in the reaction could have been recovered as a separate valuable product or recycled to the hydroperoxides by procedures such as dehydratation of olefin, hydrogenation of olefin and oxidation to hydroperoxide. Almost simultaneously, Atlantic Richfield Co. came up with similar process, using catalysts on molybdenum basis such as molybdenum oxide, molybdenum chloride and molybdenum hexacarbonyl. The acids and the corresponding salts, where the molybdenum is contained in the anionic portion of the molecule, were used as well.[23] Halcon and ARCO subsequently formed a joint venture, the Oxirane Corporation, to exploit this novel technology. The resulting "oxirane process" was responsible for almost 45 % of the production of propylene oxide in 2002.[24]

Another successful partnership between the German BASF, the US company DOW and Belgium's Solvay, laid the foundation of the first plant for production of propylene oxide using hydrogen peroxide as an oxidant.[25] The hydrogen peroxide to propylene oxide (HPPO) - Process sketched in Figure 2.1 makes use of titanium(IV)-silicate (TS-I) as catalyst, first introduced by chemists at Enichem in 1983.[26] TS-I has been obtained by the hydrothermal crystalization of a gel obtained from a mixture of tetraethyl orthosilicate (TEOS) and tetraethyl orthotitanate (TEOT), in the presence of tetrpropylammonium hydroxide. The zeolite like material has partially substituted Si atoms for Ti in its lattice, with the composition $xTiO_2(1\text{-}x)SiO_2$ where x is between 0 and 0.04 M. The unique catalytic properties of this material are noticed by the catalytic oxidation with hydrogen peroxide. The catalyst is not deactivated by the water present in the system what is typicall for all other early transition metals, that are deactivated through hydroxylation. The lack of lewis-acidic sites, due to the electronic balance between titanium and silicium atoms also minimizes the possibility of an epoxide - ring opening, reaction typically for similar, zeolite - like materials. A Ti-peroxo species is assumed as an active species in this reaction.

In the HPPO process propene is oxidized in a slurry containing the catalyst, hydrogen peroxide and methanol as a preferred solvent. After this reaction a mixture is obtained comprising of 8 to 13 wt% of propylene oxide, 2 to 7 wt% unreacted propene 0.01 to 1 wt% propane and 0.02 to 0.5 wt% oxygen. In the following step propylene oxide is separated by distillation

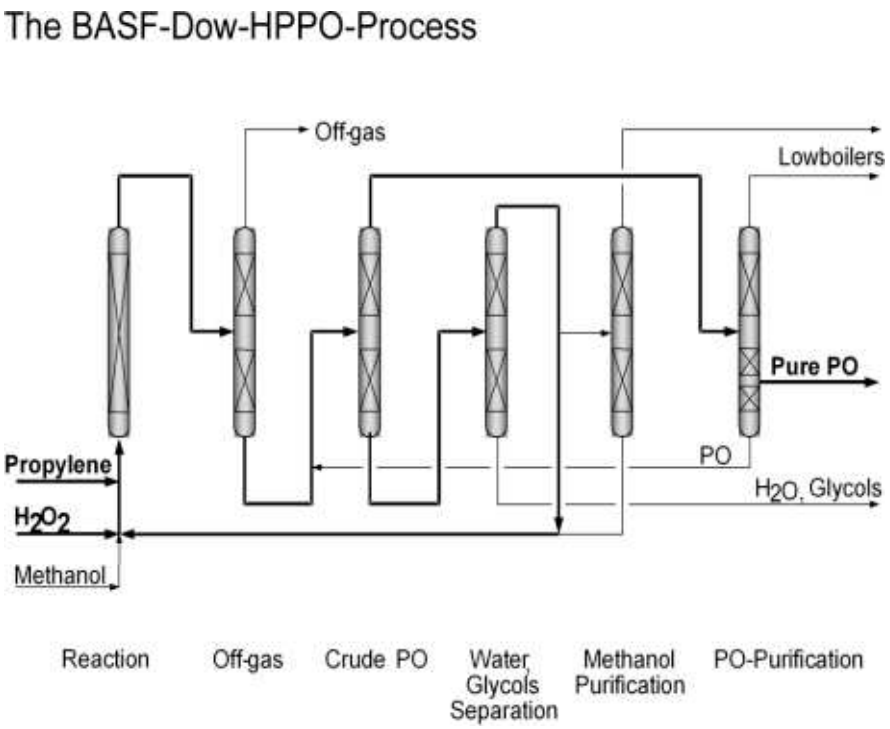

Figure 2.1. Scheme of the BASF/Dow/Solvay HPPO plant, Belgium

and purified. The final purification procedure removes oxygen by hydrogenation on a heterogeneous catalyst containing tin and at least one nobel metal on α-Al_2O_3. The purified propene containing 10 ppm oxygen at most is re-introduced in the oxidation reaction.[25]

2.1. Rhenium catalysts in the epoxidation of olefins

Using rhenium based compounds as a catalyst is a relative new concept in the metallorganic chemistry. In 1989, Joergensen stated that "the catalytic activity of rhenium in epoxidation reactions is low".[27] Shortly after that, the catalytic variety of this compound class, particularly MTO, was discovered.[28,29]

2.1.1. Dirhenium heptaoxide and derivatives

Dirhenium Heptaoxide (Re_2O_7) synthesized by burning of rhenium at 400 °C in oxygen atmosphere is the main raw material in the Re(VII) chemistry. Its features are defined by its unusual polymer like structure having Re-atoms in octahedral and tetrahedral coordination connected over an oxygen bridge. Important in this context is that the bridging Re-O bounds are longer

than the terminal ones. Also, the four different oxygens bound to a tetrahedrally coordinated Re center differ from each other only about 10 pm in length while the octahedrally coordianated Re atoms form three longer and three significantly shorter Re-O bonds.[30]

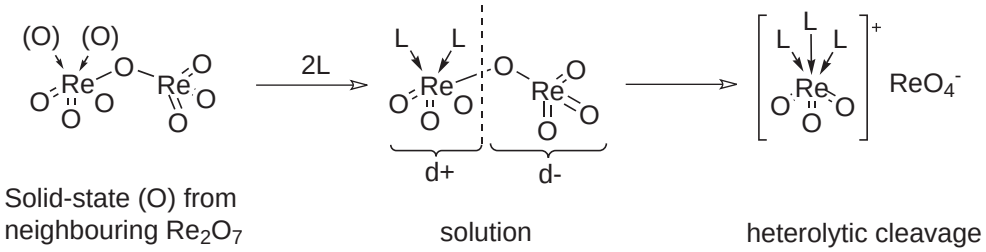

Scheme 2.2. The behavior of Re_2O_7 in coordination solvents

This structure shows its advantage when dissolved in coordinating solvents. Two solvent molecules always coordinate on only one Re-atom enhancing its coordination number to six. Bidentate ligands, like bipyridine and N,N'-dicyclohexyldiimine coordinate on only one Re-atom as well (Scheme 2.2).[31] The tridentate ligands show the same behavior, coordinating on only one rhenium atom, breaking the bridging Re-O-Re bound and forming an ionic complexes (Scheme 2.2). The discovery of this lability of the Re-O-Re bound opened new possibilities for the preparation of inorganic and organic perrhenyl compounds, partially presented in Table 2.2 together with their activity in the epoxidation catalysis. The foundation of an abundant class of compounds containing the ReO_3^+ fragment stabilized with different ligands which modulated its activity was also discovered.

2.1.2. The carboxylato rhenium complexes

Out of all compounds discussed in Section 2.1.1 the carboxylato complexes emerged as the most valuable precursor class in the Re(VII) chemistry. They are synthesized either by a reaction of Re_2O_7 with carboxylic anhydrides or by reacting perrhenates (especially silber perrhenates) with carboxylic chlorides in AN or THF as solvents (Scheme 2.3).[44]

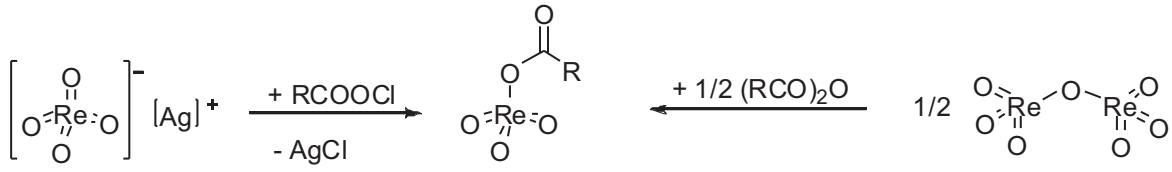

Scheme 2.3. Synthesis of various carboxylato complexes

Table 2.2: Activity of various rhenium compounds in olefin oxidation[32]

Compound	t /h	Yield [a] /%	Ref.
CH_3ReO_3	0.08	95 (25 °C) [b]	
$Na[ReO_4]$	16	0	
$NH_4[ReO_4]$	16	0	
$[N(nC_4H_9)_4][ReO_4]$	16	0	
$(CH_3)_3Sn[OReO_3]$	16	0	28,33
$(CH_3)_3Si[OReO_3]$	16	0	33
Re_2O_7[c]	18	0 (25 °C)	
	18	50 (65 °C)	
$Cp^\star ReO_3$	5	0	34
$[CpMe]ReO_3$	5	0	35
$CpReO_3$	5	0	35
$(\sigma-\text{Mesityl})ReO_3$	5	0	36
$(\sigma-\text{Phenyl})ReO_3$	5	0	37
$Cp^\star Re(CO)_3$	5	0	38
$Re_2(CO)_{19}$	5	0	
$Cp^\star ReOCl_2$	1	48	39
$Cp^\star ReOBr_2$	1.5	45	39
$Cp^\star MeReOCl$	2	68	40
$Cp^\star(tC_4H_9C)ReCl_2$	2	27	41
$CF_3COORe(CO)_5$	1	0	42
$CF_3CORe(CO)_5$	1	40	43

[a] Reaction conditions: 0.2 mmol catalyst, 10 mmol (1ml) of cyclohexene, 10% H_2O_2 in 1,4-dioxane (5 ml), T=90 °C unless otherwise noted. Product is *trans*-1,2-Cyclohexanediol

[b] Due to very high catalyst activity, the reaction mixture starts to boil (T=100 °C)

[c] Re_2O_7 is also active in THF solution (10 % H_2O_2) at 65 °C (50 % yield)

These complexes are all strong Lewis acids containing at least one solvent molecule pro Re atom. The coordinated solvent can be substituted only with strong coordinated ligands like TMEDA or py (Scheme 2.4). The crystal structures of these molecules reveal an octaehedral coordination of the metal center, with the carboxylic ligand being η^2-coordinated with monodentate ligands, and η^1-coordinated with bidentate ligands.[45] The hapticity also depends on the nature of the organic group of the carboxylic ligand. Hydrocarbons are forming η^2-complexes with one solvent molecule coordinated on the metal and perhalocarboxylates η^1-complexes with two coordinated solvent molecules. Apart from the crystal structure analysis that can not always be determined of these compounds, IR-spectroscopy is a valuable tool giving the necessary structural information. Typical carbonyl vibrations of the monodentate carboxylato ligands are between 1770 - 1790 cm^{-1} where the bidentate carboxylates differ immense with vibration spectra around 1440 cm^{-1} for the symmetric vibrations and 1490 cm^{-1} for the asymmetric vibrations. Several perrhenyl carboxylates were synthesized in the last couple of years by J. Mitterpleininger in our group who used *in situ* - IR for the characterization of the carboxyl ligand.[46] This method enabled the characterization of complexes that escaped isolation.Some of the perrhenyl carboxylate characterized in this work are summarized in Table 2.4.

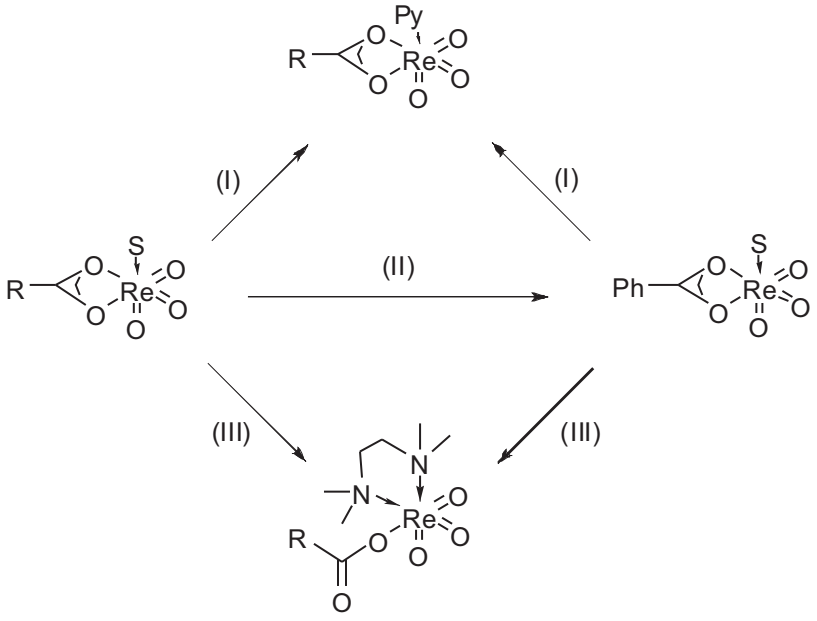

Scheme 2.4. Synthesis of trioxorhenium carboxylates and related compounds (R = Me, CF_3, or ^{t}Bu; S = THF, AN) (I) py; (II) $PhCO_2H$; (III) TMEDA

Table 2.4: νCO vibration of perrhenyl carboxylates in acetonitrile at room temperature[46]

Compound	$\nu_{\text{asymm.}}$CO [cm^{-1}]	$\nu_{\text{asymm.}}$CO [cm^{-1}]
$CH_3(C{=}O)OReO_3$	1493	1448
$C_2H_5(C{=}O)OReO_3$	1490	1440
$C_3H_7(C{=}O)OReO_3$	1487	1435
$C_4H_9(C{=}O)OReO_3$	1487	1435
$(CH_3)_2CH(C{=}O)OReO_3$	1495	1452
$(CH_3)_3C(C{=}O)OReO_3$	1499	1456
$C_6H_5(C{=}O)OReO_3$	1509	1487
$C_{10}H_7(C{=}O)OReO_3$	1512	1489
$o{-}C_6H_4[(C{=}O)OReO_3]_2$	1501	1456

2.1.3. MTO synthesis and useage as epoxidation catalyst

MTO is the most active epoxidation catalyst in the group of Re-based compounds (Table 2.2).[47] It is also the most versatile catalyst in its substance class, being active in the olefin metathesis, aldehyde olefination and oxidation of alcohol, ethers and aromatic compounds.[48]

First synthesized in 1979 by R. J. Beattie and P. Jones in tiny amounts, MTO was characterized but no catalytic properties were examined.[49] Oxidation of the $(CH_3)_4ReO_2$ with air over few weeks was the main step of this first synthetic approach. The first applicable route was discovered almost ten years later by Herrmann et al. alkylating the Re_2O_7 with tetramethyltin.[28] This reaction was widely used in the heterogeneous olefin metathesis catalysis where Re_2O_7/Al_2O_3 as a catalyst was activated with a small amount of tetramethyltin as co-catalyst.[50] From the diverse alkylating agents examined over the years, only the alkylzink and alkyltin reagents resulted in high yields and not in reduction of the metal center (Scheme 2.5).[51,28]

The drawback of these reactions was the loss of rhenium in form of perrhenate, not allowing yields higher than 50 % relative to the initial rhenium amount. None of the synthetic pass warp in Scheme 2.5 could be generalized, mainly due to the harsh conditions required in the synthetic procedure under which the desired rheniumalkyls (long-chain alkyl-ReO_3 and Aryl-

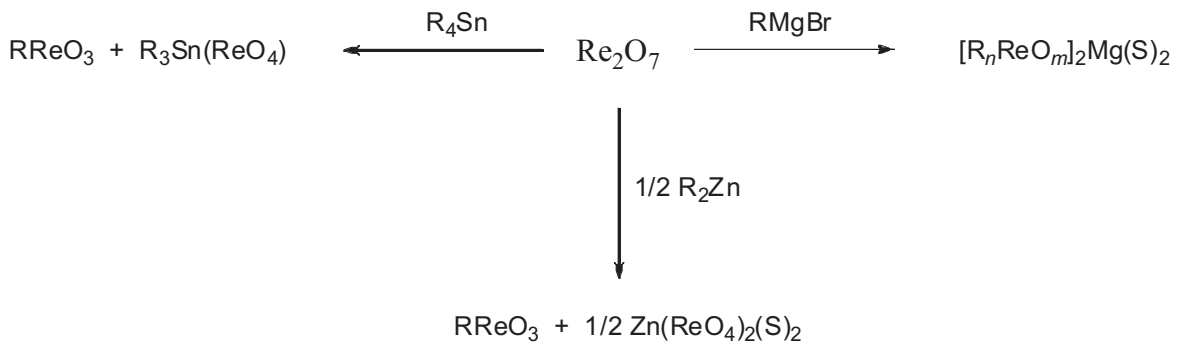

Scheme 2.5. Various synthetic procedures for the synthesis of $RReO_3$; (R = alkyl or aryl; S = THF or AN; *n=m, 2m, 4m*

ReO_3) were not stable.[52] Looking for optional starting materials Herrmann et al. came up with the acetyl perrhenates (see Section 2.1.2), which exchanged the acetyl group with an alkyl group by a reaction with alkylating reagents.[53] These reactions require low temperatures, and with accurate design of the acetyl group, the synthesis of the entire class of compounds was made possible.[48]

The growing interest in the sustainability of industrial catalysis in the last twenty years requires the use of non toxic and environment friendly reagents. The custom synthesis of $RReO_3$ had to be modified to fulfill these demands. In 2007 Herrmann et al. made the first step in this direction using the mild non toxic reagent methyl zinc acetate as a methylating reagent in the synhtesis of MTO.[54] This new synthetic method reduced the cost of production on a laboratory scale to ca. 42 euro/g from 834 euro/g that were needed with the first synthesis in 1979. The pyrophoric dimethylzinc was substituted with more user friendly methyl zinc acetate that further opened the possibility of using the waste product - zinc acetate - as a feedstock (Scheme 2.6).

Reaction conditions were optimized to use minimum amounts of solvent and to be as close to ambient conditions as possible in order to reduce the amount of waste generated and the consumed energy. The use of auxillary substances were eliminated entirely in the purification and recovery of MTO, as this complex is isolated by sublimation.[54]

The catalytic activity of MTO in the epoxidation of olefins was noticed soon after it was accessible in higher amounts.[29] However the breakthrough in the understanding of the role of MTO in the oxidation reactions was made by discovering the mono- and bis(peroxo) complexes, formed in the reaction of MTO with H_2O_2 in water, described in Scheme 2.7.[55,56]

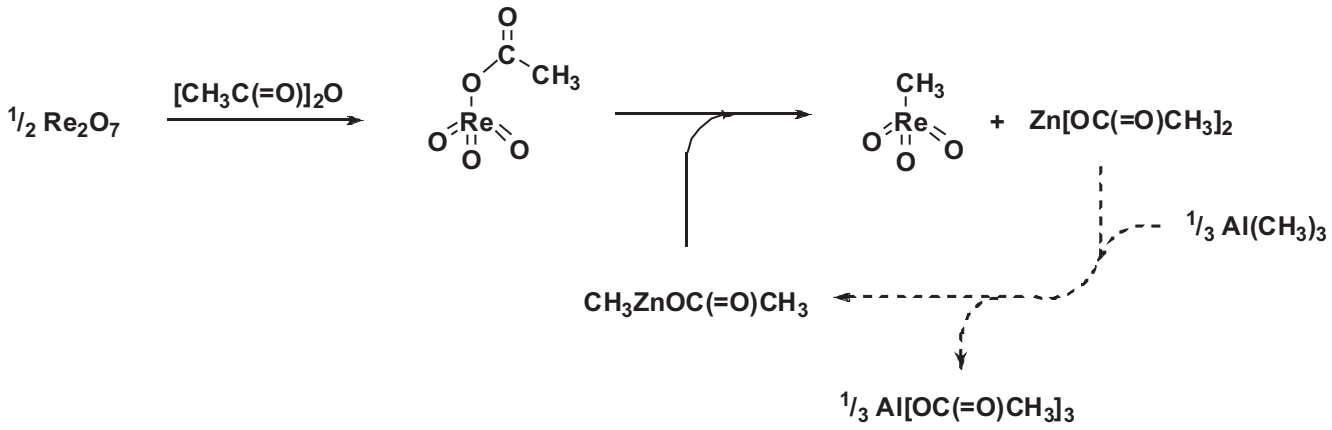

Scheme 2.6. Novel method for the synthesis of MTO using methyl zinc acetate synthesized *in situ* from zinc acetate and trimethyl aluminum

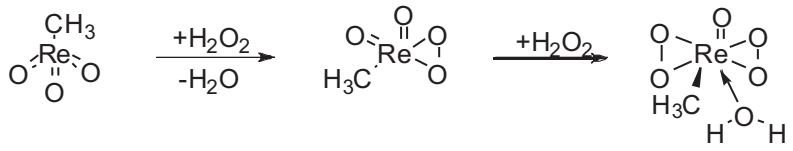

Scheme 2.7. The reaction of MTO and H_2O_2 yielding the peroxo- and bis(peroxo)-complexes, respectively; key intermediates in the olefin oxidation catalysis

The bis(peroxo) complex of stoichiometry $CH_3Re(O_2)_2O \cdot H_2O$ was the first isolated peroxo-metal complex with a metal-alkyl group that is stable to hydrolysis, light, acid, peroxides and evaluated temperatures. Its structure was determined with ^1H and ^{13}C NMR spectroscopy as well as with the elucidation of the crystal structure of its diglyme adduct. The spectroscopy results show one water molecule coordinating on the metal center having two very acidic protons. A fast exchange process of this water molecule can be observed by ^{17}O-NMR spectroscopy in solution indicating the lability of this ligand. The mono(peroxo) complex was also spectroscopically detected by a reaction of equal amounts of MTO and peroxide. In fact, it has never been isolated.

The direct reaction of the bis(peroxo) complex with olefins without additional peroxide demonstrated the activity of this compound in the epoxidation reactions. Kinetic experiments and DFT calculation supported these results and established the mono and bis(peroxo) complexes as key intermediates in the olefin epoxidation catalysis.[57,58,56]

The catalytic cycle is depicted in Scheme 2.8. The kinetic results found a similar rate constant for the reaction of the two peroxo intermediates proving that the two catalytic cycles proceed simultaneously and can not be distinguished. The oxygen transfer to the olefin occurs in

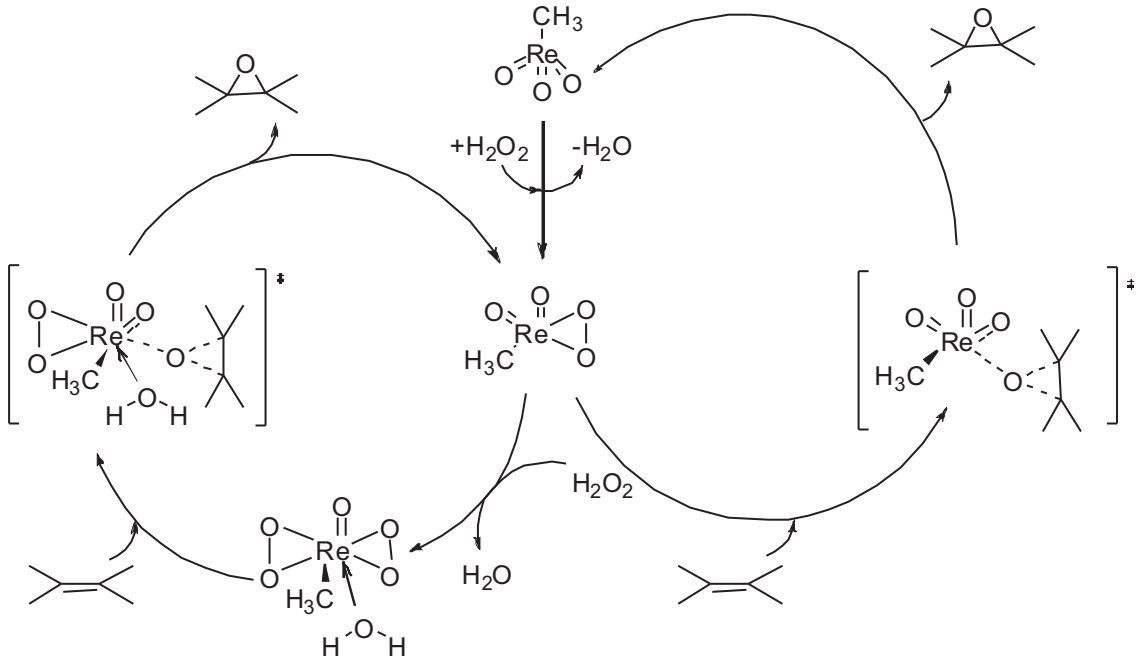

Scheme 2.8. The mechanism of the catalytic oxidation with MTO as catalyst

a concerted mechanism from the peroxo ligands, analogous to the mechanism postulated by Sharpless et al. for similar molybdenum catalysts.[59]

After the efficiency of MTO as epoxidation catalyst was established, its application in the epoxidation of various olefins grew bigger. It was than noticed that many of the synthesized epoxides reacted further with the water presented in the system forming glycols, a behavior originating from by the intrinsic Lewis acidity of the catalyst.[32] Since removing the water out of the system was impossible the proposed solution to the problem was to decrease the acidity of the metal center. In the next five years mainly the groups of Herrmann and Sharpless presented many additives that not only reduced the Lewis acidity of the metal center but also enhanced its catalytic activity.[32,60] These additives, some of which are presented in Table 2.5, contained pyridine or pyrazole structure elements and all are coordinated on the metal center instead of the water molecule accelerating the formation of the peroxo complex. The 3-cyanopyridine and especially pyrazole as Lewis bases proved to be the most efficient one.[61,62]

2.1.4. MTO as a heterogeneous catalyst

In order to use the benefits of the heterogeneous catalytic systems (see Section 1.2) many attempts were made for an MTO immobilization. NaY zeolite emerged as a suitable host

Table 2.5: MTO-catalyzed epoxidation of alkenes using H_2O_2[a,21]

Alkene	No additive [b]	Pyridine [c]	3-Cyanopyridine [c]	Pyrazole [c]
Cyclohexene	90 (5)	96 (6)		
Cyclooctene	100 (2) [c]	99 (2)		89 (0.02)
Styrene		84 (16)	96 (5)	96 (5)
Indene	48 (37)	96 (5)		
α-Methylstyrene		82 (6)	74 (1.5) [d]	93 (1.5)
1-Phenyl-1-Cyclohexene		98 (1)	96 (1) [d]	95 (1)
trans-4-Octene	95 (2)	91 (24)	97 (12)	
1-Decene	75 (72)	82 (48)	99 (14)	99 (14)

[a] Yield % (reaction time [h]).

[b] Anhydrous H_2O_2 in ^{t}BuOH.

[c] Aqueous H_2O_2 (30 %).

[d] Pyridine and 3-cyanopyridine (6 mol% of each).

material already in 1995 from the work of Ozin et al.[63] MTO was sublimed on pre-activated zeolite under strictly anhydrous conditions and used by Bein and co-workers as a catalyst in the olefin metathesis of 1-hexene. Unfortunately, the same catalyst used in the epoxidation catalysis resulted in very low conversion and product selectivities in olefin metathesis. Main reason for this behavior was the high concentration of Lewis acidic centers present in the dehydroxylated zeolite that facilitated the ring oppening of the epoxides. The next generation of MTO-zeolite catalysts were developed by Adam et al. who used nonactivated zeolites as support. The MTO was introduced in the cavities of the solid material by mixing it with the reaction solution, without substrate.[64] This relatively easily prepared catalyst was used in silane oxidation and epoxidation giving high product selectivities with 85 % H_2O_2.

Immobilisation of MTO on polymers is another alternative in the process of synthesizing a heterogeneous catalyst for the oxidation purposes, originally used by Herrmann et al. in 1992.[65] Similar method was used by Saladino et al., who described the preparation and characterization of novel heterogeneous rhenium compounds with general formula $(polymer)_n$ / $(MTO)_m$ (the n/m coefficient express the ratio by weight of the two components Scheme 2.9). Poly(4-

vinylpyridine) and polystyrene were preferably used as a support.[66]

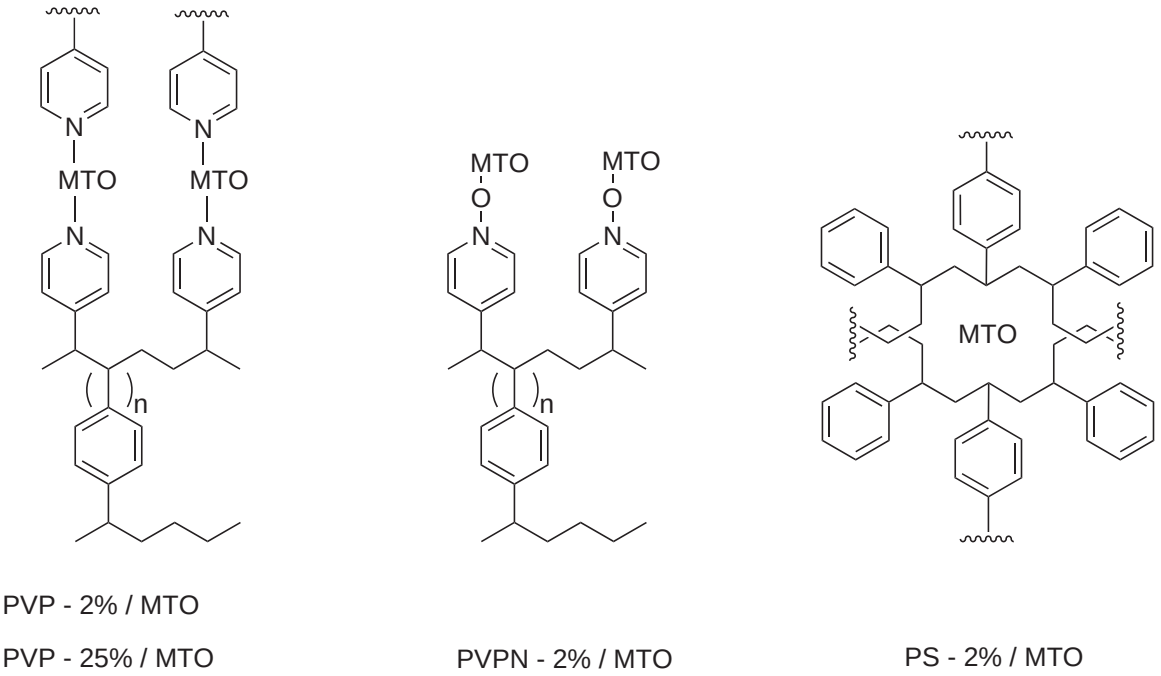

Scheme 2.9. Structure of polymer supported MTO catalysts

The Re-N bound in this polymer bound MTO is abnormally short showing a strong coordination of MTO moiety to the surface. The positive influence of the Lewis-base aducts discussed in Section 2.1.3 made this polymer supported MTO an efficient and selective catalyst for the olefin epoxidation. The catalytic activity was reported to be maintained for at least five recycling experiments.[66]

Ionic liquids, emerging as a non-volatile sustainable solvents in organic chemistry, are also used as medium for the MTO immobilization.[67] These systems pool together the advantages of the homogeneous and heterogeneous catalysis using UHP as an oxidant, which happens to be soluble in ionic liquids, same as the peroxorhenium species.[67c] The products, that are formed in good to excellent yield, can be removed by an extraction with diethyl ether which is not miscible with the ionic liquid. Water solution of H_2O_2 can not be applied because water results immediately with ring opening of the epoxide. Nevertheless, H_2O_2 was used in Bayer-Villiger reaction and the oxidation of aromatic aldehydes and ketones resulting in a high yields and selectivities. The catalyst is stable under these conditions and reusable for six consecutive runs.[67]

2.2. Molybdenum catalysts in the epoxidation of olefins

2.2.1. Dioxomolybdenum(VI) complexes with Mo-C σ-bonds

The discovery of the catalytic capability of molybdenum-based compounds in the epoxidation of olefins with the "oxirane-process",[23] triggered the research for developing new catalytic systems on molybdenum basis for similar reactions.[68,69] A rather old compound, MoO_2Cl_2 discovered by J. J. Berzelus in 1826, was used as a pattern in the early research stages. Unfortunately, the instability of the molybdenum oxides hindered the application in the oxidation catalysis.[70]

Introducing organic fragments instead of the chlorides, increased considerably the stability of these molybdenum oxides and made the variation of their activity possible. $MoO_2(Mes)_2$ was the first oxide synthesized in 1976 by Heyn and Hoffmann using this method.[71] Substituting the chlorides in MoO_2Cl_2 using Grignard reagents in particular MesMgBr, resulted in a crystalline, air and moisture stable compound. Although, molybdenum was coordinative unsaturated, no base adducts could have been isolated. $MoO_2(Mes)_2$ was not used as a catalyst for oxidation of olefins but it can be used as a precursor for synthesizing chiral molybdenum compounds by exchanging the mesityl ligands with H_2BINOL, yielding MoO_2(S−BINOL)$(THF)_2$.[72] The later compound gave good results in the epoxidaton of *cis*-cyclooctene, *trans*-β-methylstyrene and limonene when used on room temperature with TBHP as an oxidant. An enantiomeric excess was found in neither case.[72]

Realizing the function of molybenum(VI) in the enzyme nitrogenase gave an additional impulse for synthesizing novel molybdenum complexes that mimic this behavior in chemical processes.[73] For this reason, reactions of MoO_2X_2(Bipy) with Grignard reagents were thoroughly explored yielding two new types of compounds, MoO_2XR(Bipy) and MoO_2R_2(Bipy) respectively, where (X = Cl or Br and R = various organic moieties some of which are listed in the Scheme 2.10 below). These, temperature and air stable compounds with highly distorted octahedral structure prepared and examined by Schrauzer et al. offered various possibilities for specific changing of the metal environment and with it a specific modulation of its catalytic properties.[74,75]

This compound class expended further with the replacement of the Bipy-ligands with other bidentate Lewis-base ligands, introduced by the research groups of Gonçalves, Kühn and Romão.[76] A wide range of compounds were synthesized, bearing a variety of bidentate lig-

X = Cl, Br

R = CH_3, C_2H_5, *n*-C_3H_7, *i*-C_3H_7, *n*-C_4H_9, *i*-C_4H_9, $CH_2C(CH_3)_3$, c-C_5H_9, c-C_6H_{11}, C_6H_5, *o*-$CH_3C_6H_4$, *p*-$CH_3C_6H_4$, *p*-ClC_6H_4, *p*-$CH_3OC_6H_4$, $CH_2C_6H_5$, *o*-$CH_3C_6H_4CH_2$, *p*-$CH_3C_6H_4CH_2$,$CH_2CH_2C_6H_5$, $CH_2Si(CH_3)_3$

= 2,2'-bipyridyl, substituted bypiridines, 1,4-diazobutadiene and phenanthroline

Scheme 2.10. Summary of Mo(VI)-bipy-class of compounds[68a]

ands based on 1,4-diazobutadiene structure with different organic groups, phenantroline and substituted bypiridines (Scheme 2.10). The different stereochemical and electronic characteristics of these ligands impart distinct reactivities to the MoO_2R_2 core. They also provide access to more soluble complexes, making these better amenable to reactivity and spectroscopic characterization than the modestly soluble Bipy-complexes.

Many of these novel compounds were used in the epoxidation of olefins with TBHP as an oxidant. Unlike Re(VII)-compounds no activity is observed with hydrogen peroxide as an oxidant. The conversion is strongly dependent of the electronic properties of the ligand, with electron-attracting ligands resulting in higher conversions, rendering the molybdenum center electron deficient. Increase of the temperature and the reaction time leads also to significant increase in the product yield. However, sterically demanding ligands result usually in low conversions by shielding the metal center to external influences.[68] The possibility of directed change of the ligands affords a synthesis of specially designed complexes for immobilization on silica surfaces and ionic liquids. These heterogeneous systems show excellent reactivity and selectivity to the epoxides combined with excellent recyclability.[77]

2.2.2. Dioxomolybdenum(VI) complexes with cyclopentadienyl ligands

Dioxomolybdenum(VI) complexes bearing Mo-C π bonds were the second major class of compounds recently developed as a very active catalysts for olefin epoxidation.[68,69] The first complex of this type, the $CpMoO_2Cl$, synthesized in 1963 by Cousins and Green, was one of the

first monomeric high oxidation state organometallic complexes.[78] It was made in a low yield synthesis through an air oxidation of $CpMo(CO)_2(\pi-C_3H_5)$ in the presence of HCl. Its potential in catalysis was not realized back than, and follow up work was done only in improvement of the synthetic procedure.[79]

Further progress in this molecule class has not been made until 1988, when the chemistry of complexes bearing metals in high oxidation state started to boom with the discovery of their utilization as catalyst in olefin metathesis and oxidation reactions.[80] In the same year, Legzdins et al. published a new dioxomolybdenum complex $Cp'MoO_2R$ with alkyl instead of the chloro ligand. The synthetic procedure was based on oxidation of the 16-electron dialkyl nitrosyl complexes $Cp'Mo(NO)R_2$ [Cp′ = Cp and Cp⋆; R = CH_3 and $CH_2Si(CH_3)_3$] with molecular oxygen in water.[81,82] This method gave yields higher than 80 % and was also used for equivalent tungsten complexes. Its broad application has further been proven in 1996 when Hubbard et al. synthesized the dioxomolybdenum - chloro derivatives using chloro bis nitrosyl complexes as precursors.[83] Unfortunately, the $[Mo-CH_3]$ entity was more sensitive to molecular oxygen than the nitrosyl ligands, so this method could not be used for the synthesis of complexes bearing longer alkyl chains.

Almost simultaneously Faller and Ma published a new Dioxomolybdenum chloro complex with a Cp⋆-Ligand, $Cp^\star MoO_2Cl$. Similar to the first synthesis of Cousins and Green, carbonyls were used as precursor, $[Cp^\star Mo(CO)_2]_2$ in particular.[84,85] This carbonyl dimer was oxidized with oxygen in chloroform to the η - oxo bridged compound that was further reacted with PCl_5 to the mononuclear dioxo compound. This novel complex had the same piano stool structure as the one bearing a Cp - ligand but it was considerably more stable and could be isolated and handled easily. In 1994 Bottomley et al. improved this method by applying hydrogen peroxide as an oxidant followed by an immediate addition of HCl yielding almost quantitatively the desired product.[86]

Afterwards, the carbonyls, easy to synthesize and very stable compounds, became the most used precursors for the synthesis of the dioxomolybdenum(VI) - compounds. In 1991 Bergman et al. applied the oxidative decarbonylation to make various dioxomolybdenum(VI) - chlorides.[87] Oxygen, was used as an oxidant, purged in toluene solutions under UV-irradiation. The use of chloride carbonyl compounds as precursor eliminated the need to conduct the reaction in chlorinated solvents.

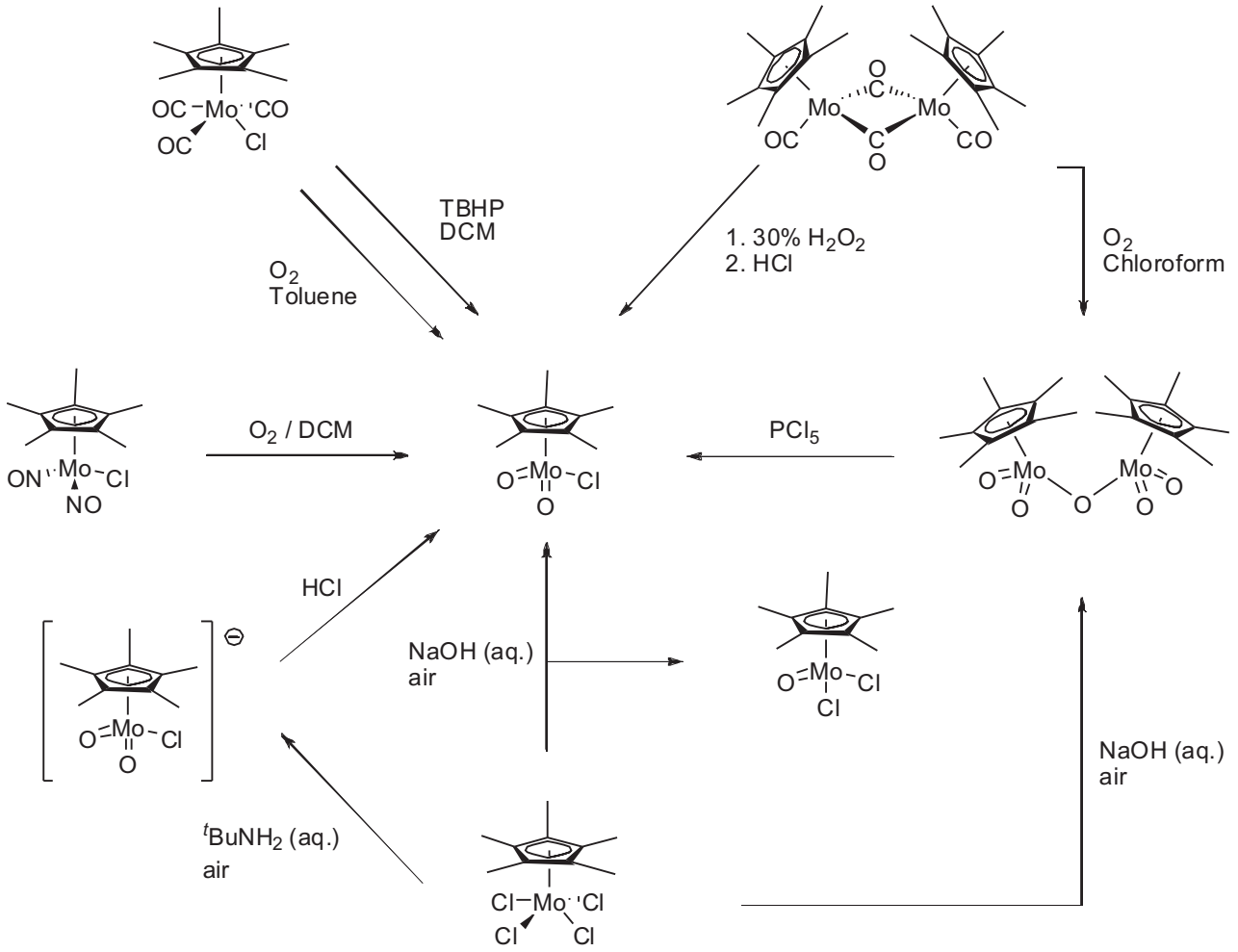

Scheme 2.11. Various synthetic procedures for making of $Cp^{\star}MoO_2Cl$[68]

The oxidative decarbonylation was also implemented in more recent works of Kühn et al., and Romão et al..[68,69,88] They developed a general and straightforward method for the synthesis of dioxomolybdenum(VI) - compounds, which could be applied on complexes bearing various Cp ligands and chloride. Its applicability was further extended to the complexes having an alkyl group instead of the chloride. The reaction was performed using alkyl peroxides as an oxidating agent in dichloromethane as a solvent. Studies undertook on the novel complexes synthesized by the two groups once again proved that the stability depends on the steric bulk of the Cp ligand, with $(CpBz_5)MoO_2Cl$ being more stable than its Cp and $Cp^{\star}$ counterparts.[88a]

Slightly different preparation methods for $(C_5Bz_5)MoO_2Cl$ were presented by Martins, Romão and Poli et al.[88b] Treatment of the η^2-acyl complex $(C_5Bz_5)MoCl_3(COCH_3)$ with excess TBHP in DCM originated $(C_5Bz_5)MoO_2Cl$. The obtained yield is much higher than the yields previously reported for other cyclopentadienyl complexes. An X-ray structure of $(C_5Bz_5)MoO_2Cl$

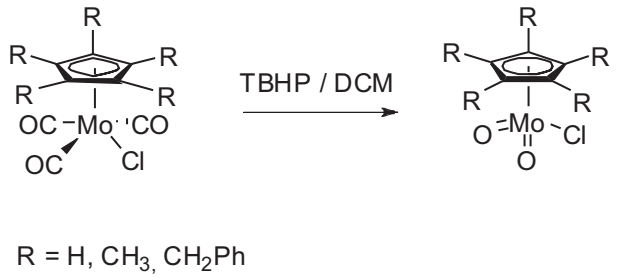

R = H, CH_3, CH_2Ph

Scheme 2.12. Oxidative decarbonylation of $Cp'Mo(CO)_3Cl$

has also been obtained. However, attempts to extend this method for alkyl groups instead of chlorine by alkylating the $(C_5Bz_5)MoO_2Cl$ with allylmagnesiumbromide and $ZnMe_2$ failed.

Another precursor who gained importance was Cp^*MoCl_4, which could be oxidized by air in aqueous NaOH.[89] It resulted in a mixture of Cp^*MoO_2Cl and Cp^*MoOCl_2 as the logical intermediate to the dioxo complex. The reaction time was to be kept low, otherwise the products, which are vulnerable to hydrolysis reacted further to Cp^*MoO_2OH, which underwent a condensation reaction to the $[Cp^*MoO_2]_2O$ dimer. The base used in the process also has an influence on the products formed. In fact, when Cp^*MoCl_4 was reacted with tBuNH$_2$ in the presence of water and air, an anionic trioxo complex $[Cp^*MoO_3]^-$ was formed that could be isolated as its ammonium salt. The treatment of this complex with gaseous HCl resulted in a clean formation of Cp^*MoO_2Cl.

Realizing the importance of molybdenum(VI) compounds in oxidation reactions Bergman et al. first applied these cyclopentadienyl-dioxomolybdenum(VI) derivatives as catalysts for the olefin epoxidation.[87] Similar to the Mo-C σ bound complexes, the Cp^*MoO_2Cl (the catalyst used by Bergman) performed the catalysis effectively when TBHP was applied as oxidant. Other alkyl peroxides showed similar reactivity apart from Ph_3COOH and hydrogen peroxide which exhibit no reaction whatsoever. Bergman related this behavior with the formation of the peroxo intermediate $Cp^*Mo(O)_2OCl$ that was isolated and proved not to be active in the catalysis. This intermediate was formed with TBHP as well, but only in absence of the olefin. This unusual behavior, knowing the reactivity of similar Re(VII)-complexes and their importance as catalyst (see Section 2.1.3), was proven once again by H. W. Rosky et al. who obtained an X-Ray structure of this peroxo intermediate and showed its instability under the applied reaction conditions.[90]

The oxidative decarbonylation developed by Kühn, Romão et al. was also implemented in

the catalysis using excess alkyl peroxide. Under such conditions the dioxo species, created *in situ*, was again the active intermediate, reacting further with the rest of the peroxide and the olefin in the catalytic cycle.[88,68,91] The advantages of the molybdenum carbonyls as precursors are:

- Their straightforward synthesis
- Their stability. All compounds are stable under air for a short period of time and indefinitely under inert gas atmosphere.
- The ligand variability. The cyclopentadienyl and the alkyl - ligand are easily modified, altering the electronic properties of the metal center and thus its catalytic activity. Designing task-specific ligands for immobilization of these compounds is also an important issue.[77,88,92]

Table 2.6: A summary of cyclopentadienyl dioxomolybdenum(VI) - complexes, their ^{95}Mo NMR chemical shift and catalytic activity[a][68,93]

Compound	^{95}Mo [b]	Yield % [c]	TOF / h^{-1}
$CpMoO_2Cl$	-448	100	1200
Cp^*MoO_2Cl	-399	50-60	800
$(CpBz_5)MoO_2Cl$	-282	100	1200
$CpMoO_2CH_3$	-346 (-1726)[d]	95	820
$Cp^*MoO_2CH_3$	(-1596)[d]	68	270

[a] The catalysis was performed on 55 °C using cyclooctene as a substrate with catalyst:cyclooctene:TBHP - ratio of 1 : 100 : 200.

[b] ^{95}Mo NMR spectra measured in $CDCl_3$ at room temperature

[c] Yield calculated after 4 hours reaction time.

[d] ^{95}Mo NMR spectra of the carbonyl compound measured in $CDCl_3$ at room temperature

Various dioxomolybdenum(VI) compounds generated *in situ* from their carbonyl precursors are summarize in Table 2.6. A direct correlation between the substitution pattern of the Cp

ligand and the ^{95}Mo-NMR signals is observed. Knowing the importance of the molybdenum spectroscopy, as a tool for predicting the electronic properties of the metal center in complexes with similar structure, this correlation can be used as a measure for the electronic influence of the diverse ligands.[94] Unfortunately, by increasing the electron density on the metal center beginning with Cp, Cp* to $CpBz_5$ the NMR signal shifts to low field. The same trend has been perceived in the carbonyl complexes with alkyl substituents. This unusual behavior was also documented by Masters et al. on different series of molybdenum carbonyls ((mes)$Mo(CO)_3$, (p−xyl)$Mo(CO)_3$, (tol)$Mo(CO)_3$).[95] However, the ^{95}Mo-NMR chemical shifts are still premature to attempt a detail explanation of the trends observed. Nevertheless, correlations with the experimental results will guide future theoretical studies, and an interesting correlation does exist.

The catalytic activity of the complexes is summarized in the Table 2.6. After four hours reaction time, the complex bearing Cp and $CpBz_5$ ligands reach maximum conversion. The complex with a Cp* ligand reaches only about 50 - 60 % conversion under the same conditions.[88a] A difference between the activity of the complexes with Cp and the $CpBz_5$ ligand can be first noticed after the second and third run, made by addition of new charges of substrate to the reaction mixture. While the $CpBz_5$ complexes maintains their reactivity, the Cp derivatives lose it due to a decomposition reaction. The catalyst with $CpBz_5$ ligands shows even higher activities when used in lower concentrations. By an $(CpBz_5)MoO_2Cl$: cycloctene ratio of 1 : 1000 the TOF was higher than 4000 h^{-1} and by a ratio of 1 : 10000 the TOF reached even 20000 h^{-1} which is even higher than the activity achieved with MTO/H_2O_2 system (14000 h^{-1}).[96] Reducing the catalyst amount even further failed because of the small quantities of water present, that enhanced the catalyst decomposition in this concentration range.

The fact that the complex with $CpBz_5$ ligand is more active than the compounds bearing Cp and Cp* ligands, despite its significantly greater steric bulk, might be ascribable to its pronounced stability in comparison with the two other congeners. Another possible contribution to the higher activity of this compound might come from its lower electron density at the Mo center, due to a weaker Mo-ring bond as reflected in the ^{95}Mo-NMR spectroscopy (see above).

Within the group of complexes bearing a methyl group instead of the chloro ligand similar trends are observed.[93] A direct comparison between these two types of molybdenum catalysts revealed that the chlorid containing compounds were better catalyst when used in a 1:100, cat-

alyst to substrat ratio. This behavior was mostly due to the electronic - withdrawing property of the chlorid ligand. With lower catalyst to substrat ratio the methyl congeners showed higher catalytic activity due to their higher moisture stability. Another major difference between the two types is the catalytic active species. While the dioxomolybdenum(VI) chloro complexes can be isolated in an oxidation of the molybdenum(II) - chloro carbonyls with TBHP as an oxidant, an oxoperoxomolybdenum(VI) - $Cp'MoO_2O(CH_3)$ was the main product of this oxidation with the methyl bearing complexes.[93] Preliminary results obtained by Kühn et al. proposed this oxoperoxomolybdenum(VI) species as the active intermediate in the epoxidation catalysis, indicating a different catalytic cycle as by the complexes with chlorid ligands.

2.2.3. Mechanistic studies of the olefin epoxidation catalysis with dioxomolybdenum(VI) - complexes

After the importance of the dioxomolybdenum(VI) - compounds in the catalytic, as well as the stoichiometric epoxidations of olefins was established, several research groups began with mechanistic investigations of these reactions. The most promising results came from Mimoun et al. and Sharpless et al. both presenting a possible mechanism for this process (Scheme 2.13), initiating a long scientific debate about the accuracy of each model.[59,97,58,98]

The first studies, conducted on a stoichiometric reactions with $[MoO(O_2)_2(OP(NMe_2)_3)]$, by Mimoun et al. supported a complexation - insertion of the olefin to form a five-membered peroxo metallocycle Scheme 2.13.[97] These preliminary results were further verified on the *cis* - dioxomolybdenum (VI) complexes bearing bidentate ligands, introduced under catalytic conditions.[97b] The initial step of this mechanistic preposition saw the olefin coordinating at the vacant coordination site on the metal atom. The speed of the reaction was accelerated by increasing the nucleophilicity of the olefins used. Strong inhibition occurred when strong basic ligands or coordinating solvents were added, which competed with the olefins for the vacant sites on the metal. The coordinated olefin further inserted in the Mo - peroxo bonding, creating a five-membered metallacycle (metalla-2,3-dioxolane), known for the late transition metals.[99] The epoxide was than formed by cycloreversion of the metallacycle.

In 1977 Sharprless et al. synthesized the ^{18}O marked peroxo - intermediate of the $MoO_2(acac)_2$ complex.[59b] Reacting it with various olefins no incorporation of the labeled oxygen in the epox-

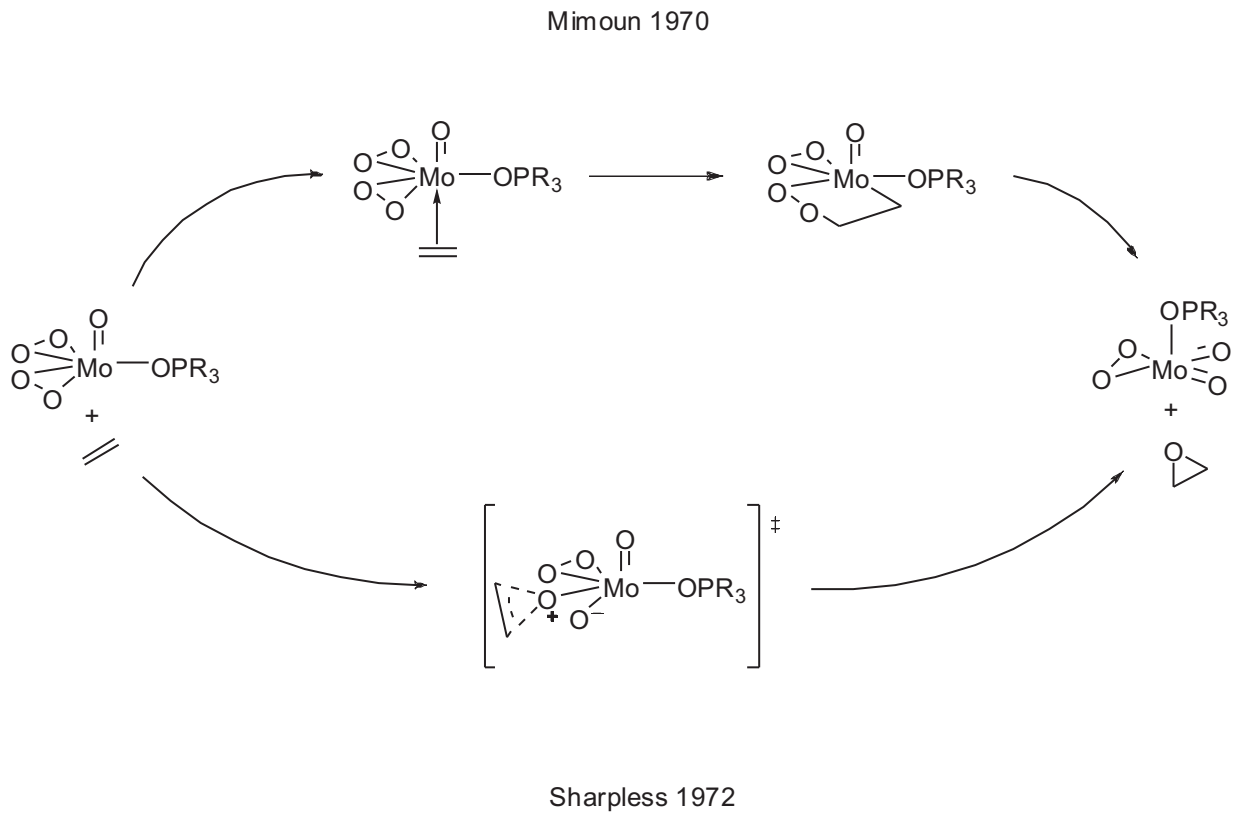

Scheme 2.13. Mimoun and Sharpless mechanistic pathway for the olefin epoxidation

ide product was found. On the base of these experiments and already established theories from Sheldon and Zajacek, Sharpless postulated a concerted oxygen-transfer pathway involving a three-membered transition state instead of the metallacycle (Scheme 2.13).[100,101]

Quantum chemical calculations performed on these two systems by Rösch et al. gave further insights on the mechanism of the oxygen transfer.[58] The main controversies, the catalytic and the stoichiometric oxygen transfer, the electronic character of the oxygen transfer and the stereo-selectivity of this process, were all addressed in this computational effort. The most important conclusions drawn, were:

- The oxygen transfer proceeds via concerted mechanism postulated by Sharpless. The formation of a metala-2,3-dioxolane as an organometallic intermediate is not favorable, and its decomposition would give aldehydes rather than epoxides
- The oxygen attacks the olefin in an electrophilic manner, forming a five-membered transition state (Scheme 2.14).
- In catalytic reactions, an intra or inter molecular proton transfer to the η^2-peroxo species is

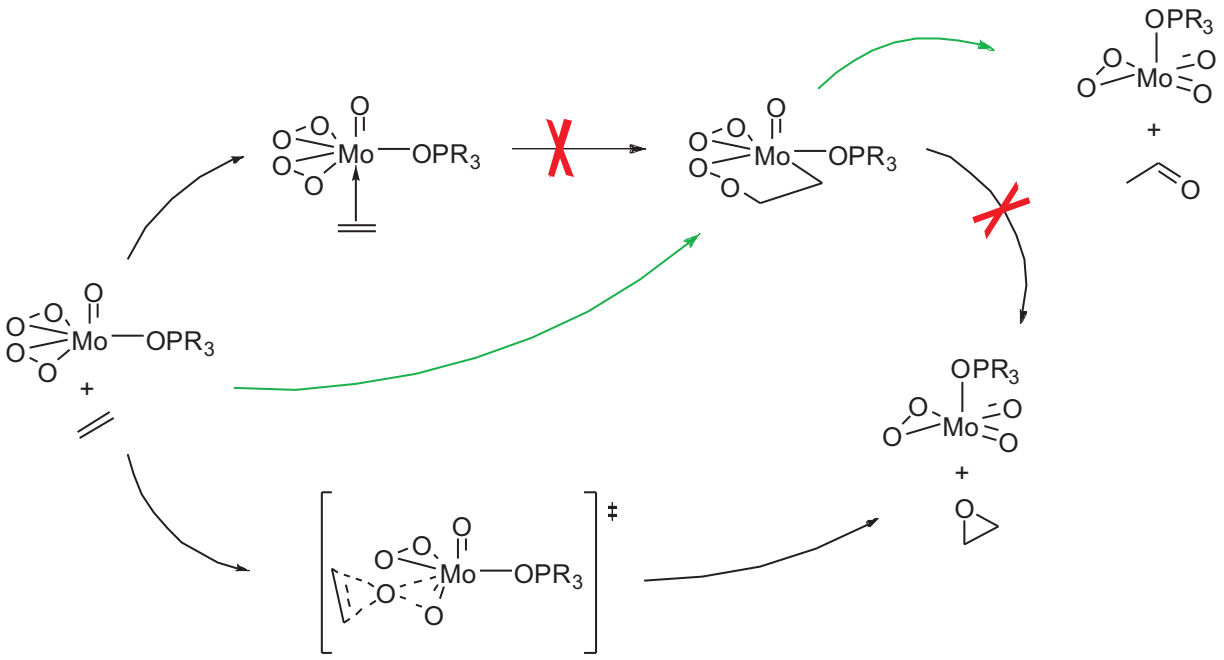

Scheme 2.14. Quantum chemical calculations support the concerted mechanism, whereas the stepwise mechanism would give the wrong product

the process with the lowest energie. The resulting η^1-peroxo species is superior in the catalytic epoxidations (assumption, later experimentally proven, by Thiel et al. (Scheme 2.16))

- The epoxidation can be done stereoselectively as well, when the olefin adheres an functional group that coordinates on the et al.

Calhorda et al. also drew similar results calculating the epoxidation of olefins with dioxomolybdenum(VI) complexes as catalysts.[98] In Calhordas mechanistic proposal, the TBHP used as oxidant first transfers a proton on the oxygen atom of the complex, coordinating itself in a η^1-fashion on the et al. The olefin inserted afterwards in between Mo - oxygen bound resulting in a seven membered transition state sketched in Scheme 2.15. The final step included a disintegration of this intermediate as the two products, *tert*-butanol and the epoxide, are eliminated from the complex regenerating the catalyst.

Scheme 2.15. The olefin coordination to the metal and the formation of the first C-O bond[98]

Based on his experiments with oxobisperoxomolybdenum(VI) complexes as catalysts for the

olefin epoxidation, Thiel, aware of the computational reports published, proposed a new mechanism for these reactions.[102] In the first step of the catalysis the alkyl peroxide coordinates on the Lewis acidic metal center. The coordinated alkyl peroxide was than activated by giving a proton to one of the peroxide ligands on the molybdenum simultaneously altering its position from η^1 to η^2. The following oxygen transfer occured on this peroxide analogous to the Sharpless mechanism Scheme 2.16. In the same way as the mechanism of Mimoun, Thiel observed that strong basic ligands and donor solvents suppresed completely the reaction by blocking the free coordination site of the metal, making the peroxo coordination impossible.

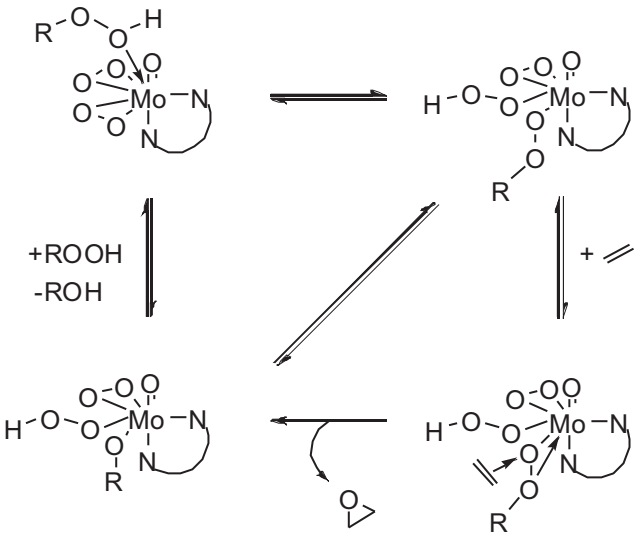

Scheme 2.16. Thiel mechanism for the olefin epoxidation[102]

The key step of this novel mechanism is the proton transfer to the peroxide instead of the oxygen atom, that is an extremely poor proton acceptor. The quantum chemical calculations performed by Thiel et al. confirmed this activation step, complementing it with the fact that the resulting alkyl peroxide changed its coordination on the metal from η^1 to η^2.[103] This ligand fluxionality was further proved applying temperature-dependent two dimensional NOESY experiments.

The only mechanistic study on dioxomolybdenum(VI) - cyclopentadienyl complexes was done on $Cp^{\star}MoO_2Cl$ in 1991 by Bergman and Trost.[87] They proved that the reaction followed the same pathway as the other molybdenum(VI) compounds even though the ligand environment was different. The cyclopentadienyl ligand was stable under the catalytic conditions applied and the only deactivation came with the formation of the peroxo - $Cp^{\star}Mo(O_2)OCl$ - complex.

With the experimental data gathered, the authors could not distinguish between the known, Mimoun and Sharpless pathways.

3. Synthesis of a novel heterogeneous rhenium catalyst for olefin epoxidation

3.1. Mobil crystalline of materials (MCM)

Among the various supporting materials studied, the mesoporous silicates, designated as MCM-41 (hexagonal) and MCM-48 (cubic) by Mobil scientists, were taken as promising candidates for the catalyst support in our experiments.[104] These materials, first synthesized in 1992, possess a unique long range ordered mesoporous framework composed of amorphous silica walls. Their structure and pore size can be altered during their synthesis, providing a great variation of materials with unique properties. Other features that make these materials ideal for catalytic application are their large surface area, that can rich remarkable 1000 m^2g^{-1}, and their high chemical and thermal stability.[105]

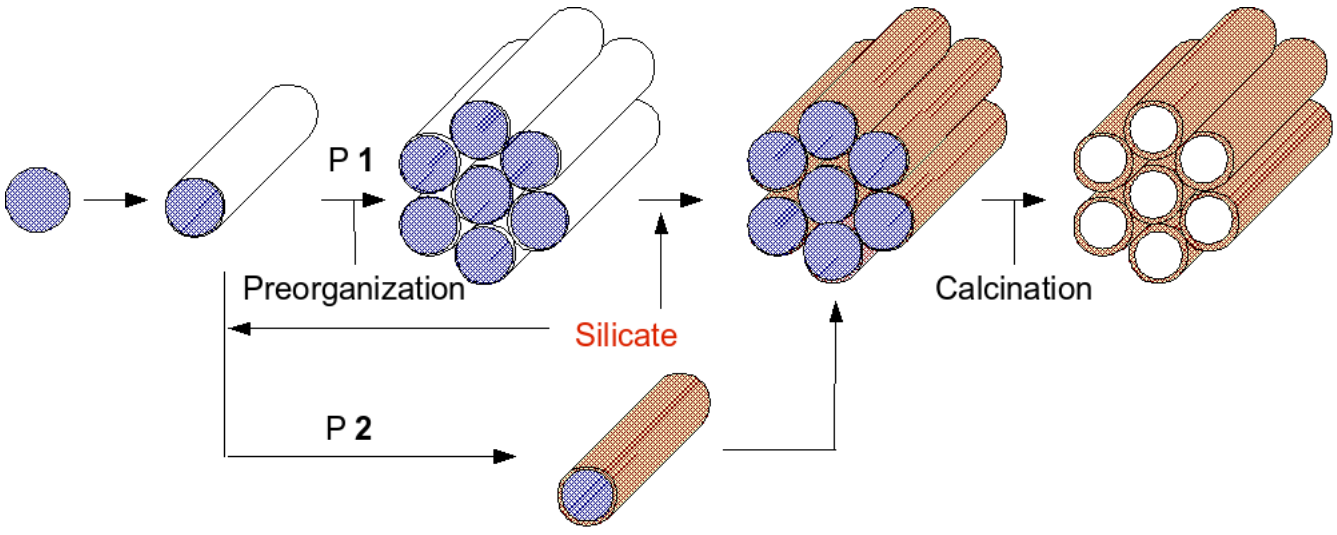

Figure 3.1. Schematic description of the liquid crystalline templating mechanism[104]

The formation mechanism of these materials is known as a Liquid Crystal Templating (LCT),

where the liquid crystalline mesophase (micelles) are acting as a template, rather than individual single molecule or ion.[106] These micelles, formed by an organic surfactant in water, can order themselves prior to the silicate addition (**P1** in the Figure 3.1) or the silicate itself can influence the ordering of the isotropic rodlike micelles to the desired liquid crystal phase (**P2**).[104] These two different pathways are depicted in Figure 3.1. Applying organic surfactants with different length, materials with pore size between 1.5 and 10 nm can be synthesized. On the other hand, by varying the surfactant to silica molar ratio four different siliceous structures can be formed: MCM-41 (hexagonal), MCM-48 (cubic) a thermaly unstable lamellar phase, and cubic octamer phase$[(CTMA)SiO_{2.5}]_8$.[106] After the lattice is formed, the surfactant is removed by calcination in air, opening the pores of the siliceous material.

3.2. The grafting of acylperrhenate on mesoporous sieves

Acylperrhenate ($AcOReO_3$) was synthesized as previously described[45,55,31] and comparison of the ^1H NMR and ^{13}C NMR data proofed that the complex is pure and identical with the literature described compound.

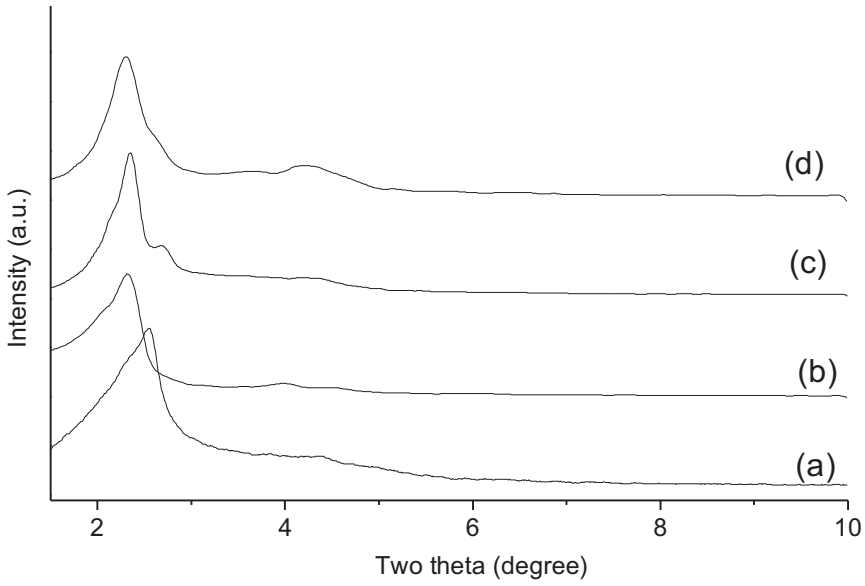

Figure 3.2. Power XRD pattern of a) MCM-41-ReO_3, (b) Al-MCM-41-ReO_3, (c) MCM-48-ReO_3, (d) Al-MCM-48-ReO_3

Dissolved in acetonitrile, this freshly prepared acylperrhenate was added to the pre-activated mesoporous materials and left reacting for 24 h. at 25 °C. After the grafting was completed,

the solvent was filtrated, and the brown solid was washed several times with acetonitrile and dried under vacuum. The characterization of these rhenium containing molecular sieves, was initiated with the examination of their mesoporous structure, done by X-ray diffraction.

Table 3.1: Textural properties of the grafted and non grafted sample

Sample	Re wt %	Interplane Distance / nm [a]	Unit Cell Parameter /nm [b]	BET Surface Area / m^2g^{-1}	Pore Volume /cm^3g^{-1}
Al-MCM-41	-	3.75	4.33	-	-
Al-MCM-41-ReO_3	0.9	3.75	4.33	-	-
Al-MCM-48	-	3.79	9.28	-	-
Al-MCM-48-ReO_3	1.3	3.82	9.36	941	0.8
MCM-41	-	3.80	4.38	839	0.8
MCM-41-ReO_3	2.8	3.46	3.99	489	0.6
MCM-48	-	3.97	9.72	1043	1.2
MCM-48-ReO_3	6.0	3.72	9.12	938	0.8

[a] d_{100} for MCM-41 and d_{211} for MCM-48.

[b] $a = 2d_{100}/3$ for MCM-41; $a = d_{hkl}(h^2 + k^2 + l^2)^{1/2}$ for MCM-48

In each case all four reflections are observed in the 2Θ range 2-8°, with an indexing corresponding to a hexagonal cell showing the (1 0 0), (1 1 0), (2 0 0) and (2 1 0) planes. Figure 3.2c and Figure 3.2d show the XRD patterns of the MCM-48-ReO_3 and Al-MCM-48-ReO_3, which exhibit a main reflection corresponding to the (2 1 1) plane along with a shoulder peak derived from the (2 2 0) plane, typical for cubic cells. These peaks together with the sextet pattern observed between the 2Θ angles 3-6, are characteristic for a cubic mesoporous MCM-48 structure.

The observed product reflections show some decrease in the relative intensity and a notable shift to higher 2Θ values compared to the parent samples.[107] These changes result from the

contraction of the unit cell, due to acylperrhenate immobilization on the channels of the molecular sieves. However, the XRD patterns clearly indicate that the structures of the mesoporous materials remain intact throughout the grafting procedure. The modified mesoporous materials contain between 1 - 6 wt.% Re according to the elemental analyses.

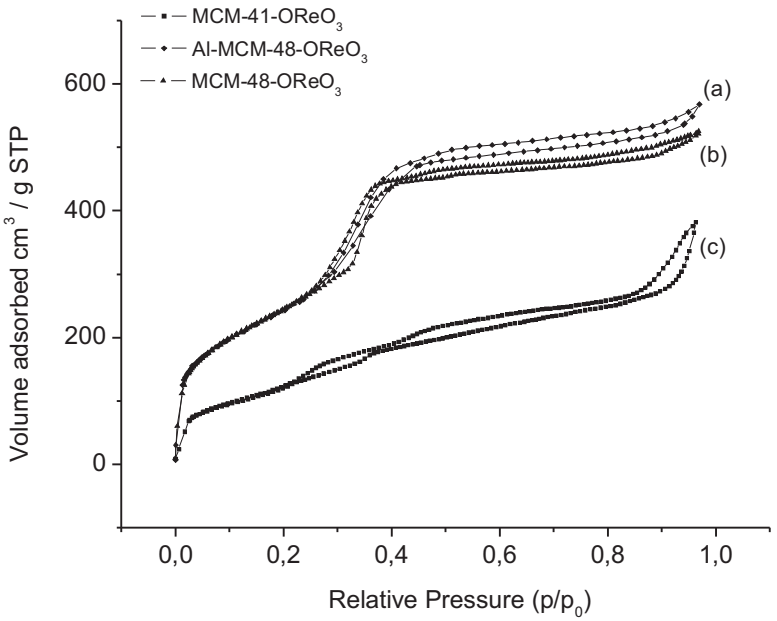

Figure 3.3. N_2 adsorption/desorptions isotherms of (a) Al-MCM-48-$OReO_3$ (b) MCM-48-$OReO_3$ (c) MCM-41-$OReO_3$

The low temperature N_2 adsorption/desorption isotherms of parent MCM-41 and MCM-48 are of type (IV) according to the IUPAC nomenclature[108] and characteristic for mesoporous solids. A well-defined sharp inflection is observed between the relative pressure ($p/p0$) of 0.3-0.4 due to capillary condensation of nitrogen inside the primary mesoporous channels of the molecular sieves. The calculated textural parameters using XRD and adsorption/desorption isotherms are summarized in Table 3.1. All grafted samples show a decrease in the unit cell value, surface area and the pore volume. This is probably due to the grafting of the acylperrhenate complex on the internal surfaces of the mesoporous materials. The TEM images (Figure 3.4) of the grafted samples show a high uniformity in pore size, providing strong evidence that the mesoporous structures retain long range ordering[104,105] through out the grafting process and the channels remain accessible. A representative electron diffraction pattern of the (1 0 0) and (1 1 0) planes supports further the long range ordering of the grafted samples.

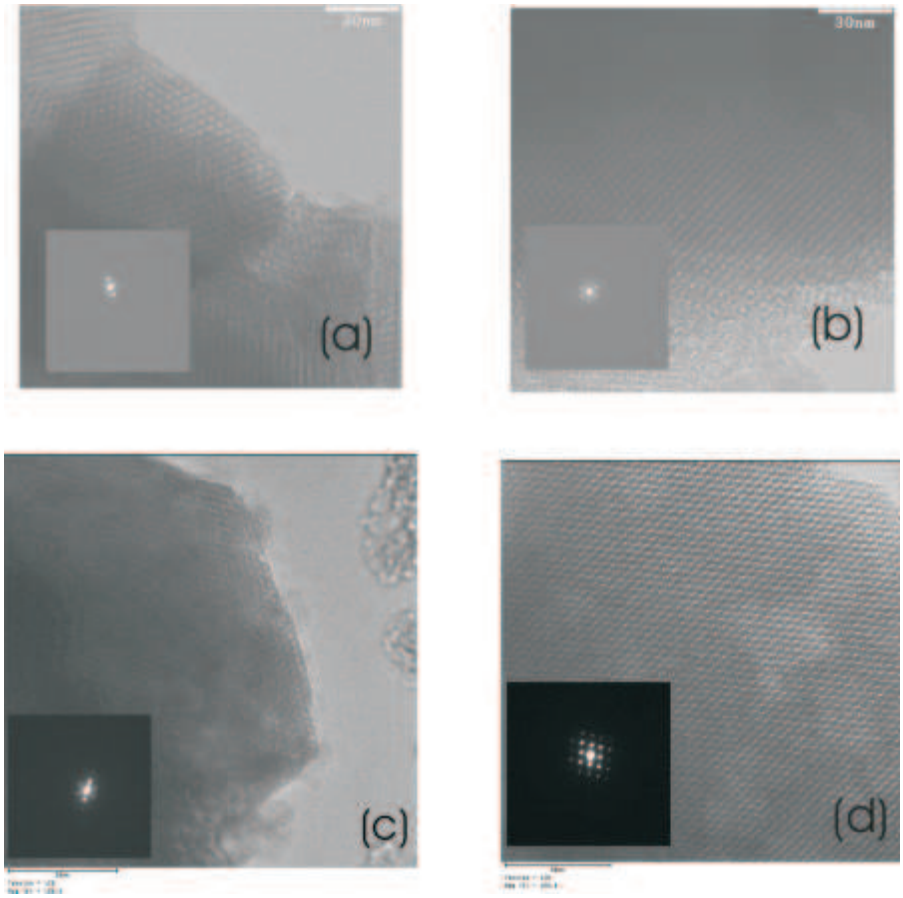

Figure 3.4. Transmission electron micrograph images of (a) Al-MCM-41-$OReO_3$ (b) Al-MCM-48-$OReO_3$ (c) MCM-41-$OReO_3$ and (d) MCM-48-$OReO_3$

The FT-IR spectra of parent Al-MCM-41/Al-MCM-48 and the grafted samples are depicted in Figure 3.5. The bands at 3500 cm^{-1}; 960 cm^{-1}, 1080 cm^{-1} and 800 cm^{-1} are attributed to stretching vibration of the surface (Si-OH, Si-O-Re, Si-O-Si and Si-O-Si).[109] The peak broadening between 930 and 970 cm^{-1} is an indication for the existence of the trioxo rhenium species, its asymmetric stretching vibration $[Re{=}O]_{vs}$ appearing usually at 920 - 960 cm^{-1}.[45,55,31] The symmetric stretching vibration $[Re{=}O]_{w}$ that should be detectable around 980 cm^{-1}[45,55,31] is,unfortunately, masked by the strong [Si-O-Si] vibration of the carrier material in this region.

3.2.1. A model of the grafting process

The determination of the exact nature of the catalyst-precursor grafted on MCM-41 and MCM-48 proved to be quite difficult. In order to confirm the possible grafting mode of acylperrhenate and to develop an idea how the structure of the grafted complex may look like, a similar reaction

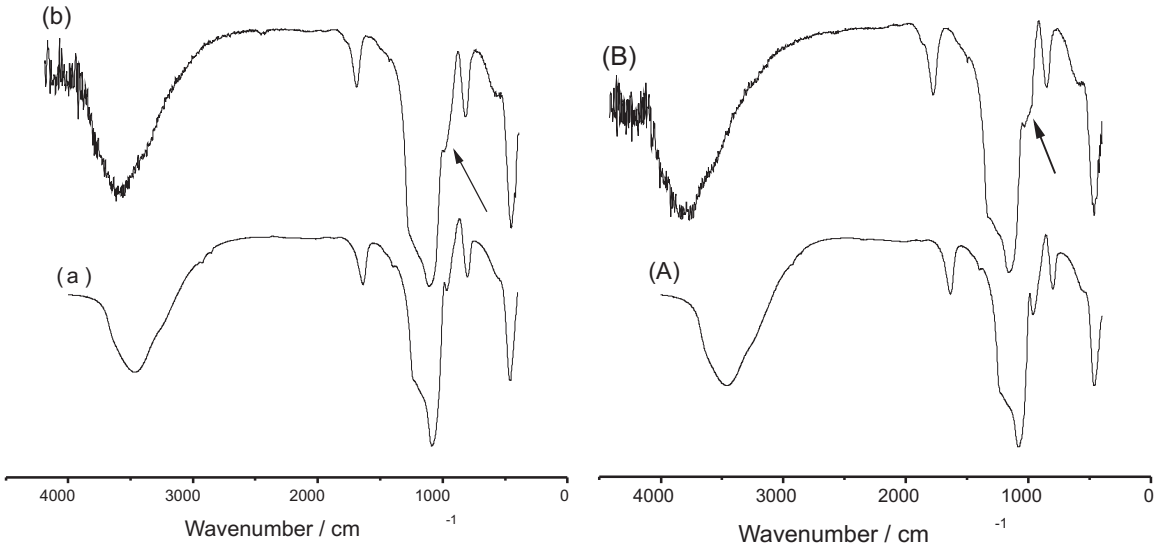

Figure 3.5. FT-IR spectra of (a) Al-MCM-41, (b) Al-MCM-41-$OReO_3$, (A) Al-MCM-48, (B) Al-MCM-48-$OReO_3$.

in liquid phase by using trimethylsilanol as a model for the surface was performed (Scheme 3.1). This liquid phase reaction proceeding under the same conditions as the grafting process was monitored by ^{1}H-NMR.

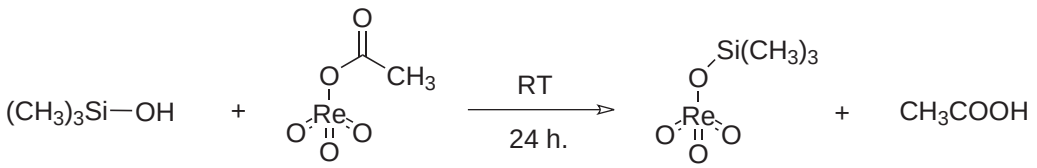

Scheme 3.1. Trimethylsilyl perrhenate synthesis from trimethylsilanol and acylperrhenate

It can be clearly seen that the peak at 0.099 ppm (9H, $(CH_3)_3Si$) originating from the trimethylsilanol moiety decreases in intensity and a new peak at 0.483 ppm, representative for trimethylsilyl perrhenate is formed. After crystallization, colorless crystals are isolated. The analytical and spectroscopic results (^{1}H-NMR, ^{13}C-NMR, elemental analysis) are identical with the literature data of trimethylsilyl perrhenate.[44,110] (Figure 3.6).

This reaction proofed once again that the [Si-O-Re] moiety can be formed under the reaction conditions applied, and accordingly, the formation of similar, [$\equiv SiOReO_3$] species, on the surface should be expected.

3.2.2. Catalytic applications

The grafted samples are applied for olefin epoxidation with cyclooctene being the substrate

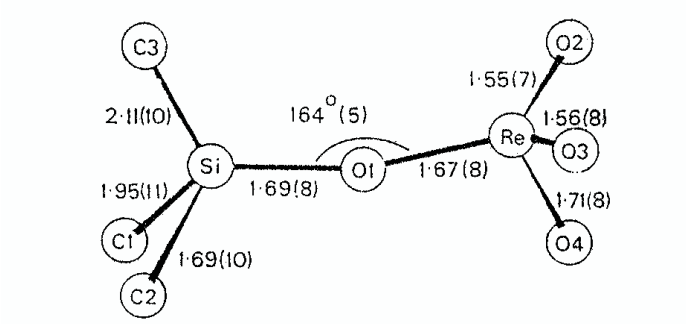

Figure 3.6. The molecular structure of trimethylsilyl perrhenate[111]

Table 3.2: Cycloocten oxidation with peroxorhenium catalyst grafted on mesoporous materials

Sample	Time				TOF h^{-1}
	4h		24h		
	Conversion %	Selectivity %	Conversion %	Selectivity %	
MCM-41-$OReO_3$	46	100	82	84	63
MCM-48-$OReO_3$	45	94	86	72	86
Al-MCM-41-$OReO_3$	20	79	59	73	37
Al-MCM-48-$OReO_3$	34	90	70	73	51

and H_2O_2 as the oxidizing agent. The results are summarized in Table 3.2, and the kinetic curves of the same catalysis with all catalysts are shown in Figure 3.7. In all the cases the initial activity is high (see Table 3.2 and Figure 3.7) and slows down as the reaction proceeds, which is due to the consumption of substrate and possibly enhanced by the formation of H_2O as a by-product thus lowering the concentration of the catalytic active species by partial hydrolytic decomposition.[112] When using a 30 % H_2O_2 solution in water as oxidizing agent for conducting the olefin epoxidation (Table 3.2) no reaction could be observed. This observation supports the assumption of negative effects of the formed water on the catalyst.

Further more, the catalysts grafted on surfaces without aluminium show much higher reactivity (82 % conversion after 24 h, for MCM-41-$OReO_3$ and 86 % for MCM-48-$OReO_3$) than the catalysts on surfaces containing aluminium (59 % conversion after 24 h., for Al-MCM-41-$OReO_3$ and 70 % for Al-MCM-48-$OReO_3$). A probable cause for this behavior is the stronger electron donating capability of the aluminium containing surfaces, which reduces the Lewis

Table 3.3: Recycling experiments with MCM-41-$OReO_3$ as a catalyst, and different oxidizingagents

Catalyst	Oxidazing agent	Time			
		4h		24h	
		Conversion %	Selectivity %	Conversion %	Selectivity %
MCM-41-$OReO_3$	H_2O_2 in H_2O	0	0	0	0
	H_2O_2 in EtOAc	41	86	78	77
	Second run	20	84	39	78
	Third run	6	88	19	74
	TBHP [a]	13	87	19	86
	Second run	2	61	15	62
	Third run	3	57	10	40

[a] 5-6 M Solution in decane, used as purchased from Sigma-Aldrich

acidity of the metal center followed by a reduction of its catalytic activity.

In order to examine the extent of leaching, the catalytic reaction is interrupted after a conversion of 50 % is reached. The solution is filtrated off and the filtrate is examined for its remaining catalytic activity. The filtrate obtained from a catalyst on a MCM-41 - type of surface (hexagonal structure) is negligible (< 2 %). On a contrary, the filtrate originating from the catalyst immobilized on a MCM-48 surfaces (cubic structure) shows relatively high activity (15 %) originating clearly from a catalytically active species present in the solution as a result of a more pronounced leaching during the reaction. The three dimensional pore-structures of the late surfaces render the active sites obviously more sensitive, resulting in a higher extent of leaching.

Recycling experiments have been carried out with MCM-41-$OReO_3$, as the most active and the most stable catalyst, under the conditions applied. After the reaction the catalyst was filtered, washed with dichloromethane, dried under vacuum and reused under the same reaction conditions as previously applied. The catalytic activity decreases somewhat in each step of this process, as can be seen in Table 3.3, the selectivity, however is largely maintained. These results indicate that the active species on the silica surface is continuously destroyed during

the catalytic reaction. A possibility for this occurrence is the formation of water, as a by-product of the epoxidation, that could partially coordinate to the catalytic active species on the surface and results in activity loss. Such reaction, however, is not necessarily accompanied by a concomitant leaching.

In order to minimize the water influence in this experiments the epoxidation reactions were attempted additionally with TBHP as oxidizing agent. TBHP lowers the reactivity of this catalytic system considerably, but it improves its recycling ability to a certain degree. The lower initial activity in the second and the third run of the recycling experiments might indicate that as the reaction proceeds, organic molecules, like *tert*-buthanol (^{t}BuOH), epoxide and TBHP are absorbed on the silica surface hindering the diffusion to, and away from the catalytically active centers. As a result a notable decrease of the initial activity of the catalyst can be observed. Furthermore, the selectivity losses are more pronounced than in the presence of H_2O_2 being the oxidant.

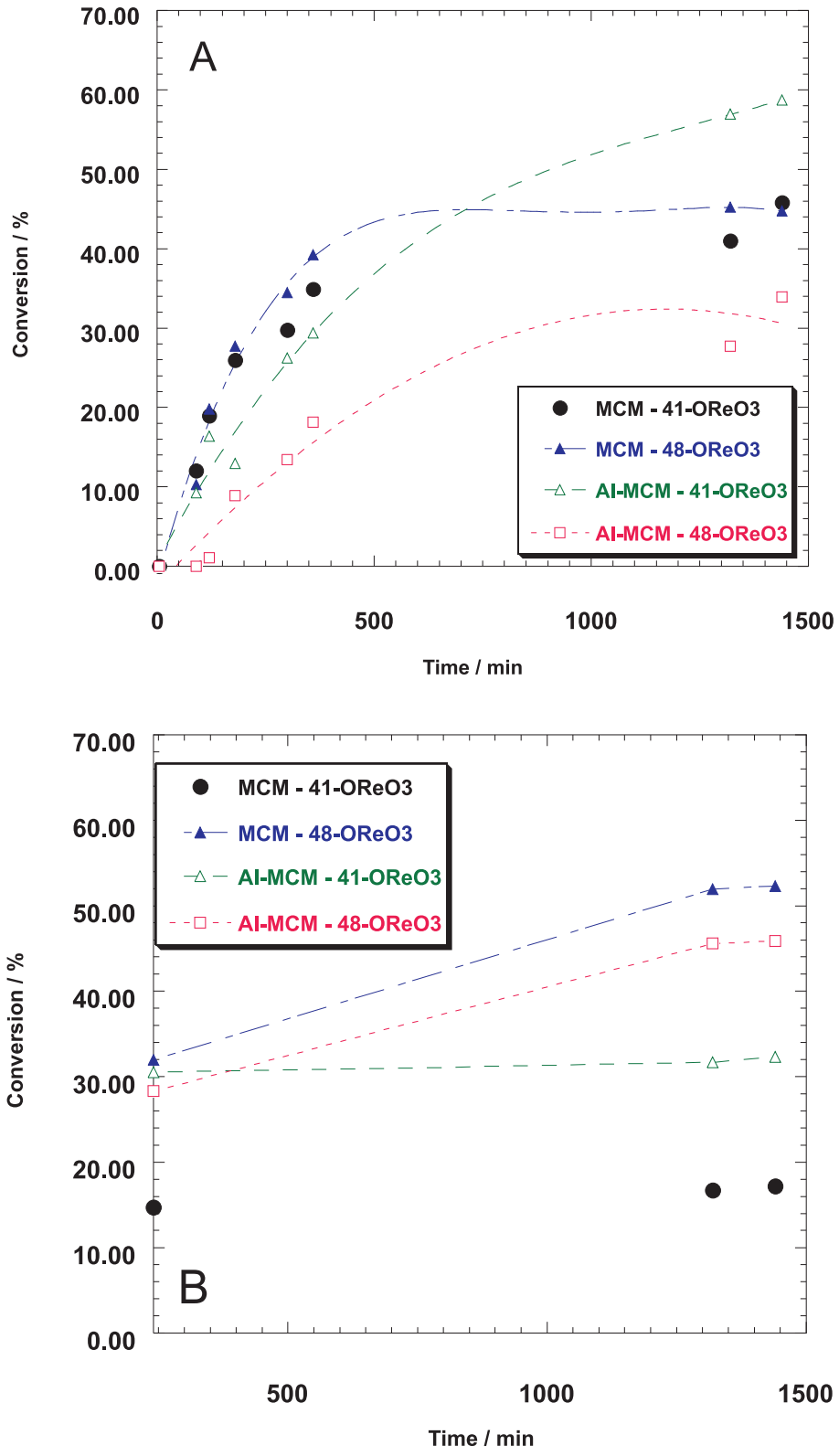

Figure 3.7. (A) Epoxidation of cycloocten over various catalysts and (B) leaching test over various catalysts. (Reaction conditions: 7 mmol Cyclooctene, 7 mmol hydrogen peroxide (23.8 ethyl acetate), 0.014 mmol catalyst and 1 g mesitylene (GC-Standard). Reaction temperature is 323 K). The TOF was determined after 90 min. for each catalyst

4. Kinetic studies on the oxidation of $CpMoCH_3(CO)_3$ with TBHP

Between 2004 and 2006, A. Sakthivel and J. Zhao from the group of Prof. Kühn at the Technische Universität München, successfully grafted various Molybdenum carbonyls on mesoporouse silica materials. Two different immobilization procedures were applied, both presented in Scheme 4.1 and Scheme 4.2. The first one, involved a direct grafting on the carrier materials mostly by exchanging a ligand with a silanol group of the surface. The $CpMo(CO)_3Cl$ was successfully grafted on MCM-41, MCM-48 and SBA-15 surfaces using this direct grafting method, by a reaction of the chloro ligand with the hydroxyl group of the surface.[113]

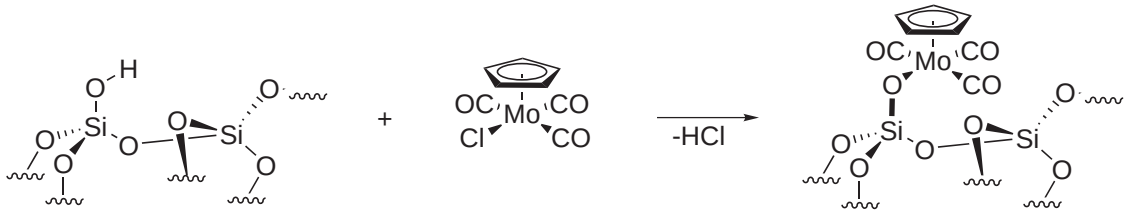

Scheme 4.1. Direct grafting of $CpMo(CO)_3Cl$ on silica.[113a, b]

The second method applied, was the covalent attachment of the coordination complexes to the mesoporouse materials via a spacer ligand. These spacers, linked to the metal itself or to the Cp-ligand, contained a siloxane groups, which reacted in a condensation reaction with the surface silanols, attaching the complex to the surface moiety.[92,114] Several examples of this grafting methodic are given in Scheme 4.2.

Applying these materials as heterogeneous catalysts in the epoxidation of olefins, it was soon discovered that their activity drastically changed by making only small changes to the metal center itself. Even more surprising, was the change in reactivity of the same materials synthesized by two different procedures, behaviour observed with $CpMo(CO)_3{-}(CH_2)_3{-}Si(OCH_3)_3$ grafted

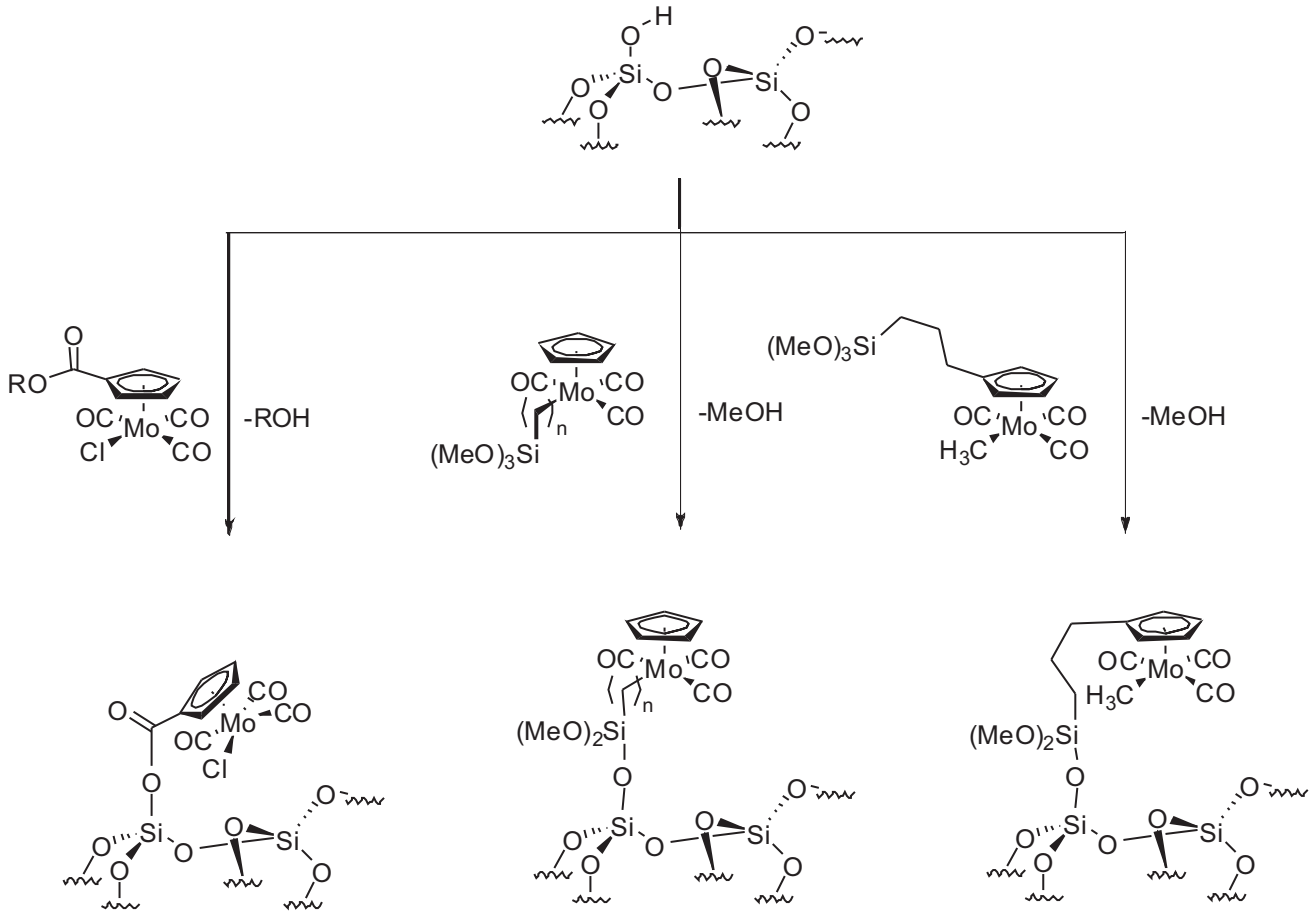

Scheme 4.2. Covalent attachment of $CpMo(CO)_3Cl$ and $CpMo(CO)_3CH_3$ on silica using a siloxane containing spacer[92]

on MCM-41 surfaces.[69] Trying to explain these phenomena, was soon proofed impossible, due to the lack of understanding of the catalyst formation and the catalytic cycle itself.

In order to explain the catalytic behaviour of these, and similar Molybdenum based systems, kinetic and DFT studies were initiated, using the $CpMo(CO)_3CH_3$ as a representative of this compound class. The title compound, $CpMo(CO)_3CH_3$ was synthesized and purified using a slightly modified literature method.[115,92] When treated with a TBHP excess of at least three equivalents in dichloromethane, the Mo(VI)oxo-peroxo complex is formed and can be isolated in good yields.

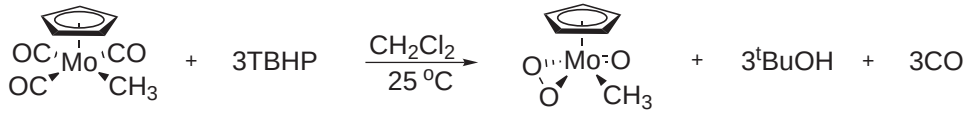

Scheme 4.3. Synthesis of Mo(VI)oxo-peroxo compound

The Mo(VI)oxo-peroxo compound was fully characterized by UV-vis, IR and NMR spectroscopy, and the structure was determined by single crystal X-ray diffraction. The single crystal X-ray crystallographic analysis reveals that its solid-state molecular structure displays a slightly distorted "three-legged piano stool" conformation, in which the midpoint of the peroxo ligand is one of the legs of the piano stool. Two other structurally characterized Mo oxo-peroxo compounds and three W(VI)-oxoperoxo compounds of composition $CpW(O_2)O(CH_2Si(CH_3)_3)$ and $Cp^{\star}WO(O_2)Cl$ have a similar structural arrangement according to the literature.[87,90,82,85]

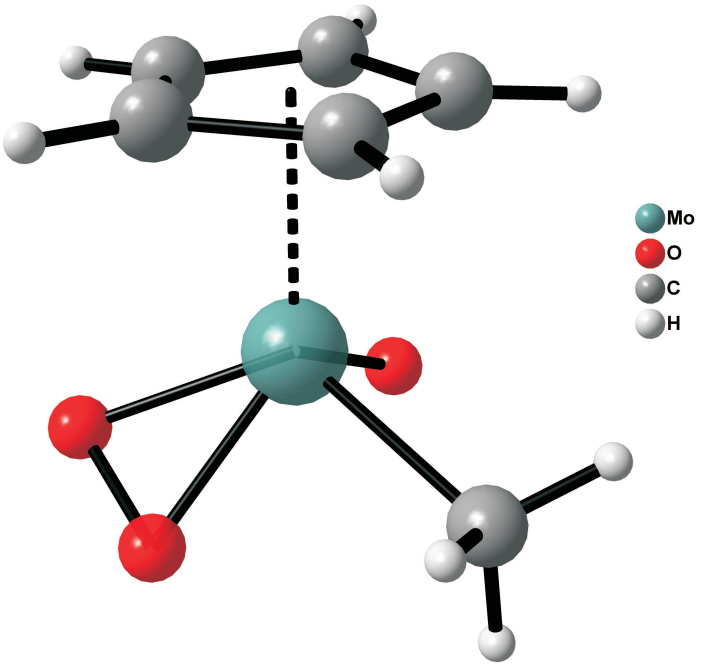

Figure 4.1. Ball and stick model of compound $CpMo(O_2)OCH_3$ in the solid state

The reaction of $CpMo(CO)_3CH_3$ with TBHP, carried out in dry $CDCl_3$ and dry CH_2Cl_2 at room temperature, was followed by NMR and UV-vis spectroscopic techniques, respectively. The changes in the chemical shifts of the cyclopentadienyl (Cp) ligand and/or the methyl protons in the NMR spectra were particularly informative. When 0.06 mol of $CpMo(CO)_3CH_3$ and 10 equivalents of TBHP were mixed in 0.5 ml $CDCl_3$, the reaction started immediately. The signal of the carbonyl compound at 5.27 ppm decreased with time and a new signal at 6.33 ppm appeared. The area of this new signal reached a maximum after 15 min whereas the carbonyl compound peak was reduced to around 60% of its original size. The reduction of the signal at 6.33 ppm that followed, was associated with the build up of a new signal at 6.29

ppm. After 2 hours, the Cp signal of the carbonyl compound and the Cp signal at 6.33 ppm disappeared completely and only the signal at 6.29 ppm remained. The signal intensity-time curves are shown in Figure 4.2A. The ^{95}Mo-NMR examination showed similar results. After 2 h the ^{95}Mo signal of $CpMo(CO)_3CH_3$ at -1424 ppm vanished completely, and a new peak at -609 ppm, which was assigned to the complex $CpMo(O_2)OCH_3$ was the only one observed.[68]

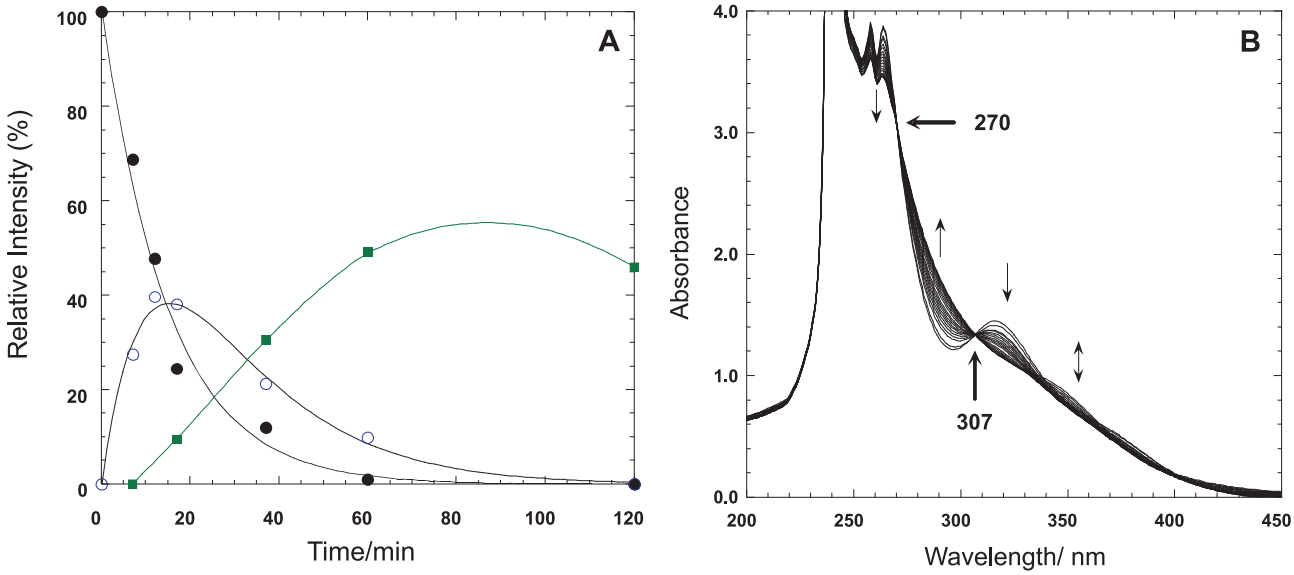

Figure 4.2. (A) The changes in the relative peak intensities with time of $CpMo(CO_3)CH_3$(•)(at δ= 5.27 ppm), and its products $CpMoO_2CH_3$ (○)(at δ= 6.33 ppm) and $CpMo(O_2)OCH_3$(at δ=6.29 ppm) during the reaction of $CpMo(CO_3)CH_3$ (0.06 mmol) with 10 eq. of TBHP in $CDCl_3$, at 20 °C (B) UV-vis spectral changes (at 6 min intervals for the first 1 hour and then every 10 min) for the reaction of $CpMo(CO_3)CH_3$ (0.33 mM) with TBHP (10 eq.) in CH_2Cl_2 at 20 °C

An experiment was designed to examine the intermediate (at 6.33 ppm), which is usually formed shortly after mixing TBHP with the carbonyl compound and later disappears. The above reaction was repeated and quenched after 15 min by adding MnO_2. The filtrate was evaporated to dryness and extracted with diethyl ether to give a yellow solid. This product was subsequently analyzed by ^{1}H and ^{95}Mo - NMR spectroscopy. The ^{1}H-NMR showed a signal at 6.33 ppm and a signal at 1.45 ppm with 5:3 relative intensities, respectively. The ^{95}Mo-NMR showed one signal at -346 ppm. A similar reaction profile was obtained when the reaction was carried out in C_6D_6 under the same conditions and the chemical shifts match with the NMR data known for the dioxo-Mo(VI) compound, $CpMoO_2CH_3$.[81] These results suggest that the formation of $CpMo(O_2)OCH_3$ from the reaction of the carbonyl compound with TBHP proceeds via compound $CpMoO_2CH_3$ as shown in Scheme 4.4.

The yield of the final, peroxo, product in the NMR experiments described above is less

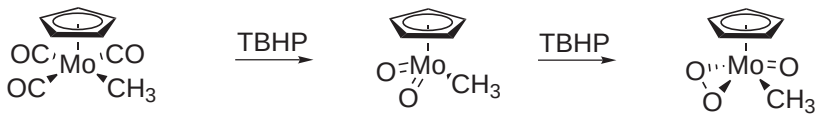

Scheme 4.4. Proposed reaction pathway for the oxidation of compound $CpMo(CO)_3CH_3$

than 60% (with respect to the carbonyl edukt), due to a side reaction which forms a highly insoluble precipitate. The later was isolated as a blue solid, containing 42.3 % Mo, 18.7 % C and 2.9 % of H. Further characterization attempts were unsuccessfully due to its insolubility in all available solvents. The blue solid could not be re-dissolved even after adding excess of TBHP, an attribute known for decomposition products of $Cp^{\star}MoO_2Cl$.[90] However, this side product has been tested as a catalyst in epoxidation reactions, and was found to be completely inactive, even after prolonged reaction times. The yield of $CpMo(O_2)OCH_3$ can be increased by increasing the TBHP : $CpMo(CO)_3CH_3$ ratio, suggesting that the major reaction pathway, which leads to the relatively stable product $CpMo(O_2)OCH_3$ is favored. The side reaction pathway is totally suppressed with addition of substrate in the catalytic reaction.

The reaction progress was also followed by UV-vis spectroscopy with different concentrations and catalyst/TBHP ratios in CH_2Cl_2. $CpMo(CO)_3CH_3$ has strong absorptions at λ_{max} = 256, 267 and 316 nm, and a shoulder peak at λ_{max} = 370 nm. When the carbonyl complex (0.33 mM) is treated with a 10-fold excess of TBHP at 25 °C, the absorbance at 316 nm decreases with time and the absorbance in the range 207 - 270 nm increases to give two clear isosbestic points at 307 and 270 nm (Figure 4.2B). These changes in absorbance are due to the formation of complex $CpMoO_2CH_3$. The reaction of $CpMo(O_2)CH_3$ with TBHP proceeds leading to an additional absorbance decrease in the range 307 - 335 nm and a slight increase in the absorbance in the range 335 - 400 nm, due to the formation of $CpMo(O_2)OCH_3$. However, the isosbestic points due to this change are not very clear. A possible explanation, based on further experimental evidence is given in the next subchapter. It is worth mentioning, however, that under UV experimental conditions no precipitate was observed, possible due to the higher TBHP excess that may decrease catalyst decomposition or side reaction.

The intensity-time curves and the changes in the UV-absorbance with time were used to determine the rate constants for the oxidation of the carbonyl compound with TBHP to yield $CpMoO_2CH_3$, and the formation of the oxo-peroxo compound in the following reaction. In the presence of excess TBHP, the reactions follow pseudo-first-order kinetics, and the decrease in

the intensity of the signal at 5.27 ppm (Cp protons of the carbonyl compound) with time fits to a first-order exponential decay equation ($I_t = I_\infty + I_0 - I_\infty exp(-k_\psi t)$). The value of the observed-first-order rate constant was obtained from this fitting to be $k_\psi = (1.12 \pm 0.15) \cdot 10^{-3} s^{-1}$. This indicates that the reaction is first-order with respect to the concentration of the carbonyl. The build up and the decay of the signal intensity at 6.33 ppm (Cp protons of $CpMoO_2CH_3$) was fitted to a biexponential (build up and decay) equation to determine the pseudo-first-order constants for the formation of $CpMoO_2CH_3$, ($k_f = (1.25 \pm 0.35) \cdot 10^{-3} s^{-1}$) and for its reaction with TBHP ($k_r = (8.5 \pm 0.3) \cdot 10^{-4} s^{-1}$). The rate constant k_f is also valid for the reaction of the carbonyl compound with TBHP and is in accord with the value obtained above from the time-dependent decrease of the carbonyl signal. Previous studies on similar (cyclopentadienyl)-tricarbonyl-molybdenum(II) compounds, such as the chloro derivative, indicated that the Mo-dioxo moiety is rapidly formed and reacts more slowly with the peroxide to yield the final Mo-oxoperoxo product.[87,82,81,85] From the results obtained here, it appears that the presence of a methyl group instead of a chloro ligand does not affect the initial oxidation rate from Mo(II) to Mo(VI) much. However, it enhances significantly the displacement rate of the oxo with the peroxo group on the Mo(VI) center. This may also influence further reactions between $CpMo(O_2)OCH_3$ and TBHP, thus explaining the observed catalytic activity of $CpMo(O_2)OCH_3$, a behavior which has not been previously reported for similar CpMo(VI)-oxoperoxo derivatives with a Cl ligand.[87]

4.1. Reaction of $CpMo(O_2)OCH_3$ with TBHP

When $CpMo(O_2)OCH_3$ reacts with a large excess of TBHP (>100 eq) in the absence of an olefin, a slight change of its UV-vis spectra occurs. After mixing a 0.3 mM solution of $CpMo(O_2)OCH_3$ in CH_2Cl_2 with 0.015 mmol TBHP at room temperature, the absorbance at 335 nm decreases exponentially with time, and levels off after $\sim$ 20 min. By adding more TBHP, the absorbance decreases further but never becomes zero even with very high TBHP excess ($\sim$ 1500 eq), as shown in Figure 4.3. This must be due to the formation of an intermediate (**I**) which exists in equilibrium with $CpMo(O_2)OCH_3$.

The equilibrium constant and the extinction coefficient of the intermediate were determined from the variation of the final absorbance with [TBHP] using Equation Eq.4.6 derived as follows:

$$A_{335} = A_p + A_I = \varepsilon_p[peroxo] + \varepsilon_I[I] \tag{4.1}$$

where A_p and A_I are the absorbance of the $CpMo(O_2)OCH_3$ complex and the intermediate (**I**), and ε_p and ε_I are their extinction coefficients, respectively.

With the total mass balance expression, $[Mo]_T = [peroxo] + [I]$, Eq.4.1 can be written as fellow:

$$A_{335} = (\varepsilon_p - \varepsilon_I)[peroxo] + \varepsilon_I[Mo]_T \tag{4.2}$$

Using the equilibrium expression:

$$K_{eq} = \frac{[I]}{[TBHP][peroxo]} = \frac{[Mo]_T - [peroxo]}{[TBHP][peroxo]} \tag{4.3}$$

and therefore,

$$[peroxo] = \frac{[Mo]_T}{1 + K_{eq}[TBHP]} \tag{4.4}$$

Replacing $[peroxo]$ in Eq. 4.2 by using Eq. 4.4

$$A_{335} = \frac{\varepsilon_p - \varepsilon_I[Mo]_T}{1 + K_{eq}[TBHP]} + \varepsilon_I[Mo]_T \tag{4.5}$$

and

$$\frac{A_{335}}{[Mo]_t} = \varepsilon_I + \frac{(\varepsilon_p - \varepsilon_I)}{1 + K_{eq}[TBHP]} \tag{4.6}$$

A plot of $A_{335}/[Mo]_T$ against [TBHP] is shown as an inset in Figure 4.3. The data were fitted to equation 4.6, and the values of $K_{eq}(= 1.23 \pm 0.49)$ and $\varepsilon_I(= 748 \pm 430 M^{-1}cm^{-1})$ were determined.

The absorbance-time curves in Figure 4.3 are exponential, and fit to a 1st-order exponential equation,$A_t = A_\infty + A_0 - A_\infty exp(-k_\psi t)$, to determine the values of k_ψ at each [TBHP]. The observed-first-order rate constants (k_ψ) vary linearly with [TBHP] in a relatively large intercept (Figure 4.4).

Since the reaction between TBHP and $CpMo(O_2)OCH_3$ is reversible, the observed-rate con-

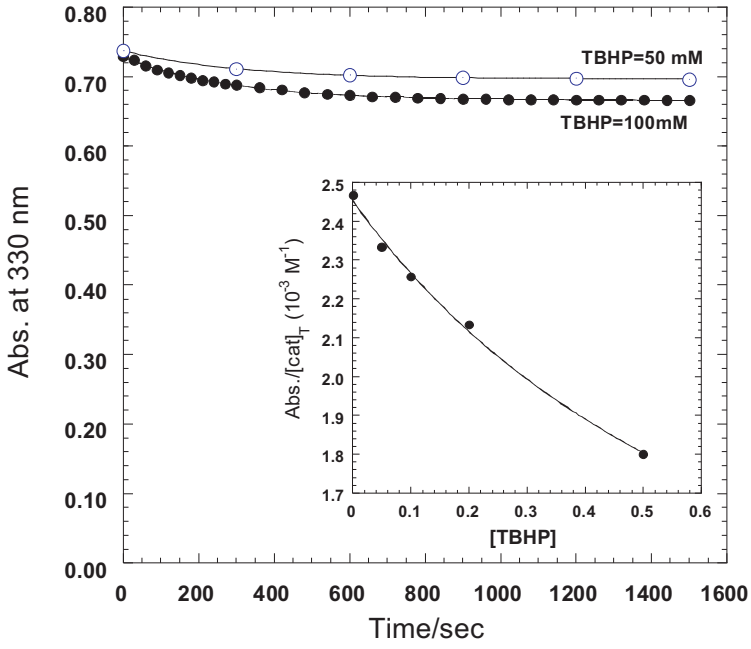

Figure 4.3. Changes in absorbance with time at 330 nm for the reaction of $CpMo(O_2)OCH_3$ with TBHPin CH_2Cl_2 at 20 °C. The inset shows a plot of $\frac{A_{335}}{[Mo]_t}$ against [TBHP], the solid line represents the calculated values with based on Eg. 4.6 with K_{eq}=1.23, ε_I=748 $M^{-1}cm^{-1}$ and ε_p= 2460 $M^{-1}cm^{-1}$

stant is the sum of the forward and the reverse rate constant. With TBHP being present in large excess over the catalyst, the observed-rate constant can be expressed as:

$$k_\psi = k_p[TBHP] + k_{-p} \tag{4.7}$$

Therefore, the intercept of the straight line represents the value of the reverse rate constant ($k_{-p} = 0.0032 \pm 0.0002 s^{-1}$), and the slope expresses the forward rate constant ($k_p = 0.0047 \pm 0.0003 M^{-1}s^{-1}$). The value of the equilibrium constant ($K_{eq} = 1.47 \pm 0.36$) calculated from these kinetic data agrees with the value ($K_{eq} = 1.23$) obtained from Eq. 4.6 within the experimental error range of these measurements. After the equilibrium is established, a slow decrease in the absorbance continues with time, probably due to the decomposition of the catalytic system, which is usually observed in the absence of the olefin, and increases with the TBHP concentration and the solvent polarity.

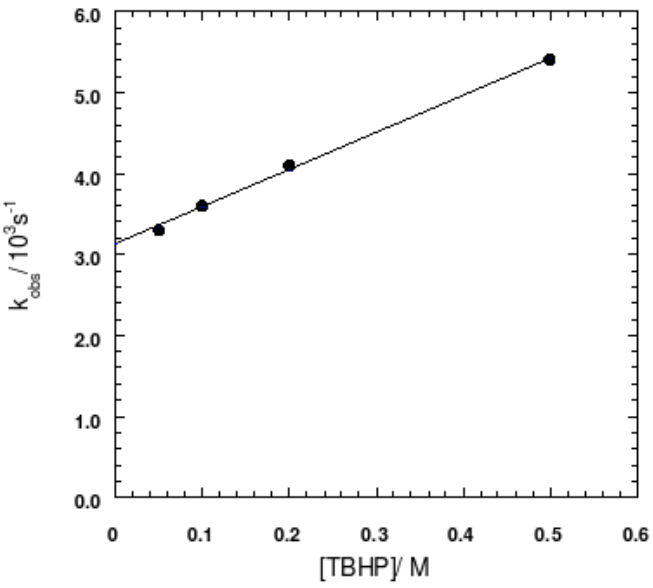

Figure 4.4. A plot of the observed-first-order rate constant (k_{abs}) against [TBHP] for the reaction of $CpMo(O_2)OCH_3$ (0.3 mM) with TBHP in CH_2Cl_2 at 20°C

4.2. Catalytic epoxidation

4.2.1. Epoxidation catalyzed by $CpMo(CO)_3CH_3$

Since the olefin does not react with TBHP without the catalyst being present, no corrections were needed for the uncatalyzed process. In the presence of an olefin, the epoxide is formed and the conversion to the epoxide proceeds to completion.Figure 4.5 shows the formation of cyclooctene oxide with time in an NMR experiment initially started with $CpMo(CO)_3CH_3$ (0.05 mol), TBHP (0.6 mol) and cyclooctene (0.44 mol) and carried out in $CDCl_3$ at 20 °C. When TBHP was added last to a mixture of the catalyst and the olefin, the epoxide appears slowly in the first 10 minutes of the reaction. The rate then increases and becomes linear in the next 20 minutes, and the build up continues exponentially.

This kinetic behavior is typical for a catalytic reaction where the catalyst precursor initially reacts with the oxidant to produce the active species in rates slower or similar to the rate of the reaction of the active species with the substrate. In addition, the reaction rate in the later stages of the reaction becomes slower, indicating that the catalyst is partially deactivated, decomposing or forming less active species.

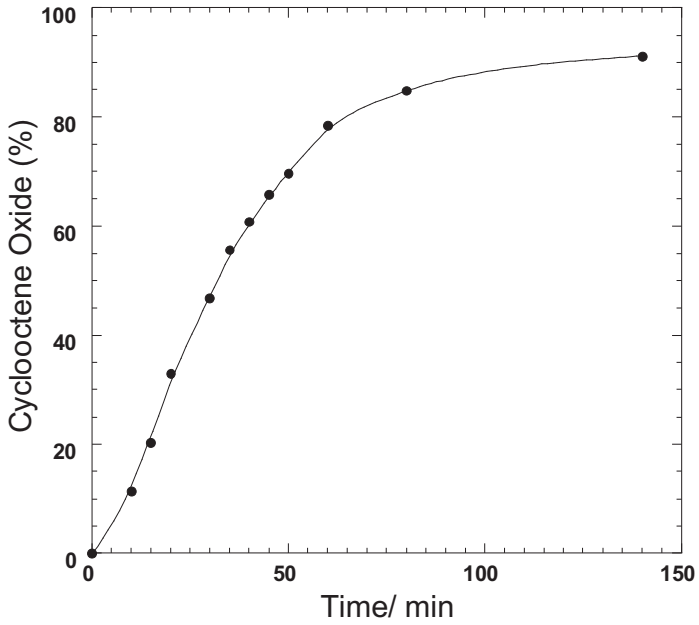

Figure 4.5. Yield of cyclooctene oxide against time. The reaction was carried out using 0.44 mol cyclooctene, 0.6 mol TBHP and 0.05 mol $CpMo(CO_3)CH_3$ in $CDCl_3$ at 20 °C

In this catalytic system, $CpMo(CO)_3CH_3$ reacts with TBHP to form $CpMoO_2CH_3$ and $CpMo(O_2)OCH_3$. One or both of them could be the active species, directly epoxidizing the olefin or acting as catalysts to activate TBHP toward epoxidation. To examine each Mo species separately, $CpMoO_2CH_3$ and $CpMo(O_2)OCH_3$ were isolated or prepared under controlled conditions *insitu* and their catalytic activities were investigated with different substrates (cyclooctene, β-methylstyrene and β-methoxystyrene).

In the absence of TBHP, both Mo(VI) species are inactive toward the epoxidation of cyclooctene and β-methoxystyrene at room temperature. However, when excess TBHP is added, the catalytic reaction proceeds. The epoxidation of cyclooctene and β-methylstyrene leads to the corresponding epoxides only, whereas the oxidation of β-methoxystyrene produces benzaldehyde. Similar behavior was observed for the oxidation of β-methoxystyrene with Re(VII)-peroxo species as a catalyst. The reaction initially produces the epoxide, which is not stable due to the electron donating ability of the methoxy group, and undergoes C-C bond cleavage leading to benzaldehyde as the final product.[56]

A general pathway (Scheme 4.5) for this catalytic reaction can thus be proposed, involving three Mo species: the carbonyl, the dioxo, and the oxo-peroxo complexes. Kinetically, it is

possible to investigate the proposed pathways by studying each species separately.

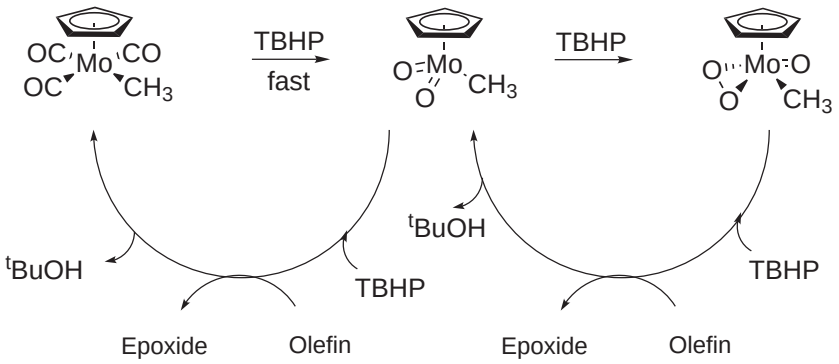

Scheme 4.5. General reaction scheme for the oxidation of $CpMo(CO)_3CH_3$ by TBHP, and the epoxidation activity of the oxidation products, $CpMoO_2CH_3$ and $CpMo(O_2)OCH_3$

4.2.2. Epoxidation catalyzed by $CpMo(O_2)OCH_3$

Compound $CpMo(O_2)OCH_3$ was found to catalyze the epoxidation of cyclooctene and styrene with TBHP as oxidizing agent at room temperature. Figure 4.6 shows the change in the absorbance with time at 265 nm due to the epoxidation of β-methoxystyrene by the TBHP/ $CpMo(O_2)OCH_3$ system. In the absence of TBHP, the olefin is not oxidized, nor does it react in any form with $CpMo(O_2)OCH_3$ (when $CpMo(O_2)OCH_3$ was mixed with cyclooctene or β-methoxystyrene no changes were observed by NMR and UV spectroscopy). However, as discussed above, UV experiments show that $CpMo(O_2)OCH_3$ reacts with TBHP in the absence of olefin. This suggests that the epoxidation of the olefin is carried out by an active intermediate **I**, which is formed by the reaction of $CpMo(O_2)OCH_3$ with TBHP (Scheme 4.6).

Although homolytic and heterolytic activation of peroxides by metal catalysts are possible, activation of TBHP by a homolytic cleavage of the O-O bond (which would generate reactive radicals, such as $RO^{\cdot}$ or $HO^{\cdot}$) does not occur due to the reaction insensitivity against oxygen. Also, the olefin reactivity, which was found to increase with the olefin nucleophilicity rather than with the radical stability, does not support a radical mechanism. Furthermore, radical mechanisms have not been proposed by the previous studies on epoxidations catalyzed by similar Mo compounds.[87,102,116,97] Therefore, the reactive intermediate (**I**), in equilibrium with the catalyst, should transfer an O-atom to the olefin to form the epoxide and regenerate the catalyst (Scheme 4.6).

During the catalytic reaction, the concentration of **I** can be defined by either a steady-state

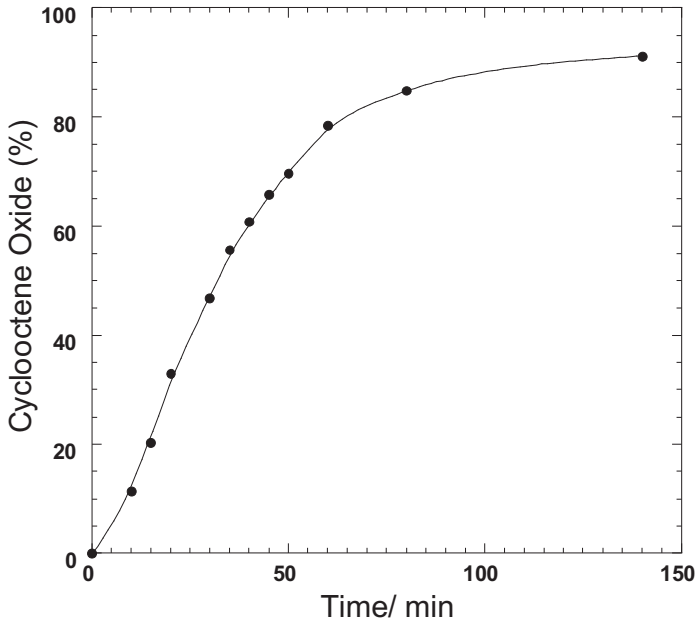

Figure 4.6. The absorbance-time curve at 265 nm for the oxidation of β-methoxystyrene (0.1 mM) with TBHP (10 mM) catalyzed by $CpMo(O_2)OCH_3$ (0.4 mM) in CH_2Cl_2 at 20 °C

approximation or a pre-equilibrium condition. The epoxidation rate according to Scheme 4.6 is expressed by Eq. 4.8:

$$rate = \frac{-d[alkene]}{dt} = k_{ep}[alkene][I] \tag{4.8}$$

If the rate equation is derived by means of a steady-state approximation for [**I**], $\frac{d[I]}{dt} = 0$, and with the mass balance expression, $[Mo]_T = [peroxo] + [I]$, than the change in the intermediate described with Eq. 4.9

$$\frac{d[I]}{dt} = k_p[peroxo][TBHP] - k_{-p}[I] - k_{ep}[alkene][I] \tag{4.9}$$

transforms in

$$[I]_{SS} = \frac{k_p[TBHP][Mo]_T}{k_{-p} + k_p[TBHP] + k_{ep}[alkene]} \tag{4.10}$$

replacing the value of [**I**] in Eq. 4.8 by $[\mathbf{I}]_{SS}$ above, the rate of the reaction can be written as follows:

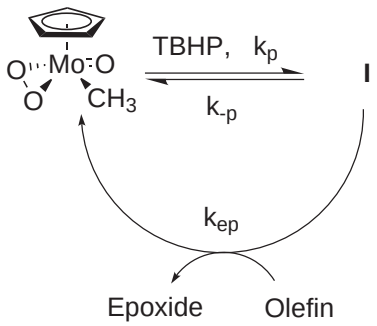

Scheme 4.6. Schematic representation of olefin epoxidation with TBHP catalyzed by $CpMo(O_2)OCH_3$

$$rate = \frac{k_{ep}k_p[alkene][TBHP][Mo]_T}{k_{-p} + k_p[TBHP] + k_{ep}[alkene]} \tag{4.11}$$

The kinetics of the epoxidation of β-methoxystyrene with TBHP catalyzed by $CpMo(O_2)OCH_3$ were investigated by following the absorbance change due to the consumption of β-methoxystyrene and the formation of the product(s) in the region 260-270 nm. Kinetic measurements were carried out with a constant concentration of β-methoxystyrene of 0.1 mM and a constant [TBHP] of 10 mM. The concentration of $CpMo(O_2)OCH_3$ was varied in the range 0.1 - 0.5 mM. Reaction mixtures were prepared in a spectrophotometric cell, the last added reagent being TBHP. The initial rates (i.r.) were calculated from the first 5% of the curves by using .

$$i.r. = -(1/b\Delta\varepsilon_\lambda) \cdot \frac{\Delta Abs_i}{\Delta t} \tag{4.12}$$

Where b is the optical path length and $\Delta\varepsilon_\lambda$ is the total change in the molar absorptivity at λ, and ΔAbs_i is the initial change in the absorbance.

The variation of the initial rate with the catalyst concentration is presented in Figure 4.7 and shows a linear dependence on $[Mo]_T$ as expected from Eq. 4.11. Using the determined values of k_p and k_{-p} (0.0047 $M^{-1}s^{-1}$ and 0.0032 s^{-1}, respectively) and the initial concentrations of β-methoxystyrene and TBHP, the value of k_{ep} ($\sim$ 16 $M^{-1}s^{-1}$) was determined from the slope.

Kinetic measurements were also carried out with a constant $[Mo]_T$ ($CpMo(O_2)OCH_3$) of 0.4 mM and a constant concentration of β-methoxystyrene of 0.1 mM, varying the concentration of TBHP in the range 5-500 mM. A low concentration of β-methoxystyrene was used to allow direct measurement of the absorbance change, since β-methoxystyrene has a very strong absorptivity in the UV region ($\varepsilon_{265} \sim 2x10^4$ $M^{-1}cm^{-1}$). A plot of the initial rate against [TBHP] is shown in

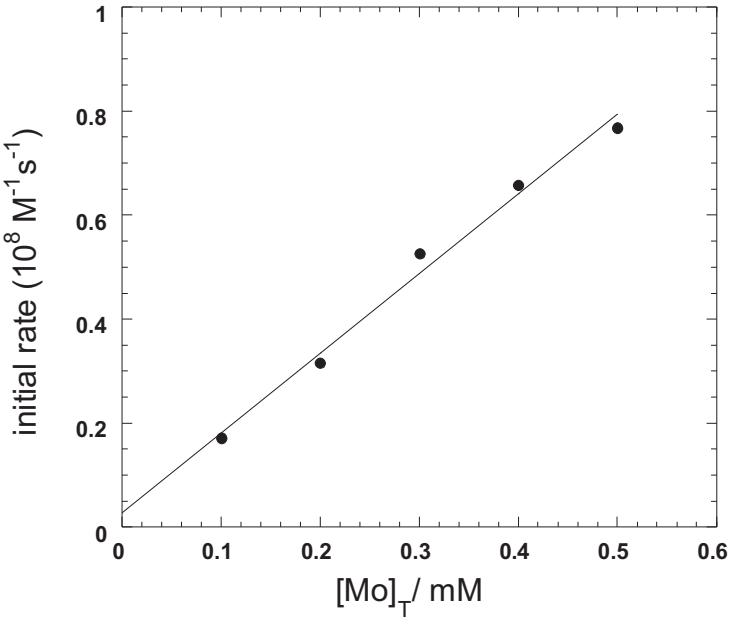

Figure 4.7. Linear variation of the oxidation initial rate of β-methoxystyrene against $[Mo]_T$ in CH_2Cl_2 at 20 °C.[TBHP] = 10 mM, [β-methoxystyrene] = 0.1 mM

Figure 4.8. At low [TBHP] ($\leq$ 20 mM), the initial rate varies linearly and is first-order with respect to [TBHP]. The order decreases with increasing [TBHP]. This kinetic behaviour agrees with the rate law derived based on a steady-state approximation (Eq. 4.11). Fitting the data in Figure 4.8 to Eq. 4.11 using the known values of k_p (= 0.0047 $M^{-1}s^{-1}$) and k_{-p} (= 0.0032 s^{-1}), leads to the epoxidation rate constant (k_{ep} = 18.3 $\pm$ 3.8 $M^{-1}s^{-1}$). This value of k_{ep} is close to the value estimated above from varying the concentration of the catalyst.

The reactions of *trans*-β-methylstyrene (UV method) and cyclooctene (NMR method) were studied similarly, and the values of k_{ep} for their epoxidation with TBHP catalyzed by $CpMo(O_2)OCH_3$ are 0.5 and 1.3 $M^{-1}s^{-1}$, respectively. These results show that the epoxidation rate constant (k_{ep}) increases with the olefin nucleophilicity:

$$\beta\text{-methoxystyrene} \gg \text{cyclooctene} > \textit{trans}\text{-}\beta\text{-methylstyrene}$$

β-methoxystyrene is the most nucleophilic olefin among the examined substrates (due to the presence of an OCH_3 group), and it is ca. 15 times more reactive than cyclooctene. Cyclooctene is more active than trans-β-methylstyrene also due to its higher nucleophilicity.[103,117,56,98]

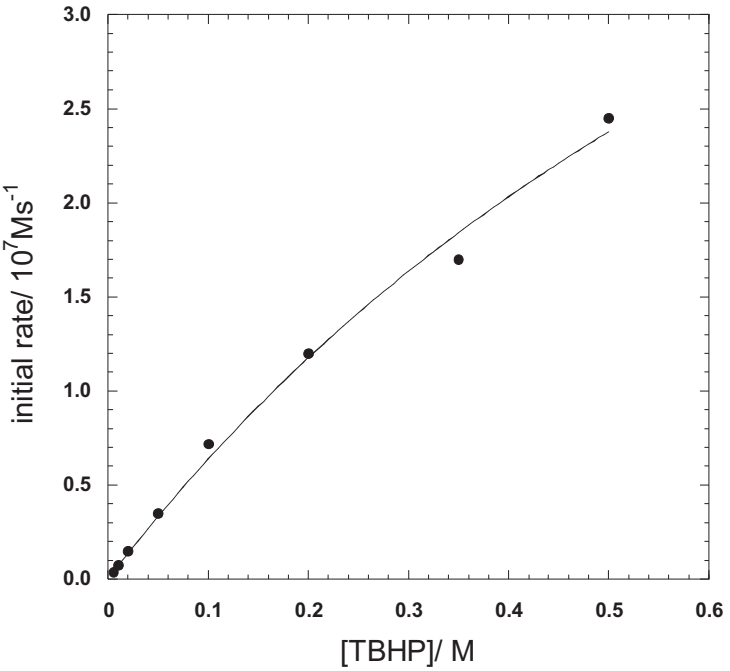

Figure 4.8. Variation of the oxidation initial rate of β-methoxystyrene (0.1 mM) with TBHP catalyzed by $CpMo(O_2)OCH_3$ (0.4 mM) in CH_2Cl_2 at 20 °C. The data was fitted to Eq. 4.11 with the values of k_p (= 0.0047 $M^{-1}s^{-1}$) and k_{-p} (= 0.0032 s^{-1}) being held constant, and k_{ep} (=18.3 ± 3.8 $M^{-1}s^{-1}$) being varied

Also, the epoxidation reaction is stereoselective. When *trans*-β-methylstyrene is oxidized only the *trans* epoxide is obtained. Epoxidations that occur by an external attack of the nucleophilic olefin onto the electrophilic oxygen of the M-alkylperoxo (or M-peroxo) group by a concerted O-transfer step are usually stereoselective.[88,93,114,118]

4.2.3. Epoxidation catalyzed by $CpMoO_2CH_3$

The profile of the reaction between $CpMo(CO)_3CH_3$ (0.05 M), cyclooctene (0.44 M) and TBHP (0.6 M) in $CDCl_3$ at 20 °C (Figure 4.6) indicates the presence of a minimum of two catalytic systems formed from the initial Mo(II) precursor. Each catalyst activates TBHP (through an active intermediate) for the epoxidation of an olefin (as shown in Scheme 4.5). It was not possible to study the catalytic activity of $CpMoO_2CH_3$ separately, because in addition to the epoxidation reaction, $CpMoO_2CH_3$ also reacts with TBHP to form $CpMo(O_2)OCH_3$, which also catalyzes the epoxidation of olefin as shown above. However, the values of the rate constants

for the reactions of $CpMo(CO)_3CH_3$ with TBHP to yield $CpMoO_2CH_3$ and $CpMo(O_2)OCH_3$ were determined in the absence of the olefin under the same conditions, and the rate constants for the epoxidation of cyclooctene by the TBHP / $CpMo(O_2)OCH_3$ catalytic system (k_p, k_{-p} and k_{ep} in Scheme 4.6) were determined separately. Therefore, it is possible to estimate the relative rates of the epoxidation reactions by $CpMoO_2CH_3$ from reactions initially started with the precursor $CpMo(CO)_3CH_3$.

In an experiment initially started with $CpMo(CO)_3CH_3$ (0.2 mM), TBHP (10 mM) and β-methoxystyrene (0.1 mM), the initial rate was $1.3 \cdot 10^{-8} M^{-1} s^{-1}$. When initially started with $CpMo(O_2)OCH_3$ under the same conditions, the initial rate was $0.32 \cdot 10^{-8} M^{-1} s^{-1}$ (see Figure 4.7). From the initial rate ratio ($1.3/0.32 = 4.1$) is obvious that the epoxidation reactions catalyzed by $CpMoO_2CH_3$ are 4.1 times higher than those catalyzed by $CpMo(O_2)OCH_3$ under the same conditions. This shows that $CpMoO_2CH_3$ is more active than $CpMo(O_2)OCH_3$. However, when TBHP is present in large excess over the catalyst, formation of $CpMo(O_2)OCH_3$ from $CpMoO_2CH_3$ occurs at the beginning of the catalytic reaction, and most of the epoxidation is carried out by $CpMo(O_2)OCH_3$ rather than $CpMoO_2CH_3$.

Part II.

Olefin metathesis

5. Introduction

"Where matters of observation are concerned,
chance favors only the prepared mind"

L. Pasteur, Address at University of Lille, France, 1854

The olefin metathesis is an organic reaction that entails redistribution of alkylene fragments by the scission of carbon - carbon double bounds in olefins.[119] The word metathesis is derived from the Greek words $\mu\varepsilon\tau\alpha$ (change) and $\theta\varepsilon\sigma\iota\zeta$ (position), first used to describe the poylmerization of cyclic alkenes by the Goodyear chemist Nissim Calderon in 1967.[120] In fact, the olefin metathesis of propene at high temperature was first observed in 1931, and the first catalyst for this process (known as alkene disproportionation at that time) was first reported by Du Pont, Standard Oil and Phillips Petroleum in 1960.[121] The catalyst used was based on molybdenum, as metal, oxide or $Mo(CO)_6$, deposited on alumina. The first power plant applying this *Triolefin process* was build in Shawinigan, Canada, producing 30 000 tonnes butene per year operating at 120-220 °C at 25-30 bar with propen conversion of 41 %.[18]

WO_3/SiO_2 and Re_2O_7/Al_2O_3 were two other catalysts developed for the Triolefin process. The tungsten catalysts operated on even higher temperatures (500 °C) and gave 42 % propen conversion. The Rhenium catalyst developed by BP was the only one active on room temperature but also it was the most sensitive one and escaped industrial application because of early deactivation.

In 1974 only seven years after its opening, the plant in Shawinigang was shut down because of abrupt change in the feedstock availability.[6] The reaction is reversible, and the potential propylene shortage motivated a reaction with the same catalysts in which 2-butene and ethylene reacted to yield propylene. In 1984 Lyondell (ARCO) built the first plant operating on this

principle yielding 136 000 ton of propene per year. The ethylene coming from the ethane - cracking was first dimerized to 2-butene process followed by a metathesis of the 2-butene to propene. The catalyst used was also developed by Phillips and comprise Nickel oxide supported on alumina or silica. This reaction proceeded at 33 °C and 12 bar to give an ethylene conversion of 93 %.

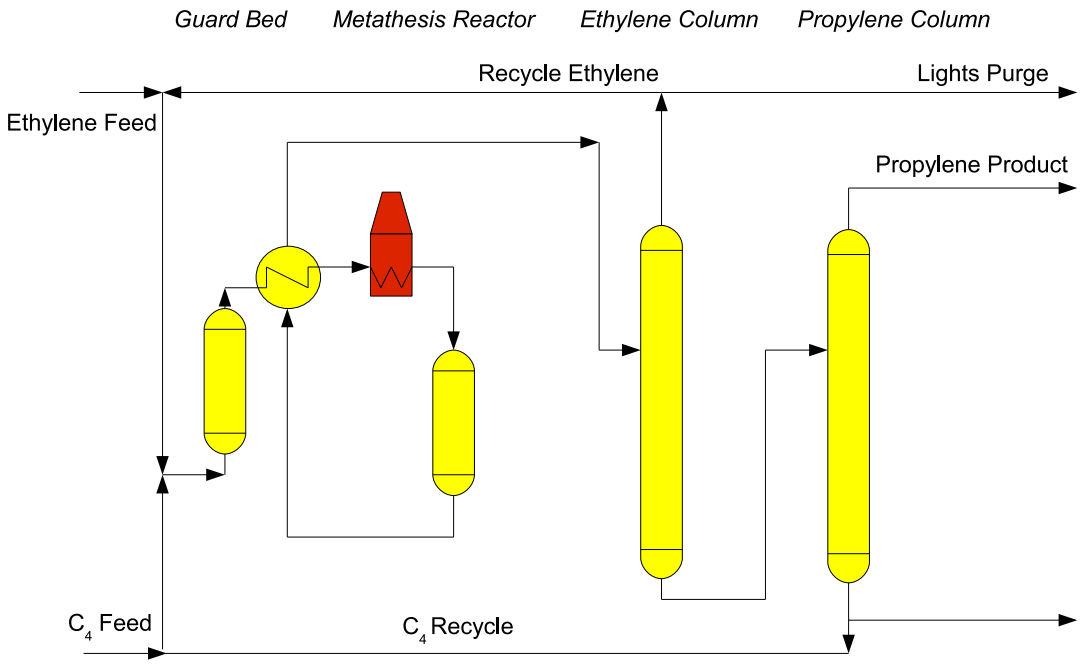

Figure 5.1. BASF-FINA olefin conversion unit flow chart

BASF-FINA a joint venture between BASF Co. and ATOFINA Petrochemicals launched the worlds largest naphtha steam cracker in 2002 at PortArthur, Texas. Together with Shell Chemicals the two companies constructed a world-scale integrated C4 olefin complex. It included a butadiene plant which received feedstock direct from steam crackers and an alkylation unit that produced a high grade octane enhancer. The alkylation unit also supplied the olefin conversion unit that operated similar to the Lyondell process using the metathesis to increase the propene output at the steam cracker. The Japanese Mitsui and the Chinese Shanghai Secco are two other companies that made use of the olefin conversion technology to enhance the propene production Table 5.1.

The Shell Higher Olefin Process (SHOP) introduced in 1977 incorporated the olefin metathesis in the production of linear higher olefins from ethene. It was a three step reaction where the ethylene was first oligomerized to give a mixture of linear α-olefins in a catalytic reaction with Nickel-phosphine as a catalyst. The oligomeres with more than 16 C-atoms and less than 4 were distilled and further isomerized to internal alkenes over solid potassium metal catalyst. In the third and final step of the production the internal olefins underwent a cross metathesis reaction yielding 10 - 15 % of the desired linear internal olefins with 11 to 14 C - atoms. The products were separated by a distillation and the higher (> 14) or lower (< 11) alkenes were recycled. The olefin metathesis was performed at 100 - 125 °C and 10 bar pressure, over a molybdate catalysts deposit on alumina. Over one million of tons of linear internal alkene per year were produced with the SHOP process to be further converted into detergent alcohols, via a hydroformylation process, or into detergent alkylates.

Concomitant to the developments in the propene production, the olefin metathesis, precisely the Ring Opening Metathesis Polymerization (ROMP), became one of the most important reaction in the polymerization industry. First patents about this subject were filled by Du Pont in 1961 about the polymerization of norbornene catalyzed by $TiCl_4/LiAl(C_7H_{15})_4$. The experiments proved that a bond has been broken in the norbornene but it was not clear which one. Seven years later, Calderon performed the same reaction with labeled compounds proving that the reaction proceeded by cleaving the alkene double bond, analog to the olefin disproportionation known from the propene chemistry.[122] Norbornene was also the first monomer polymerized on an industrial scale by CdF Chimie using ROMP. The monomer was prepared with a Diels-Alder reaction and then polymerized with ruthenium chloride catalyst in buthanol (Table 5.1). The reaction took place in an extruder and the two solution were mix in air, on a room temperature.[123] The polynorbornene was a useful elastomer and was used for oil spill recovery, as a sound barrier, or for damping.

Another polymer that marked the development of the olefin metathesis was polydicyclopentadiene, first synthesized by Hercules Inc.[124] Polydicyclopentadiene is a high branched polymer that is light but also tough, rigid and thermoset. Its low dielectric constant, low moisture uptook and an excellent impact strenght made it ideal for use as a core materials in oil & gas, marine, aerospace, and construction applications.[125]

The monomer (dicyclopentadiene) was a by product in the naphtha crackers and was first

polymerized with WCl_6 and $WOCl_4$ as a catalyst via a reaction injection molding. In this technique developed by BFGoodrich Co. two streems one including the monomer and the catalyst and the other the monomer, cocatalyst and additives are mix at first in a mixing chamber and led in the mold, where an exothermic polymerisation occurs Figure 5.2. This low temperature process typically takes less than a minute to complete, including time for mixing, curing, and demolding.[126]

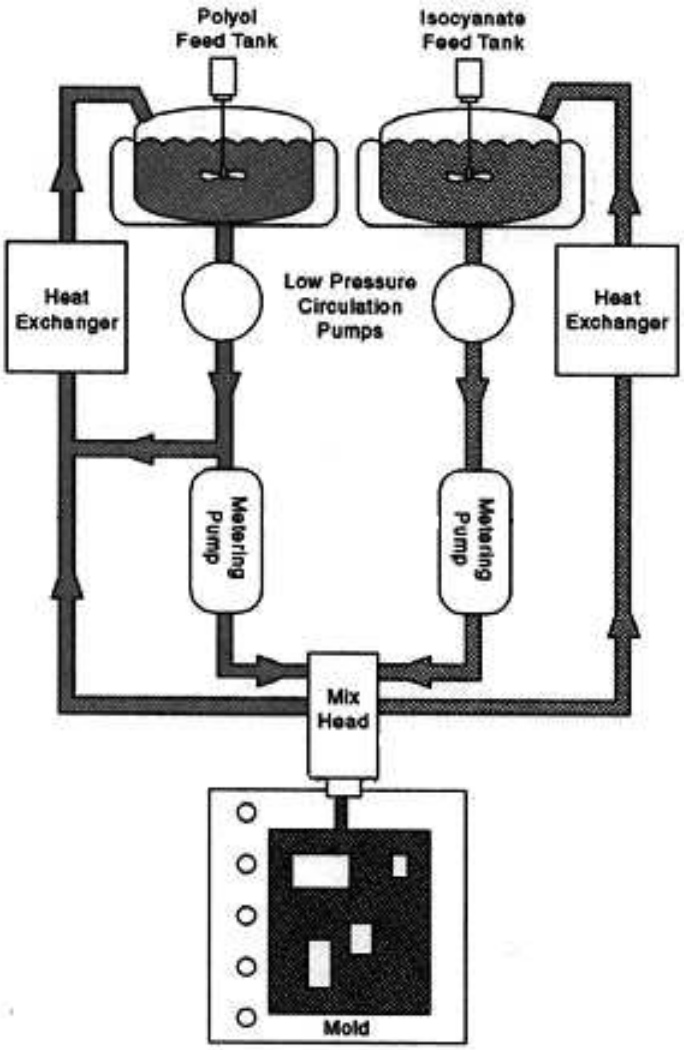

Figure 5.2. Reaction injection molding scheme[126]

Today, Materia Inc. implicate novel ruthenium catalyst developed by Grubbs et. al. in this highly important polymerisation process.[127] The P-DCPD attained with these catalysts have no odor problems due to the residual DCPD monomer in the parts and the catalysts are less sensitive to moisture and air.[128] The main market for these polyolefins that are distributed under the trade name Prometa® are the sport, recreation and marine industry.[129]

Table 5.1: Industrial processes based on the olefin metathesis [a]

Product	Process	Company	Production t / year[128]	Catalyst
Propene	OCT[a]	BASF - FINA	860 000	WO_3 / SiO_2 + MgO
		Mitsui Chemicals	420 000	
		Shanghai Secco Petrochemical	590 000	
Neodene® (Linear higher olefins)	SHOP[b]	SHELL	1 190 000	Mo/Al_2O_3
Neohexene		Chevron	1 400	WO_3 / SiO_2 + MgO
Vestenamer® 8012 (Polyoctenamer)	ROMP	EVONIK	3 000[130]	WCl_6
Norsorex® (Polynorbornene)	ROMP	CdF - Chimie[c]	5000	$RuCl_3$ / HCl
Polydicyclopentadiene	RIM[d]		20 000[e]	
Metton®		Hercules Inc.		WCL_6 + $WOCl_4$ $EtAlCl_2$ (cocatalyst)
Telene®		BFGoodrich Co.		4 ($C_{12}H_{25})_3NH[Mo_8O_{26}]$ Et_2AlCl + $SiCl_4$ (cocatalyst)
Prometa®		Materia		$(Cy_3P)_2Cl_2Ru$=CHPh

[a] Olefin Conversion Technology

[b] Shell Higher Olefin Process

[c] Is presently produced in Carling (France) by Atofina, and developed worldwide by the Japanese company Nippon Zeon

[d] Reaction Injection Molding

[e] Parts per year (considering large parts - > 5 kg or > 1 m^2)

5.1. Mechanistic studies and the development of organometallic catalysts

5.1.1. The elucidation of the olefin metathesis mechanism

Establishing itself as a valuable industrial reaction, the olefin metathesis arouse immense interest in the scientific circles as well. Especially the mechanistic aspect of this novel reaction was puzzling and many research groups started working particularly in this filed. The first concept came from Calderon in 1968 and involved a formation of an cyclobutane complex to the metal as an intermediate.[122c] However, introducing cyclobutane in the olefin metathesis systems never resulted in the formation of alkenes and no cyclobutane was formed in the olefin metathesis so this "conventional mechanism" was proved wrong. Realizing that it is impossible to bind a cyclobutane to a metal as suggested by Calderon, Roland Pettit suggested an unusual tetramethylene complex where four methylene units were bond to a central metal atom as an intermediate.[131]

At that time the French chemist Chauvin inspired by the work of E. O. Fischer about tungsten carbene and the Italian chemist Natta and his contributions to the ROP suggested another mechanistic pathway. A crucial step in this novel proposal was the formation of a metal carbene as a propagation species initiating the metathesis by an interaction with an olefin and the formation of a metallacyclobutane intermediate (see Scheme 5.1).[132] Chauvin performed a metathesis between cyclopentene and 2-pentene yielding C_9, C_{10} and C_{11} dienes in 1:2:1 ratio. This product distribution could not be explained by the conventional mechanism where only the C_{10} diene was expected. Unfortunately, the control experiment, with cyclooctene and 1-pentene gave only the conventional C_{13} diene, which could not be explained by Chauvin at that time.

Casey and Burkhardt unintentionally provided the first model for this mechanism applying metal carbenes in the cyclopropane synthesis. They realized that in the reaction of $Ph_2CH_2{=}W(CO)_5$ with isobutene a new olefin $Ph_2CH_2{=}CH_2$ was formed, probably with an exchange between the metal carbene and the isobutene.[134] Using a different olefin, $[(CH_3O)PhCH_2 = CH2]$, they further proved that both fragments of the metal carbene exchanged with both fragments of an olefin's double bond, discovering the fundamental step of the olefin metathesis.

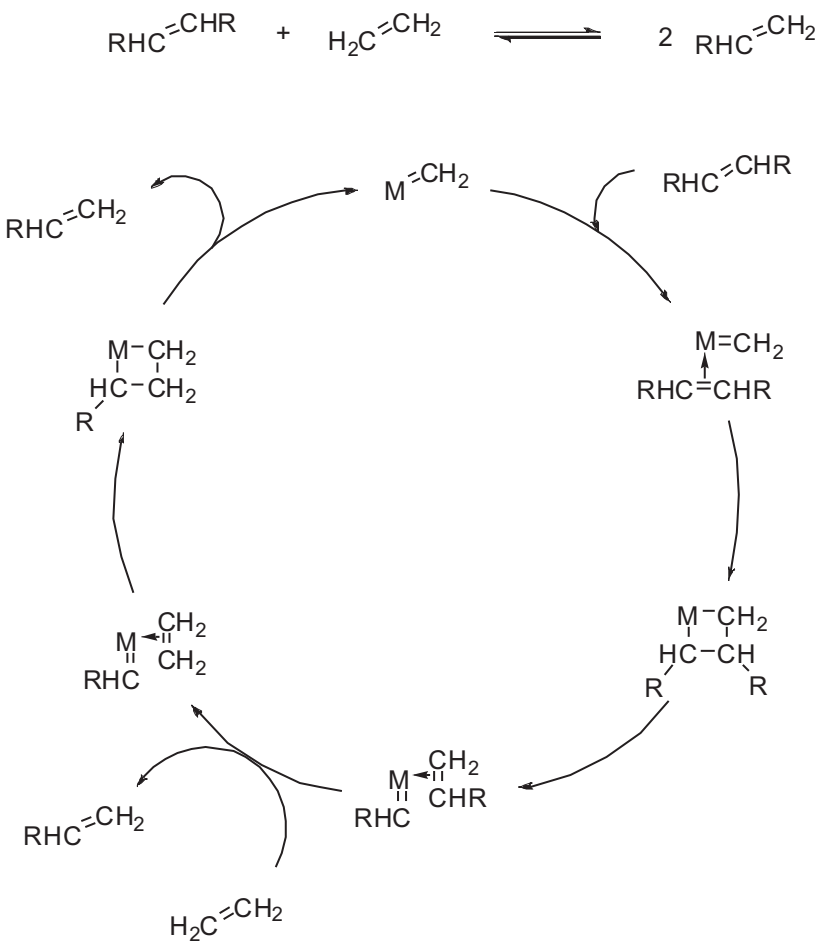

Scheme 5.1. Olefin metathesis mechanistic insights[133]

The last uncertainties of the Chauvin mechanism evolving around the product distribution were cleared by Katz et al. in 1975.[135] The group at Columbia University showed that during the metathesis of an asymmetric alkene, the stable metal carbene was primarily formed, derived by cleaving the double bond. This metal carbene was the one that reacted further with alkenes yielding only one main product. A metathesis reaction following this path would have the terminal alkenes transformed into themselves, but with their terminal methylenes interchanged. Isotopic labeling experiments provided a prove for this hypothesis.[136]

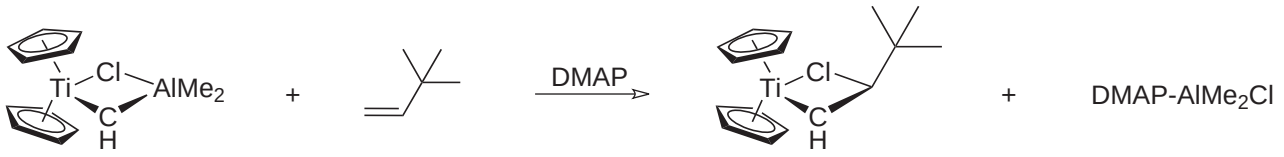

Scheme 5.2. Synthesis of a stable titaniumcyclobutene complex as a model for the active intermediate in the olefin metathesis

The first demonstration of this novel olefin metathesis mechanism in the catalysis was done by Fred Tebbe at DuPont in 1978 wile working on a titanium - methylene - aluminium compound.[137] After an extensive characterization he put this complex in a reaction with terminal, deuterium labeled olefins and obtained the unmarked alkene - the metathesis product. The starting complex bearing deuterium atoms was recovered and could be applied further on in the next reaction step. Furthermore, Grubbs used the same compound, now called "Tebbes Complex", to isolate a stable metallacyclobutane (Scheme 5.2) by reacting it with terminal olefins in a presence of a strong base. The base shifted the equilibrium to the metallacyclobutene intermediate by trapping the $Al(CH_3)_2{-}Cl$ formed during the metathesis.[138] This experiment demonstrated the role of the cocatalyst in the formation of the tantalum alkylidene as an active species in the metathesis, and the following reaction with the olefin. The experiment presented an alternative for the synthesis of a stable metallacyclobutenes, as a model intermediates, detail study of which could offer a way to explain the kinetic parameters and the stereoselectivities in various alkene metathesis reactions.

5.1.2. The discovery and development of the Schrock catalyst

At the same time when Tebbe started working on titanium complexes the central research and development department of E. I duPont began exploring the tantalum alkyl chemistry.[139] The initial compound synthesized with alkylation of tantalum chloride with lithium reagents, the $Ta(CH_3)_5$, was unstable on temperatures higher than 0 °C so a new one bearing more stericly demanding ligands was synthesized by the same procedure in attempt to stabilize the metal center. Several ligands were tested but the neopentane caught the attention giving a "tantalum ylide" instead of the expected $Ta(CH_2C(CH_3)_3)_5$ (Scheme 5.3).[140] In this complex the Ta=C bond was polarized with the positive charge localized on the metal and underwent wittig - reaction in the similar manner as the analog phosphorus ylides.[141] Later the X-ray structure revealed the double bond nature of the Ta - C bond with only 2.02 $\mathring{A}$ length.[142]

Soon it became apparent that the steric crowding around the metal distorted the ligands by opening of the Ta - C_α-C_β angle and pushing the α-hydrogen near to the metal center. The resulting agostic interaction lengthened the C - H bond making the hydrogen more acidic and easy to abstract by the nucleophilic carbon of the neighboring neopenthyl ligand, eliminating $C(CH_3)_4$ and creating a stable alkylyden complex (Scheme 5.3). This α-hydrogen abstraction

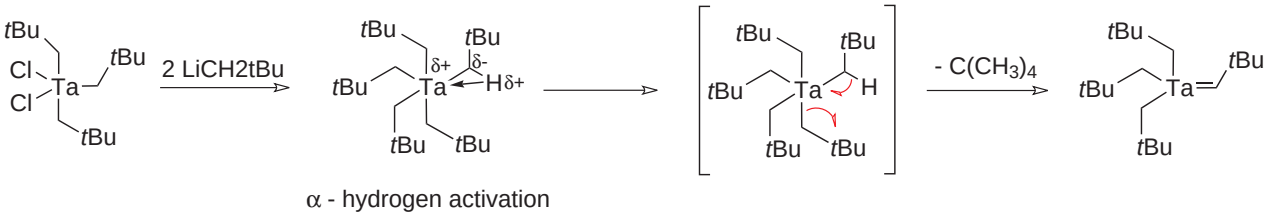

Scheme 5.3. The synthesis of the novel tantalum alkylidene complex

was also observed in d^0 complexes of Mo, W and Re.[143]

The reaction of this Ta-alkylidene complex with olefins, was studied in grate detail, because of the possibility for a metathesis reaction in the coordination sphere of the metal.[144,145] The initial experiments involving $TaCp(CH{=}C(CH_3)_3)Cl_2$ and ethene gave only the metallacyclobutene rearrangement products and a tantalacyclopentane complex with the two molecules of ethene. This rearrangement pathway was initiated by a β - hydrogen elimination, followed by a hydride transfer to the metal atom and the formation of σ - bonded alkene. This short lived intermediate underwent a reductive elimination, leaving an open coordination site for the two ethene molecules that arranged to a tantalcyclopentane.[144] Unlike complexes bearing chlorides, the compounds with alkoxides instead, like $Ta(CHtBu)Cl(P(CH_3)_3)(OtBu)_2$, gave only the expected metathesis products. All attempts to isolate the intermediates of this reaction were unsuccessful probably due to the great activity of these complexes.[145] This observation indicated that alkoxy ligands could shift the equilibrium to the metathesis products versus metallacyclobutane rearangment.

The way of stabilizing high - oxidation state alkylidene and the influence of various ligands on their activity in olefin metathesis were the two major discoveries that triggered the work of many synthetic organometallic chemists in this field. The findings made on tungsten complexes in the 1980ties by Schrock, Basset and Osborn turn out to be exceedingly fruitful.[123]

The studies were initiated by Schrock et al. with the discovery of the stable 18 e^- tungsten oxide complex $(W(=CHtBu)(O)(PMe_3)_2Cl_2)$.[146] This tungsten oxide was stable but only active in the metathesis with a $AlCl_3$ as cocatalyst probably due to a formation of an ionic species $[W(=CHtBu)(O)(PMe_3)_2Cl][AlCl_4]$.[147] The complex with only one phosphine ligand appeared to be active in the metathesis as well, which was the reason why Schrock started working on substituting the phosphine with alkoxides, creating a stable penta-coordinate species.

At the same time Kress and Osborn worked on the activation of tungsten alkylidene com-

plexes with Lewis acids, especially $AlBr_3$ and $GaBr_3$ (Scheme 5.4).[148] In the solution it appeared that one of the bromo ligands rapidly exchanged with the Lewis acid, creating a free coordination site on the metall where the olefin could coordinate. The assumptions were proven later through isolation and crystallization of this intermediate by using a cyclopentylidene ligand and $GaBr_3$ as a Lewis acid (Scheme 5.4).[148d]

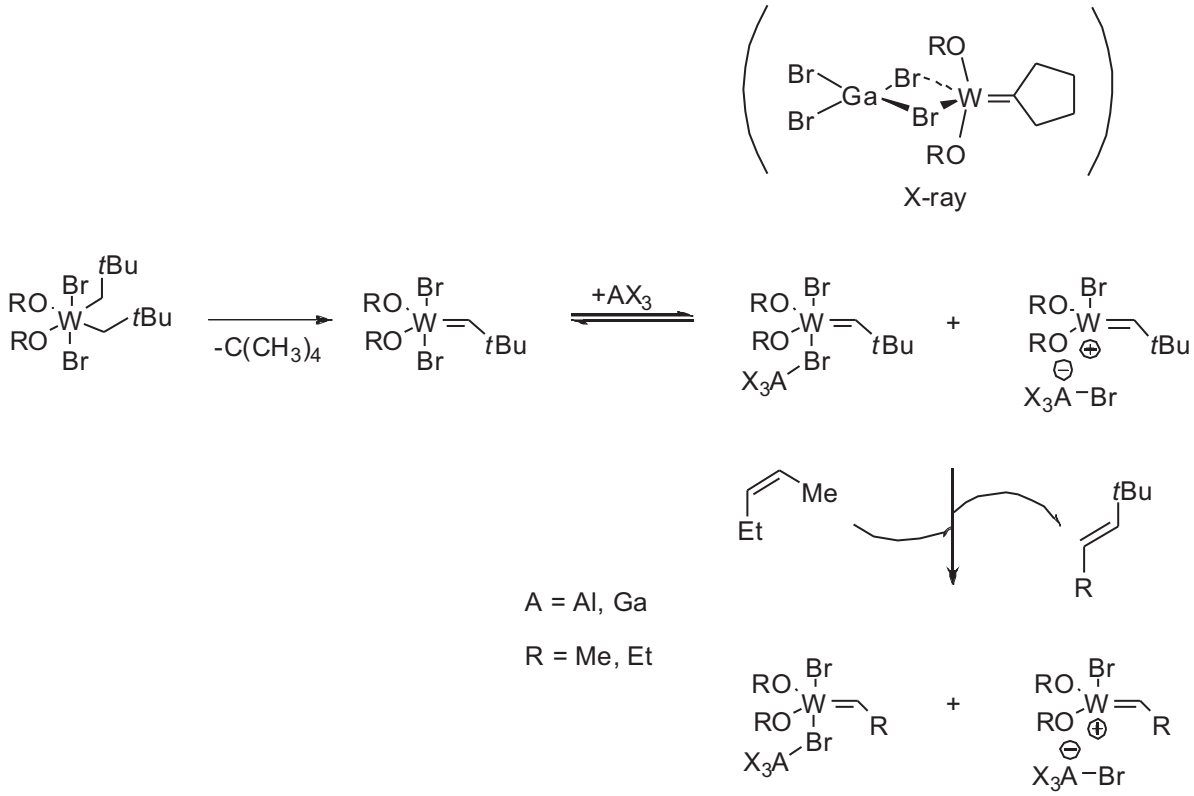

Scheme 5.4. Osborn's system and its reactivity towards olefins. X-ray characterized intermediate given in brackets

These were the first studies in which rapid metathesis of olefins analogous to classical "black box" systems was observed performed with a known d^0 alkylidene complex.[123] Alkoxides were found to be crucial for the preparation and the reactivity of tungsten-based metathesis catalysts of this type.

Expecting to stabilize these active tungsten complexes Schrock used stericly demanding imido ligands instead of the oxygen. The complex $W(=CHtBu)(NAr)(OR)_2$, synthesized as described in Scheme 5.5 turned out to be extremely active and versatile catalyst in the olefin metathesis.[149] Most important, the catalyst could be easily modified by changing the alkoxide, alkylydene and the imido ligands, which resulted in a new very rich class of olefin metathesis catalysts. Slightly

modified synthetic procedures were applied also on molybdenum complexes that turned out to be even more reactive than their tungsten analogs.[150] Due to this activity no molybdenum intermediates could be isolated and characterized.

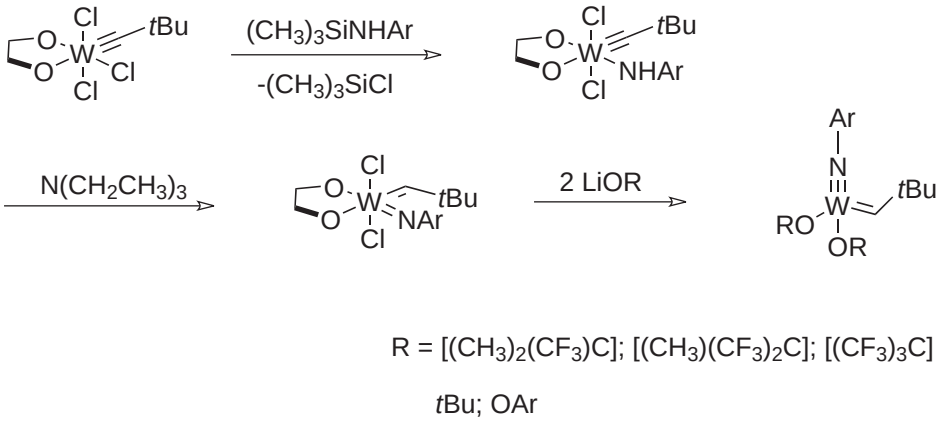

Scheme 5.5. The synthesis of $W(=CHtBu)(NAr)(OR)_2$[123]

According to these observations a hypothesis was made regarding the activity of the d^0 complexes in which more electronegative alkoxy ligands and more electropositive metals were crucial for the catalytic activity of the species. The synthesis of a family of molecular grafted Re catalysts on silica surfaces by Basset et. al (see Section 5.2) proved the deficiency of this hypothesis for the first time, and triggered intensive theoretical studies about the subject.[151,152]

The newest theoretical results for all d^0-complexes propose a four step pathway, coordination/de-coordination of olefin and the formation/oppening of the metallacycle (Scheme 5.6).[151] Assumed that the alkylyden-, Y- and the imido- ligand were all in the same plain, the olefin approached *trans* to the X substituent (**M-TSI**) coordinating on the metal center. The transition state took a trigonal bipyramidal (**TBP**) geometry that stayed unchanged through the ethen complex **M-II** as well. A [2+2] cycloaddition followed with a shift of the olefin from η^2 to η^1 coordination and elongation of the C-C bond. The metallacyclobutane had a **TBP** geometry but in some cases the square pyramidal complexes were found as a more stable minima on the potential energy surface. The oppening of the ring (**M-IV**) and the de - coordination of the olefin (**M-V**) were energetically similar with the cycloadition and the coordination of the olefin, respectively.

In the overall catalytic cycle the potential energy surface was under influence of two parameters: ease of distortion of the tetrahedral catalyst (**M-I**) and the stability of the metallacy-

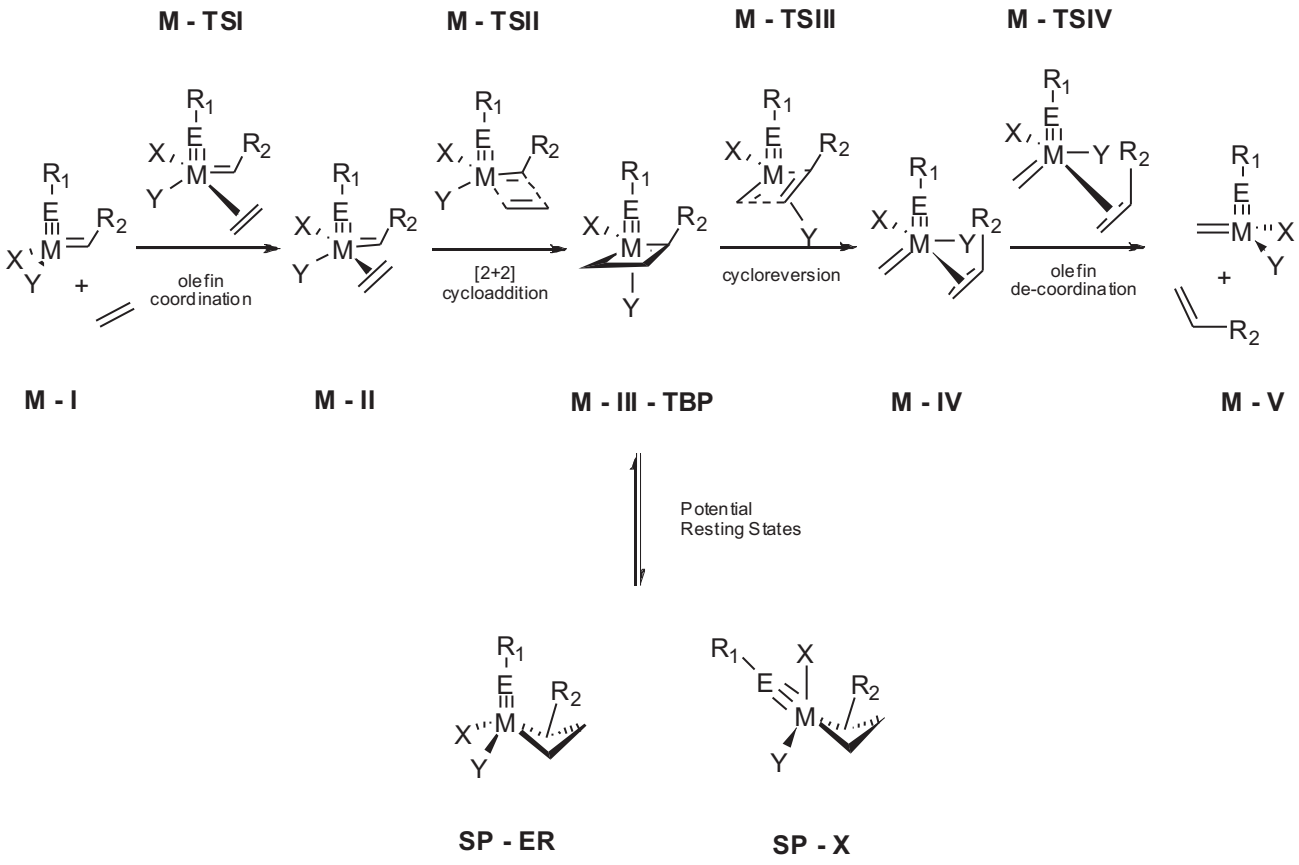

Scheme 5.6. Ethene metathesis pathway according the DFT calculation[152]

lobutane (**M-III**). The first one could be minimized by the presence of two ligands of different electron - donating ability like good donor (alkyl) and a poor σ- donor ligand (alkoxy or siloxy). The stability of the metallacyclobutane could vary by change the strength of the M - C bond.

5.1.3. The discovery and development of the Grubbs catalyst

Beeing active and well defined catalysts for the olefin metathesis, the Schrock systems dominated this research field at the beginning of the 1990ties. The air and moisture sensitivity, no tolerance to certain functional groups and difficult synthesis were the major problems accompanying them. The group of Robert Grubbs in Caltech was one of the many that pursued the idea of improving these catalysts making them more active, more stable and easy to synthesize.[123]

The first results of that work came with $RuCl_3$ as a catalyst applied in ROMP in organic solvents.[153] The problem with this system was the long initiation period of approximately 24 h, necessary for the catalysis to get started. Applying, water as a reaction medium hadn't killed the catalyst as originally expected, but actually decreased the initiation period to 30

min. The catalyst could be recycled and in every recycling step the initiation period decreased further to minimum of 14 sec. Using *p*-toluensulfonate instead of chlorid increased the activity of the system showing the same reaction trends. The active species was not isolated but well characterized by NMR - experiments as a Ru^{2+} - olefin aduct (Scheme 5.7).[154]

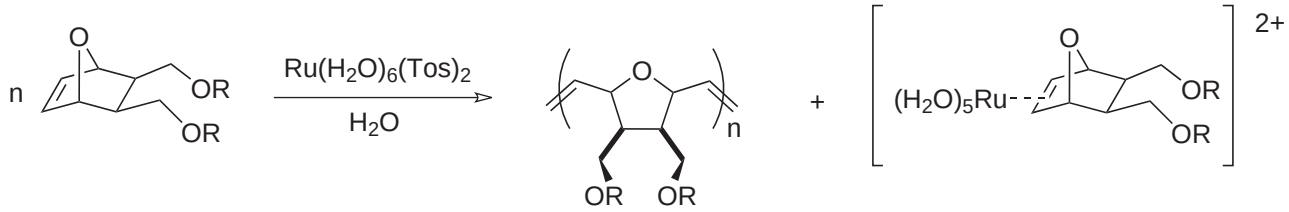

Scheme 5.7. ROMP of 7 - oxanorbornene derivative with $Ru(H_2O)_6(Tos)_2$ catalyst in aqueous medium

Two important guidelines in the ruthenium catalyst design were drawn by this experiment: Ru^{2+} - complexes performed better in the catalysis than Ru^{3+} - complexes and a free coordination site should be available on the metal center for olefin coordination. Almost at the same time, Roper synthesized the halogenated ruthenium and osmium carbene that were not active in metathesis but showed that different ligands, like phosphines, could also stabilize the formed carbene species and they had to be considered in the synthetic strategies.[155]

In 1992 Grubbs et al. integrated all this knowledge in the synthesis of the first generation Grubbs catalyst showed on Scheme 5.8.[156] 3,3-diphenylcyclopropene was used as a reagent, which was already applied by Grubbs in the synthesis of tungsten complexes of the Schrock type, particularly $(ArN)L_2Cl_2W{=}CH{-}CH{=}CPh_2$.[157] Two different routes were used to produce this catalyst on commercial-scale including the use of diazo-transfer chemistry and the rearrangement of vinyl or propargyl halide.[158]

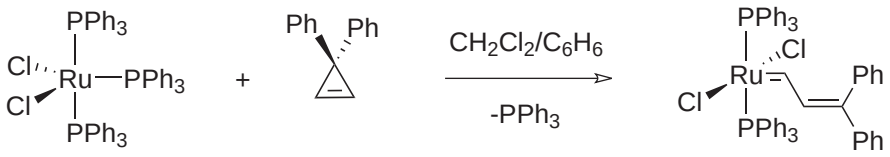

Scheme 5.8. Initial synthesis of the Grubbs first generation catalyst[156]

As anticipated, this complex was five-coordinate, $16e^-$, Ru^{2+} alkylidene species bearing phosphine and chlorid ligands. The initial catalysis tests showed, that it is a very reactive catalyst for ROMP and remarkably stable to water, acid and many other functional groups.[156]

Unfortunately the catalytic activity of $(PPh_3)_2Cl_2Ru{=}CH{-}CH{=}CPh_2$ was limited to strained olefins, and much effort was put in the improvement of this system. After many unsuccessful attempts, involving more electron withdrawing ligands instead of the chlorides the breakthrough came by changing the PPh_3 ligand to the more electron donating phosphine - PCy_3.[159] This advancement was the first indication for a new mechanism in the olefin meatathesis involving this type of catalysts.

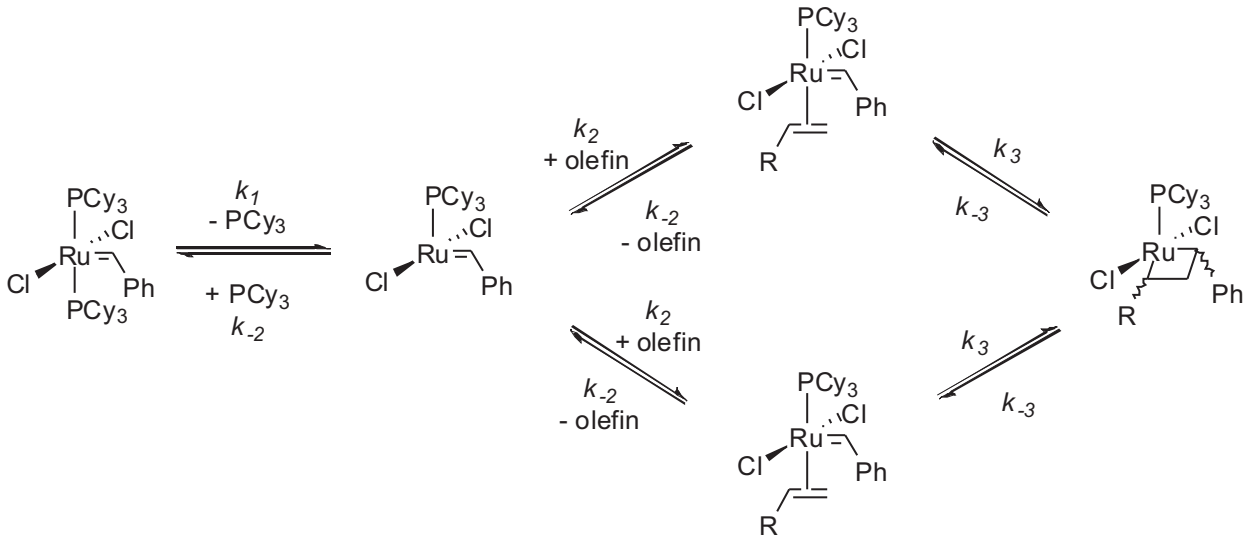

Scheme 5.9. Overall mechanism for the olefin metathesis with $(PPh_3)_2Cl_2Ru{=}CHR$ as catalyst

The initial mechanistic studies provided two important constellations: the rate of the reaction was dramatically depressed by the addition of PCy_3, suggesting that PCy_3 dissociation was crucial for the catalysis.[123] The metathesis went on with first-order kinetics in catalyst and olefin which favored a bimolecular interaction between the olefin and the ruthenim center.[160] These results ruled out an associative mechanism, which would involve an olefin coordination on the Ru center and a formation of an $18e^-$ species. The dissociative pathway accounts for more than 95 % of the catalytic activity and proceeds through a phosphine dissociation and formation of a short lived $14e^-$ intermediate. In the subsequent studies this intermediate could also be identify in the gas phase using mass spectrometric techniques.[161]

The complete mechanism is depicted in Scheme 5.9. After the dissociation as an initiation step, the highly reactive intermediate reacts with an olefin making the olefin aduct. The olefin interacts further on with the alkylidene species in the coordination sphere of the metal building the metallacyclobutane, that can dissociate productively and form the metathesis products

or regenerate the starting materials unproductively. According to this mechanism the two most important process are the dissociation of the phosphine ligand and the reaction of the generated intermediate with the olefinic substrate. By keeping the $k_2 >> k_{-1}$ the availability of $(PPh_3)Cl_2Ru{=}CHR$ will be maximized and thereby many olefin turnovers can be achieved before phosphine recoordination. It was soon established that the initiation step was not responsible by itself for the activity of the complex.[162] In the matter of fact, ligands that positively influence the initiation, decrees the overall activity of the complexes (Figure 5.3). However, this behavior is not very well understood and is still a subject of many theoretical studies.[123]

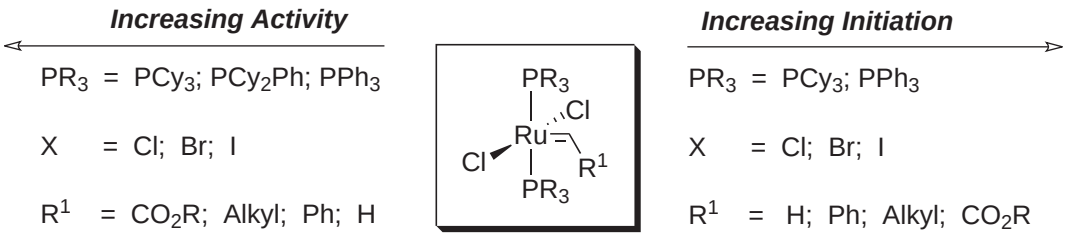

Figure 5.3. Comparison between activity and initiation

The broaden knowledge in the mechanistic insights of the metathesis supported the search for new, more suitable ligands for these catalytic reactions. A big alteration was made by Herrmann et al. by a substitution of the phosphine ligands with NHC - carbene (Scheme 5.10).[163] Although these novel bis-NHC complexes showed only slight improvement in the activity compared to the original catalyst the variable NHC - ligands were soon accepted as a standard in the following synthetic approaches done by the groups of Grubbs, Herrmann and Nolan.[164] Taking the mechanistic findings in to account, and knowing about the strong σ - bonding of the NHC ligands to the metal center, that would likely hinder the dissociation of the ligand in the initiation step, these three groups almost simultaneously successfully performed the synthesis of mono-NHC complexes, applying bulky NHCs (Scheme 5.10).[164] The strong trans influence of the NHC ligand was expected to enhanced the dissociation of the phosphine, thereby increasing the initiation rate. Besides, the NHC ligand provided the possibility for changing the elctronic and steric influence on the metal by changing the groups on the nitrogen atoms, thereby stabilizing the 14 e^-- and the 16 e^- - species, respectively.

The newly created catalysts also known as a "Grubbs second generation" catalyst, are extremely active and show remarkable tolerance to air and an array of functional groups.

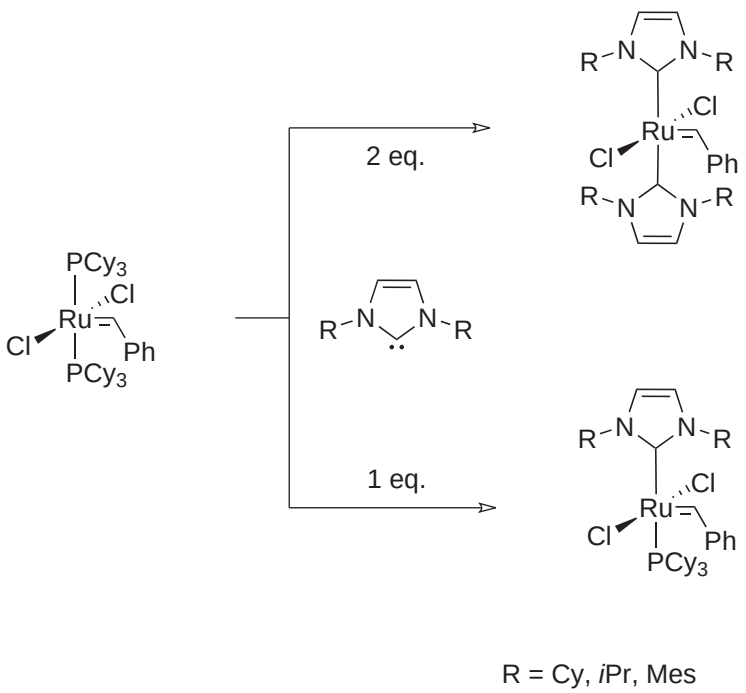

Scheme 5.10. The synthesis strategies for the second generation Grubbs catalyst

The mechanistic studies performed on these new systems showed that the increased activity was not due to the initiation step as initially expected ($k_1(\mathrm{PCy_3}) \approx 10^2 * k_1(\mathrm{NHC})$). The advancement with the implementation of the NHC was actually in the propagation step ($4 * [k_{-1}(\mathrm{PCy_3})/k_2(\mathrm{PCy_3})] \approx [k_{-1}(\mathrm{NHC})/k_2(\mathrm{NHC})$). Due to the increased donor strength of the NHC ligand, the olefinic substrate coordinates easier than the phosphine ligands .[162] In addition, the strong donor ability of the NHC relative to the phosphine allows metathesis of electron-poor and sterically demanding olefins where the first generation grubss catalysts is ineffective.[162,165]

5.2. Heterogeneous catalysts in the olefin metathese

The olefin metathesis was first discovered in the heterogeneous catalysis Chapter 5 and several systems were developed and successfully applied in industrial processes. The lack of analytic methods and instruments for precise characterization of the surface species responsible for the catalytic reaction - “the active site”, was the main reason for the marginal research interest in this area. Fortunately, this trend changed by the end of the last century with the constant development of NMR, IR, EXAFS, UV and XANES spectroscopy tools, which used together

provided an exact picture of the surface active sites (Figure 5.4):[166]

- ***in situ* IR spectroscopy**: provide information about the grafting process and the reactivity of the active site
- **NMR spectroscopy**: provide information about the ligands on the metal center and their dynamics
- **EXAFS**: provide information of the metal bindings, distances and average coordination number
- **ESR**: provide information about the oxidation state of the metal center
- **UV**: provide information about the electronic state of the metal center
- **XANES**: provide information about the geometry of the metal center.

Applying these new analytic tools Basset and coworkers defined a new approach called Surface Organometallic Chemistry (SOMC) with the purpose of combining the knowledge of the homogeneous and heterogeneous catalysts and using it in a design of well characterized, superior active site on a well defined surfaces.[166]

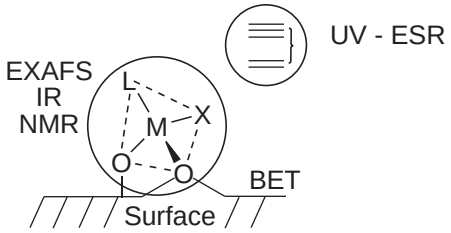

Figure 5.4. Investigation of the coordination sphere of the active site[166b]

5.2.1. Olefin metathesis catalyststst on silica surfaces

Among the first applications of this new concept was the design of a tantalum catalyst for the olefin metathesis.[167] Aware of the mechanism of the olefin metathesis in the homogeneous phase and the importance of an alkylidene species in the catalysis, Basset et al. immobilized tantalum neopentyliden species, $[Ta(=CH\textit{t}Bu)(CH_2\textit{t}Bu)_3]$, on a silica surface partially dehydroxylated on 500 °C ($SiO_{2\text{-}(500)}$) (Scheme 5.11). Neopentyl was released during the grafting procedure and

additional mass-balance analysis combined with reactivity studies gave away two active surface species, $[(\equiv SiO_2)_x Ta(=CHtBu)(CH_2tBu)_{3-x}]$ with $x = 1$ or 2. In the quest for creating a single site catalyst further experiments were conducted on silica treated on 700 °C ($SiO_{2(-700)}$) that further decreased the hydroxyl group coverage of the surface and made the formation of the bissiloxy complex, $[(\equiv SiO_2)_2 Ta(=CHtBu)(CH_2tBu)]$, spatially impossible.[168] The presence of the alkylidene ligand was strongly suggested by both deuterolysis, and pseudo - Wittig reactions with acetone, which yielded one equivalent tBuCH=C$(CH_3)_2$ pro tantal atom.[167]

The grafting mechanism was revealed using polyoligomeric silsesquioxanes (POSS) as a surface model.[169] The reaction intermediate, originated from an addition of the silanol group to the carbenic moiety Scheme 5.11, and was observed with ^{1}H and ^{13}C NMR spectroscopy. In addition, it slowly decomposed via α - hydrogen abstraction into the monosiloxy alkylidene species eliminating one neopenthyl pro tantalum atom.[169,168] This mechanism was further prooved on $SiO_{2\text{-}(700)}$ as well.

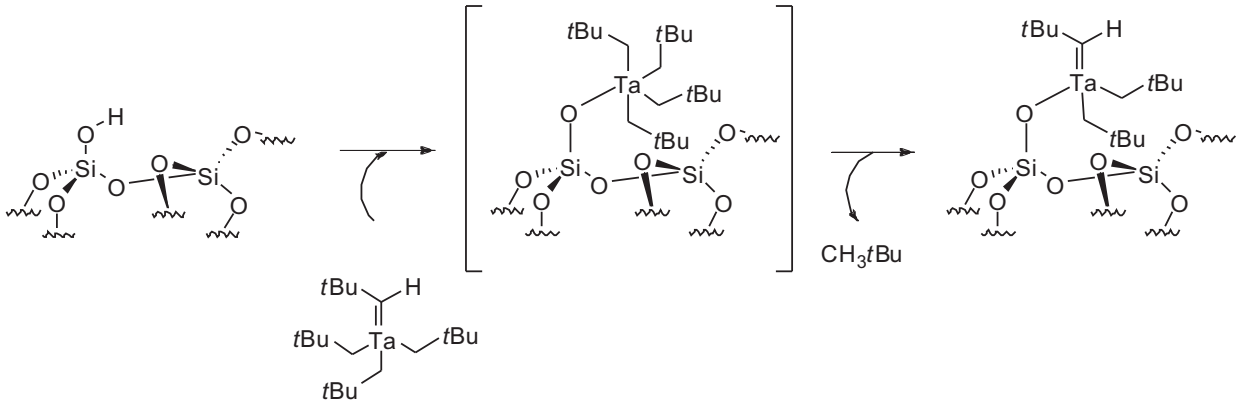

Scheme 5.11. Grafting of $[Ta(=CHtBu)(CH_2tBu)_3]$ on partially dehydroxylated silica[169]

Proving the applicability of the SOMC concept neopentyliden complexes of the 6th and 7th group transition metals were grafted so as to improve the activity of the tantalum system.[123,166] One example is the grafting of $[Re(\equiv CtBu)(=CHtBu)(CH_2tBu)_2]$ depicted in Scheme 5.12. The complexity of the starting molecule compared to the homoleptic complexes of tantalum, made use of different NMR techniques for revealing the active species essential. To improve the signal intensity ^{13}C - labeled complexes, were grafted on the surface. 2D HETCOR experiments were also applied in resolving complicated signal pattern, aroused from various carbon atoms around the metal center.[170]

Molybdenum alkylidene complexes of the Schrock type were also used to generate the sur-

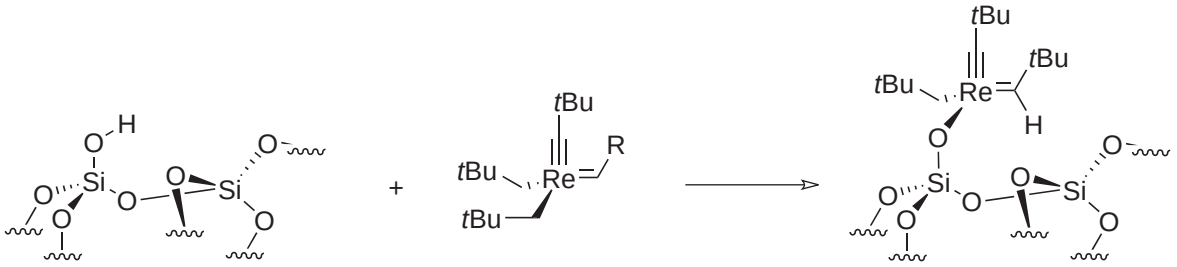

Scheme 5.12. Grafting of $[Re(\equiv C t Bu)(=CH t Bu)(CH_2 t Bu)_2]$ on partially dehydroxylated silica[170]

face species.[171] The tris(neopentyl)nitrido - molybdenum, $[Mo(\equiv N)(CH_2 t Bu)_3]$, synthesized by Herrmann et al. was a promising candidate because of it reactivity towards organosilanols in solution.[171] As expected, it reacted with silica in almost the same manner as tantalum neopentyl complexes, forming first an intermediate by addition of surface silanol accross the nitridomolybdenum fragment. α - hydrogen abstraction step subsequent to this initial grafting process, initiated at 70 °C, afforded the detachment of one neopentyl pro molybdenum atom and the formation of an active alkylidene species (Scheme 5.13).[171]

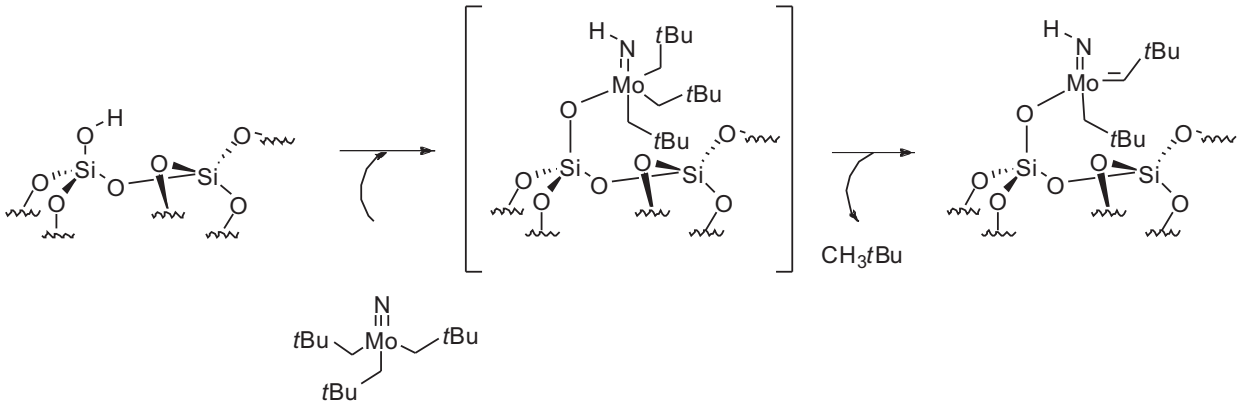

Scheme 5.13. Grafting of $[Mo(\equiv N)(CH_2 t Bu)_3]$ on silica partially dehydroxylated on 700 °C and subsequent thermolysis

The phenomenal activity and stability of this heterogeneous system in the olefin metathesis was encouraging and several molybdenum alkyl alkylidene precursors were developed by the groups of Schrock and Basset for further improvements.[172] However, in the metathesis of propene, traces of 1-butene were found which was ascribed to side reactions that involved the neopentyl ligand.[172] In 2007, Coperet and Blanc used the newly developed molybdenum bis(amido) complexes, $[Mo(\equiv NAr)(=CHC(CH_3)_2R^1)(NR^2)_2]$ with Ar = 2,6-iPr$_2$C$_6$H$_3$, R^1 = CH_3 or Ph, and $NR^2{}_2$ = pyrrolyl or NPh_2 to yield well - defined asymmetric systems having no alkyl ligands present.[173] This novel concept presented on Scheme 5.14 gave the most stable

and most active heterogeneous system known to date. The importance of asymmetric Schrock catalyst was also adopted in the homogeneous catalysis using a combination of siloxy and an alkoxy ligand in the initial Schrock complexes (see also Section 5.1.2).[174,152] The improvement was dramatic and resulted in some of the most active complexes of the Schrock type known to date.[175]

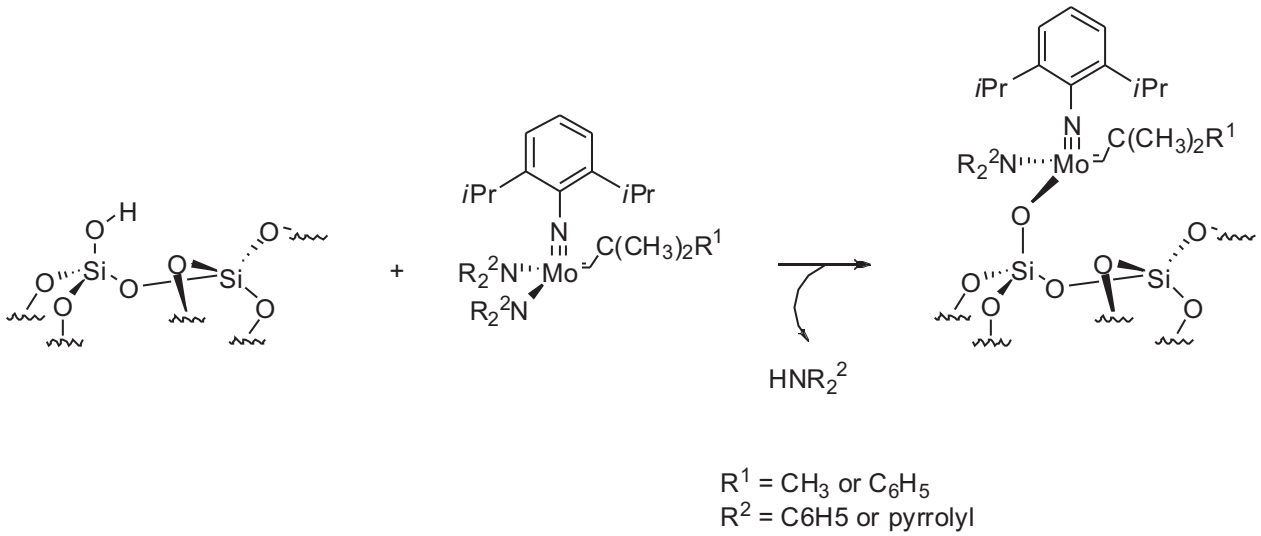

Scheme 5.14. Grafting of $[Mo(\equiv NAr)(=CHC(CH_3)_2R^1)(NR^2)_2]$ on silica partially dehydroxylated on 700 °C and subsequent thermolysis

5.2.2. MTO on γ - $Al_2O_{3\text{-}(500)}$

Although the SOMC concept resulted in the discovery of novel, very active, single site, catalysts on silica surfaces (see previous 5.2.1 section), it gave no explanation for the structure and activity of the already existing industrial catalysts. Especially catalysts on Lewis acidic surfaces like alumina, silica-alumina and nyobia, where the surface itself takes part in the catalysis could not be explained.

MTO was already known as active catalysts in the olefin metathesis, grafted on silica-alumina and nyobia surfaces.[176,28c] Knowing that without activation with tin compounds, MTO was not active in the metathesis of olefins in homogeneous phase, the asumption was made that the activity of the heterogeneous systems can only be due to a surface activation.

The especialness of γ - Al_2O_3 as a solid support in catalysis

γ - Alumina is an ionic solid having a slightly tetragonaly distorted, defect spinel structure.[177] The oxygen lattice is built up by a cubic closed-pack stacking of oxygen layers, with aluminum filling only 1/3, preferentially octahedral, cationic positions per unit cell. Several groups have successfully modeled this surface using different, experimental and theoretical, approach.[178,179] From the body of data gathered in the past several years conclusions can be drawn regarding the surface structure, its acidity and reactivity.

Knozinger and his coworkers were the first to address the structure of the γ - alumina surface layer and its activity with an empirical model.[178a] They found a maximum of five different surface hydroxyl groups with different net charges, which abundance was dependent of the relative contribution of the different crystal faces (Figure 5.5). The hydroxyl groups were divided in two main groups:

a. OH groups bounded at a single Al^{+3} cation, where alumina can adapt tetrahydral, pentahydral or octahydral coordinations.

b. OH groups linked to two or three Al^{+3} cations, in octahedral coordination

All the hydroxy groups present on the alumina were characterized with IR - spectroscopy. Sautet et al. refined the empirical model of Knözinger, using DFT calculations. The hydroxyl groups stretching frequencies observed by IR were accurately assigned (Figure 5.5) and their reactivity towards hydrogen chloride was calculated. This two methods clearly showed the difference in the reactivity of each hydroxyl group.

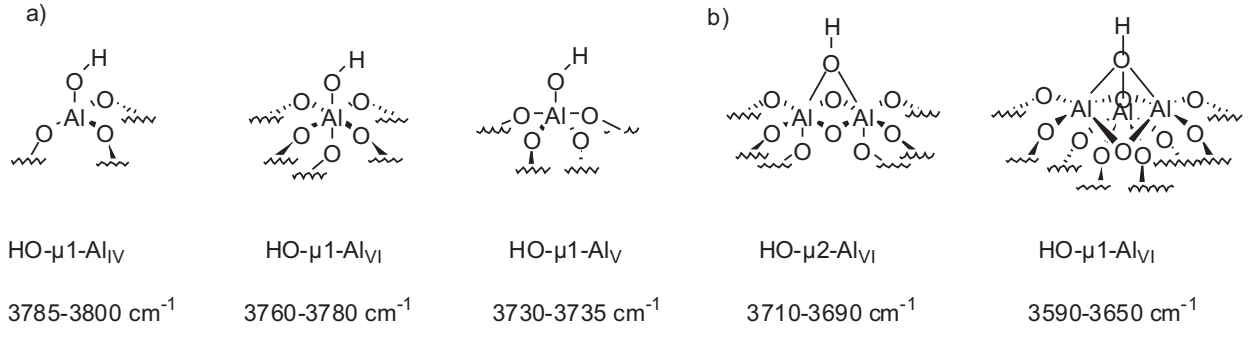

Figure 5.5. Different types of hydroxyl groups on the $Al_2O_{3\text{-}(500)}$ and their characterisation by IR spectroscopy (according to the model developed by Sautet et al.[178b])

Along the dehydroxylation process hydroxyl groups react with each other forming water, and leaving a vacant, Lewis acid sites, on Al^{+3} cations and Lewis base sites on the oxygen atoms. By increasing the dehydroxylation temperature, less reactive hydroxyl groups are activated and brought to reaction. In the specific cell of a γ-alumina partially dehydroxylated at 500 °C (γ-$Al_2O_{3\text{-}(500)}$), the density of the surface hydroxyl groups left, is approx. 4 OH/nm^2.[179] Knözinger assumed that only a few, highly charged, Lewis acidic sites (deffect sites), created by the dehydroxylation procedure can take part in the catalytic reactions initiated by these surfaces.

To characterize this "defect sites", pyridine was adsorbed under static vacuum at room temperature on a γ-$Al_2O_{3\text{-}(500)}$ surface. Under these conditions pyridine interacted with the acidic sites on the surface and each of these interactions was identified using the ν(C=C) vibration of pyridine(Table 5.2).[180]

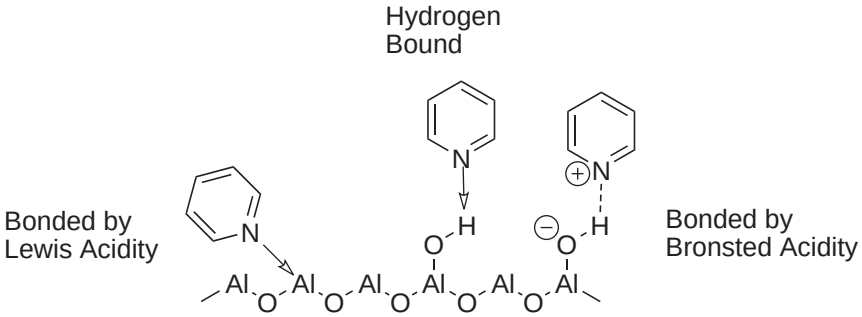

Figure 5.6. IR shift of pyridine linked with diverse acidic site[180]

Table 5.2: IR shifts of pyridine adsorbed on a different acidic site on the surface

ν(C=C)band position / cm^{-1}	Bonding Type	Desorption Temperature / °C
1438 / 1485 / 1580	Physisorption	25
1444 / 1593	Hydrogenbonding	150
1450 / 1490 / 1575 / 1606 / 1619	Lewisacidity	250 - 500
1544 / 1638	Bronsted Acidity	400

Exposing this pre-treated alumina on a high vacuum and high temperature, only pyridine adsorbed on Lewis acid sites had been detected, while no pyridine coordinated on Bronsted acidic sites was observed. This finding had strongly suggested that the activity, resulting from

the acidity of the γ-$Al_2O_{3\text{-}(500)}$, could have only occurred on these particularly defect sites.[178]

For further characterization, hydrogen and methane splitting on the γ-$Al_2O_{3\text{-}(500)}$ surface was performed, both experimentally and theoretically.[179] IR-spectroscopy played a major role in the experimental part, allowing *in situ* studies of the known heterolytic cleavage of the H-H and C-H bond by a number of alumina defect sites. The reaction of alumina with hydrogen gave rise to two different groups of IR-bands one in the 1850-1950 and a second one in 3500-3800 cm^{-1} region. The bands at 1902 and 1866 cm^{-1} were associated with the formation of Al_s-H species and those in 3800-3660 cm^{-1} with the formation of Al_s-OH species. These bands remained unchanged even after heating at 150 °C for 1h under H_2, or applying vacuum at room temperature for 1 h, which demonstrated the reaction consistency and irreversibility. Hydrolysis of the alumina treated with hydrogen for 2 h at 150 °C, yielded $1.24 \cdot 10^{-5}$ molH_2/g of solid, as a resault of the reaction of water and Al-H species. For a γ-$Al_2O_{3\text{-}(500)}$ having a specific surface area of 105 m^2/g the amount of Al-H and thereby of reactive sites is about 0.069 ± 0.003 site/nm^2. The number of active sites decreased when the surface was treated with water on 25 °C proving the difference in reactivity between the active sites.

Similar treatment of γ-$Al_2O_{3\text{-}(500)}$ surface on 25 °C with methane gave no significant change of the IR spectrum. More drastic treatment at 100 °C resulted with a formation of the aluminium methyl and aluminium hydroxyl species. Treatment with water of the so modified surface liberated $5.26 \cdot 10^{-6}$ molCH_4/g of solid what corresponds to 0.030 ± 0.003 Al_s-CH_3/nm^2.

The DFT calculations performed by Sautet et al. were in agreement with the experimental work. Al_{III} and Al_{IV} species gave a rise to an Al-H species trough out highly exo-energetic reactions (ΔE = -163 kJ/mol for the Al_{III}-site and -63 kJ/mol for the Al_{IV}-site). In the methane case only reaction with the highly active Al_{III}-species were found exo-energetic (ΔE = -25 kJ/mol).

The experimental and theoretical approach showed that defect sites were present on γ-$Al_2O_{3\text{-}(500)}$ surface. The reaction with H_2 occurred on a several Al atoms of low coordination numbers, Al_{III} and Al_{IV}, giving Al_{IV}-H and Al_V-H respectively. The CH_4 reacted selectively at 100 - 150 °C only on the more reactive Al_{III} sites forming the corresponding Al_{IV}-CH_3, in accordance with the lower number of active sites than in the case of H_2 (Only 0.030 site/nm^2, for H_2 0.06 site/nm^2 were detected).

5.2.3. The reaction mechanism and deactivation pathways

Coperet and coworkers had newly restarted the search for the active site in the MTO-γ-$Al_2O_{3\text{-}(500)}$ system, made by sublimation of MTO on a freshly prepared alumina.[181] Applying various analytic methods such as *in situ* - IR, solid state NMR EXAFS spectroscopy, and molecular modeling studies, they have succeeded in characterizing two different surface species described in Scheme 5.15.

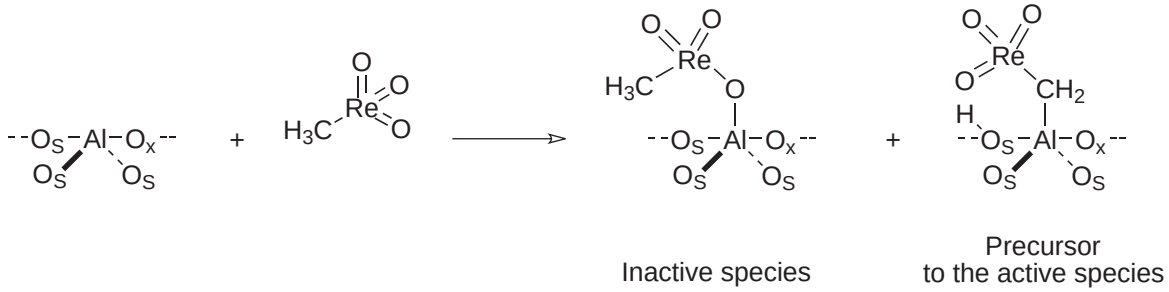

Scheme 5.15. Surface species resulting with grafting of MTO on γ-$Al_2O_{3\text{-}(500)}$[182]

The major species was formed with an interaction of one of the oxygen ligands of MTO with the Lewis acid sites of the surface. This $[(CH_3)O_2Re{-}O{-}Al_{Oh}]$, probably an inactive compound, embed 85 % of the total Re grafted on the surface. The remaining 15 % were actually responsible for the activity of the catalyst, making a $[O_3Re{-}CH_2{-}Al_{Oh}]$ species, with a C-H bond activation of the methyl group on the defect sites.[181]

Bearing a similar structure as the Tebbe reagent (see Section 5.1.2) the catalyst mechanism was derived from this, already in great detail studied, compound. The $[O_3Re{-}CH_2{-}Al_{Oh}]$ generated *in situ* the active carbene species $(O_2)(H_2C{=})Re{-}O{-}Al_{Oh}$, that reacted further with the olefins in the metathesis cycle (Scheme 5.16). This system trasformed 550 equiv of propene into a thermodynamic mixture of ethene and 2-butene, completing 190 turnovers in less than an hour, which is $\tilde{1}00$ times faster, compared to Re_2O_7/Al_2O_3.[181]

Unfortunately, this good catalytic activity was obtained only during the first hours of the catalytic reaction. When the metathesis of propene was performed at a higher flow rates of 77 ml/min (261 mol per mol of Re per min)) the conversion decreased from 12 % to 3 % in the first 710 min, reaching 0.03 % at 12000 min.[183] Modeling this phenomenon, Coperet et al. showed that the deactivation is first order in the concentration of the products especially ethene and butenes.[183] Possible deactivation pathways involving ethene as a catalyst poison, are sketched

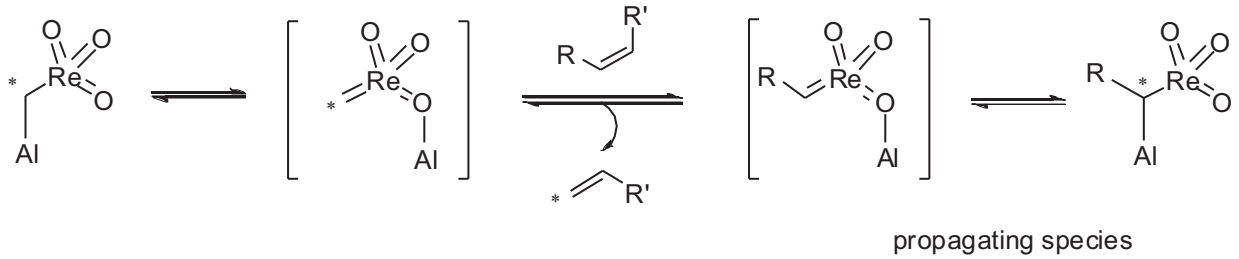

Scheme 5.16. The mechanism of the olefin metathesis with MTO-γ-$Al_2O_{3\text{-}(500)}$, as described by Coperet et al.[181]

in Scheme 5.17.

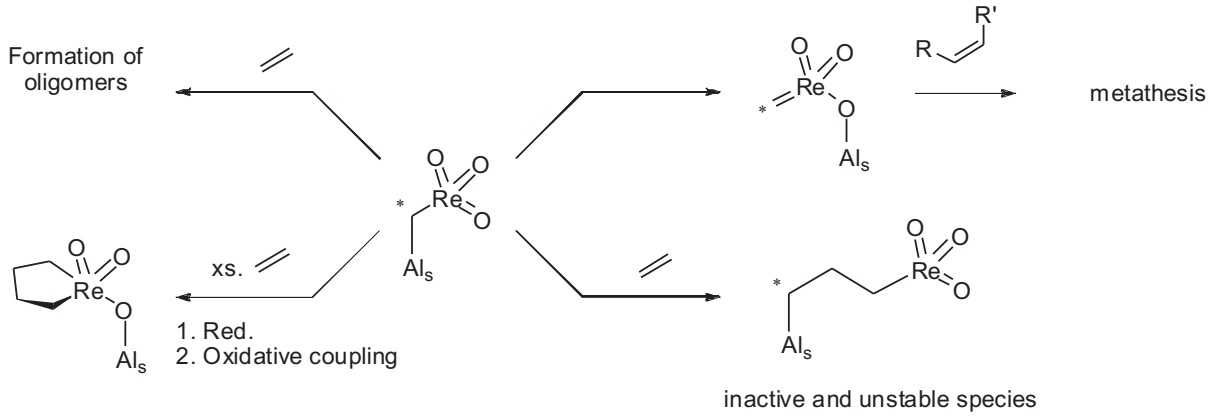

Scheme 5.17. Possible deactivation pathways of MTO-γ-$Al_2O_{3\text{-}(500)}$ with ethene[183]

The Coperet group excluded the formation of stable metallacyclopentane intermediate, as they couldn't find any spectral evidence to back up this theory. The formation of oligomers, as a reaction that occurs by contacting the alumina surfaces with ethene, could interfere with some active sites and deactivate them, but it was not considered as a main deactivation pathway. As third and likely most probable cause for deactivation the authors suggested the formation of a new Re species by an insertion of the ethene in the Al-C bond of the propagating species. Being not able to form the propagating species again, this new Re compound would quickly decompose, as common for the long chain trioxorhenium complexes, instantly destroying the active site.[184]

Further improvements of this system was achieved with silanisation of the surface hydroxyl groups with allyltrimethylsilane.[182] This approach decreased the adsorption of the metathesis product to the surface, decreasing simultaneously the unproductive metathesis pathway (isomerization of the product). Due to this feature the productive metathesis could be increased,

reaching 330000 TON per active site, which is to date the best result achieved with a rhenium-based catalyst.[182]

6. Synthesis and characterization of $CpMo(CO)_3CH_3$ on γ-$Al_2O_{3\text{-}(500)}$, a new, heterogeneous catalyst for the olefin metathesis

The understanding of the active species in the olefin metathesis catalyzed by MTO on γ-$Al_2O_{3\text{-}(500)}$ (see Section 5.2.2), opened a new application for complexes bearing [M−CH_3] groups. The immobilization of these complexes on alumina can lead to an activation of the CH-bond of the methyl group, creating a [M−CH_2−Al] species on the surface, which is accepted as an active intermediate for the olefin metathesis. Being aware of the high importance of Molybdenum compounds on alumina in the Phillips triolefin process (see Chapter 5), we assumed that grafting of $CpMo(CO)_3CH_3$ on γ-$Al_2O_{3\text{-}(500)}$ could lead to an active catalyst for metathesis as well.

6.1. An estimation of the pKa-Value of $CpMo(CO)_3CH_3$

To estimate the acidity of the methyl group of $CpMo(CO)_3CH_3$, the complex was first deprotonated, and subsequently deuteriated. The changes in the signal of the methyl protons during these consecutive reactions were monitored by ^{1}H- and ^{2}H-NMR spectroscopy.

Bases with different pKa values and different steric demand were used for the deprotonation, some of which are listed in Table 6.1. The deprotonated species reacted *in situ* with d^4-Methanol forming the deuterated, $CpMo(CO)_3CH_2D$, complex.

A clear reaction was only observed by using triethylamine as a base, predicting a pKa value of 10.7 for the $CpMo(CO)_3CH_3$ complex. No reaction of Pyridine with $CpMo(CO)_3CH_3$ was

Table 6.1: Base used for deprotonation of $CpMo(CO)_3CH_3$. pKa Values in DMSO are taken from the Bordwell pKa tables

Base	pKa
Triethylamine	10.7
Diisopropylamine	11.1
Pyridine	5.6
Lithium 2,4,6-*tert*-butyl-phenolate	10.0
2,2,6,6-tetramethyl piperidine	10.0

observed. A reaction with phenolate and piperidine proceeded unselectively, although they possess similar pKa values as triethylamine.

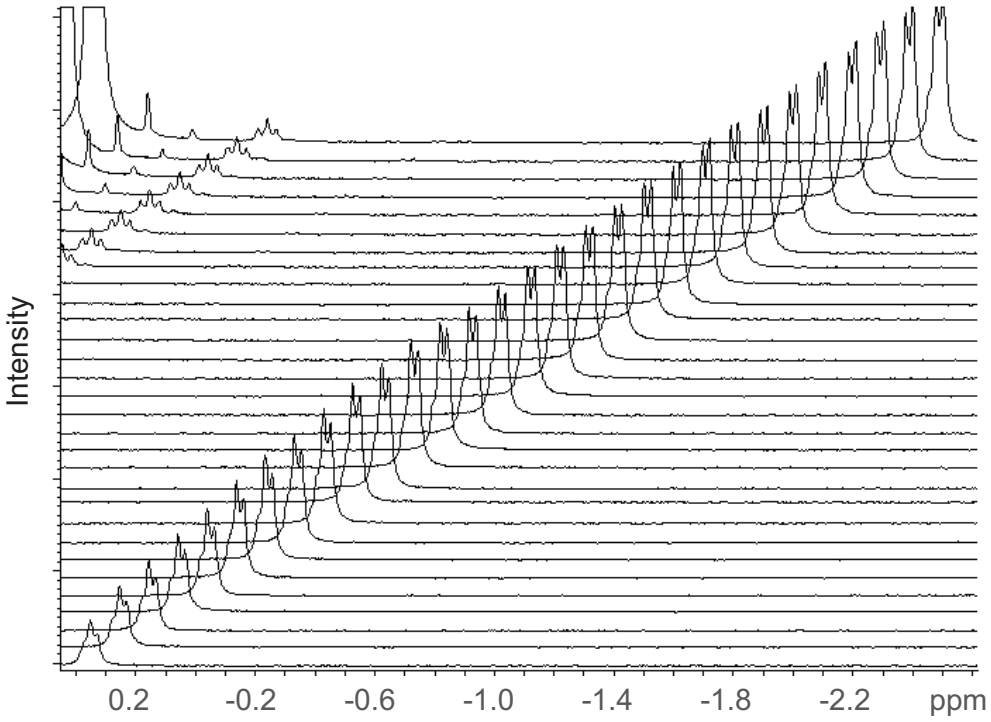

Figure 6.1. Hydrogen - Deuterium exchange on the methyl group of $CpMo(CO)_3CH_3$(0.34 ppm). Triethylamine is used as a base and methanol (D4) as a deuterium carrier.

The changes of the methyl signal in the first 10 h. using Triethylamine as base, were recorded by ^{2}H-NMR spectroscopy (Figure 6.1). As the reaction proceeded the deuterium signal not only gained on intensity but also changed its multiplicity. The triplet, formed in the first hour of the reaction, rearranged by the end of the measurement to a doublet, clearly indicating an H-D

exchange on more than one hydrogen of the methyl group.

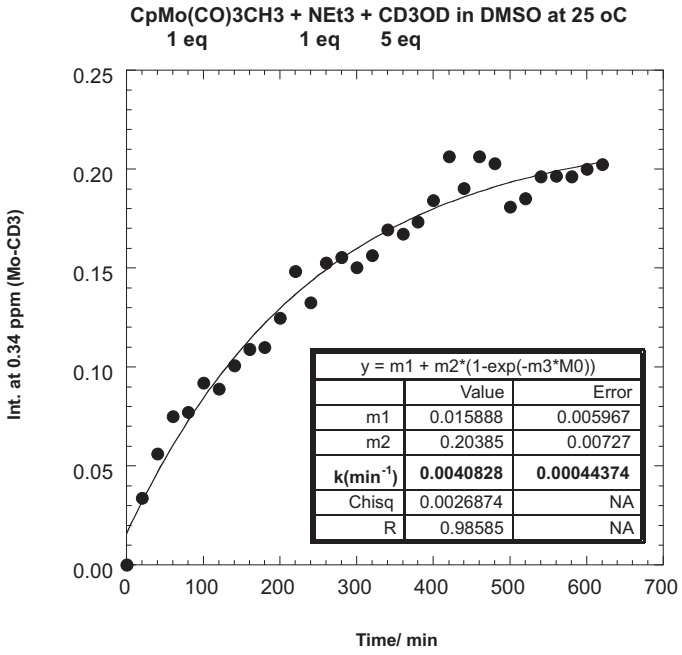

Figure 6.2. The deuteration of the methyl group is followed by NMR spectroscopy. The changes of the intensity of the signal at 0.34 ppm with time are measured. $CpMo(CO)_3CH_3$ (0.038 mmol) is deprotonated with Et_3N (0.038 mmol) in 0.4 ml DMSO using CD_4OD (0.19 mmol) as deuterium carrier

The meassured intensity against time data are shown on Figure 6.2 and fitted with a 1st-order exponential function $I_t = I_0 + I_\infty(1 - exp(k_{HD}t))$. The rate constant for the H-D exchange was calculated as $k_{HD} = (6.804 \pm 0.7395) \cdot 10^{-5}$ sec^{-1}.

The determined pKa value of 10.7 (according to the value of the corresponding Base - Triethylaluminum) for the $CpMo(CO)_3CH_3$ complex, indicated that its methyl group is acidic enough to be deprotonated on the surface of alumina (for a comparison, the methyl group of MTO has a pKa value of 7.5). With this value in mind, the grafting on $\gamma\text{-}Al_2O_3$ dehydroxylated at 500 °C (see Chapter 10 for details about the preparation) was initiated and followed by IR and NMR spectroscopy.

6.2. Spectroscopic characterization of $CpMo(CO)_3CH_3$ on $\gamma\text{-}Al_2O_{3\text{-}(500)}$

6.2.1. IR spectroscopy

$CpMo(CO)_3CH_3$ was sublimed at 60 °C under a static vacuum on a $\gamma\text{-}Al_2O_{3\text{-}(500)}$ pellet, which turned orange by the end of the reaction. The physisorbed complex was than removed by reverse sublimation and an IR spectrum was recorded. The spectra of the aluminum pellet before and after the reaction are shown in Figure 6.3.

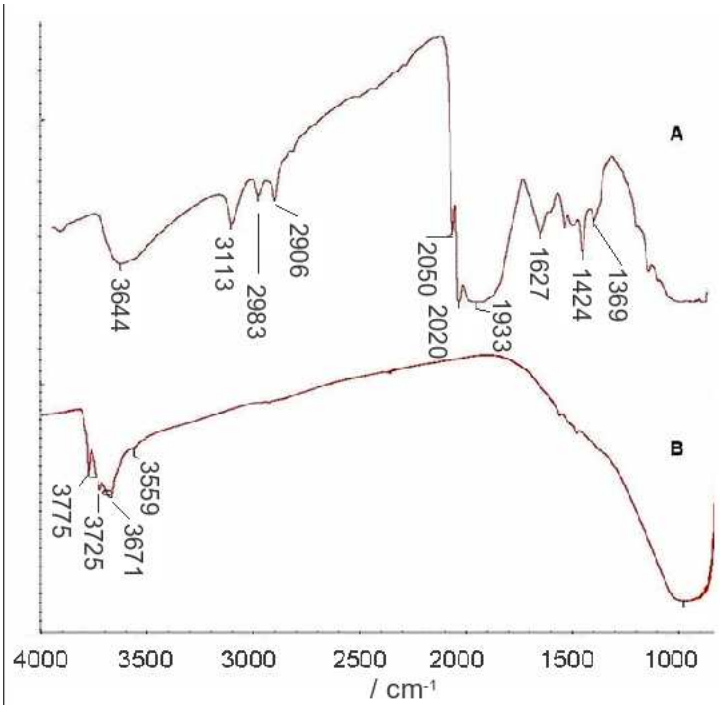

Figure 6.3. *in situ* IR-spectroscopy of the grafting of $CpMo(CO)_3CH_3$ on $\gamma\text{-}Al_2O_{3\text{-}(500)}$. **A)** after $CpMo(CO)_3CH_3$ was grafted and the physisorbed complex was removed by reverse sublimation; **B)** $\gamma\text{-}Al_2O_{3\text{-}(500)}$ after calcination and treatment at 500 °C under vacuum (10^{-5} mbar)

After the grafting procedure was completed, the familiar Al-OH bands (see Section 5.2.2 and Figure 5.5) disappeared and a new broad band centered at 3644 cm^{-1} appeared. This new band can be associate with the Al-OH groups in a new environment, interacting with the adsorbed molybdenum complex. Furthermore, three new, large signal groups corresponding to the grafted complex were also formed. The first one, containing three signals at 3113, 2983 and 2906 cm^{-1}, corresponds to the Cp-ring stretching frequency, already observed in the IR spectra of $CpMo(CO)_3CH_3$ in solution. The second group, shows three, not very well resolved

bands at 2050, 2020 and 1933 cm^{-1}, that can be associated with the terminal ν(C=O). The high adsorption of the carbonyl ligands made it impossible to distinguish between the various carbonyls on the surface, only by using IR spectroscopy.

In the third and final group, the bands at 1424 and 1369 cm^{-1} can be ascribed to the stretching frequency of the C-H bond. The signal at 1627 cm^{-1}, that doesn't exists in the initial solution spectrum of the complex, points out to a new species formed on the surface during the grafting procedure. A comparison of reactions between similar complexes and Lewis acids, revealed an insertion of one CO ligand into the [Mo−CH_3] bound, as a standard reaction under analog conditions.[185,186] The assumed acyl group [$COCH_3$] usually exhibits a CO stretching frequency in the range between 1550 and 1700 cm^{-1} and ist in agreement with the observed signal.[185,186] Considering the recorded IR spectra, the CO insertion may be one of the main reactions occurring during the grafting of the Molybdenum complex.

6.2.2. Mass balance analysis

The elemental analysis resulted in a Mo content of 1.6 wt% which corresponds to 1 Mo/nm^2, much lower than the hydroxyl group coverage of the $\gamma\text{-}Al_2O_{3\text{-}(500)}$ (approx. 4 OH/nm^2). The analysis of the gas phase, performed during the grafting procedure, showed no presence of Methane and carbon monoxide, proving that no bond breaking of the [M−CH_3] or [Mo−CO] bonds occurred.

6.2.3. Solid state NMR spectroscopy

The ^{1}H-NMR spectrum showed one narrow signal at 5.5 ppm (52 %), and a second very broad one, probably formed by the overlap of three separate signals at 2.7 ppm (16 %), 1.9 ppm (13 %) and 0.6 ppm (19 %), pointing to at least three different molybdenum species on the alumina surface.

The peak at 5.5 ppm clearly corresponds to the Cyclopentadienyl protons (5.29 ppm in solution) proving once again that the Cp - ligand remained unchanged during the grafting procedure. The peak at 0.61 ppm can be associated with the methyl group of $CpMo(CO)_3CH_3$ (in solution 0.36 ppm), physisorbed on the surface. Even after prolonged back-sublimation, this species couldn't be completely removed.

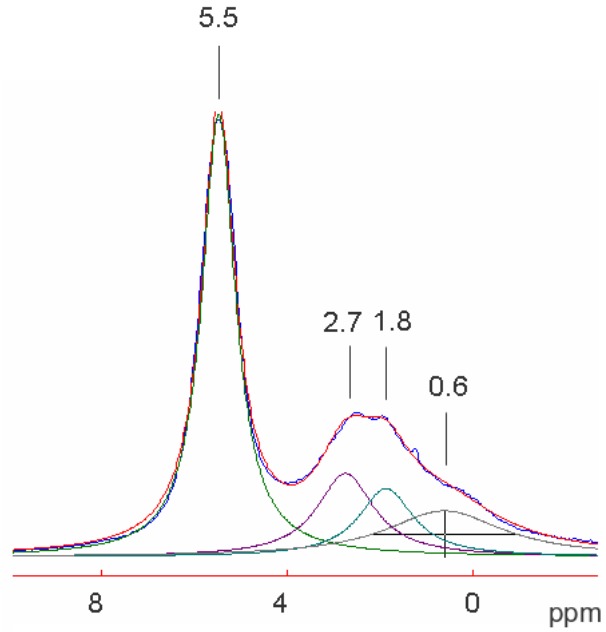

Figure 6.4. ^{1}H-NMR spectrum of $CpMo(CO)_3CH_3$ on $\gamma\text{-}Al_2O_{3\text{-}(500)}$

The additional two signals are not common for the Molybdenum complex in solution, and can only be derived from surface species formed during the grafting procedure. Considering the Lewis acid catalyzed CO insertion as a standard reaction for similar molybdenum complexes in solution, the shift of the methyl signal downfield in the spectrum could be due to a formation of Molybdenum acyl complex (**I** in Scheme 6.1). The same behavior was observed for the analog iron methyl carbonyl, $CpFe(CO)_2CH_3$, grafted on alumina.[187]

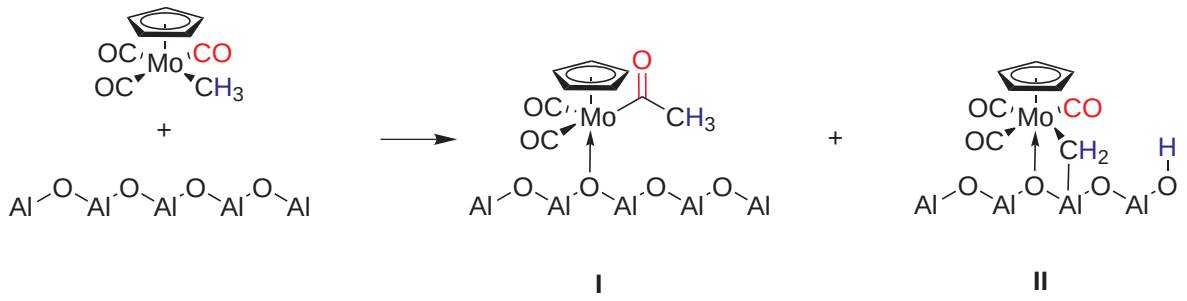

Scheme 6.1. Various molybdenum species formed on $\gamma\text{-}Al_2O_{3\text{-}(500)}$ after the grafting of $CpMo(CO)_3CH_3$ complex (The physisorbed species not included)

Further characterization of the novel surface species was done by quantitative single-pulse proton-decoupling, ^{13}C magic angle spinning (MAS) solid-state NMR-spectroscopy. The spectrum showed only one strong signal at 84 ppm, corresponding to the Cp-ligand. Due to the low surface coverage, the signals for the methyl group could not be detected. To improve the

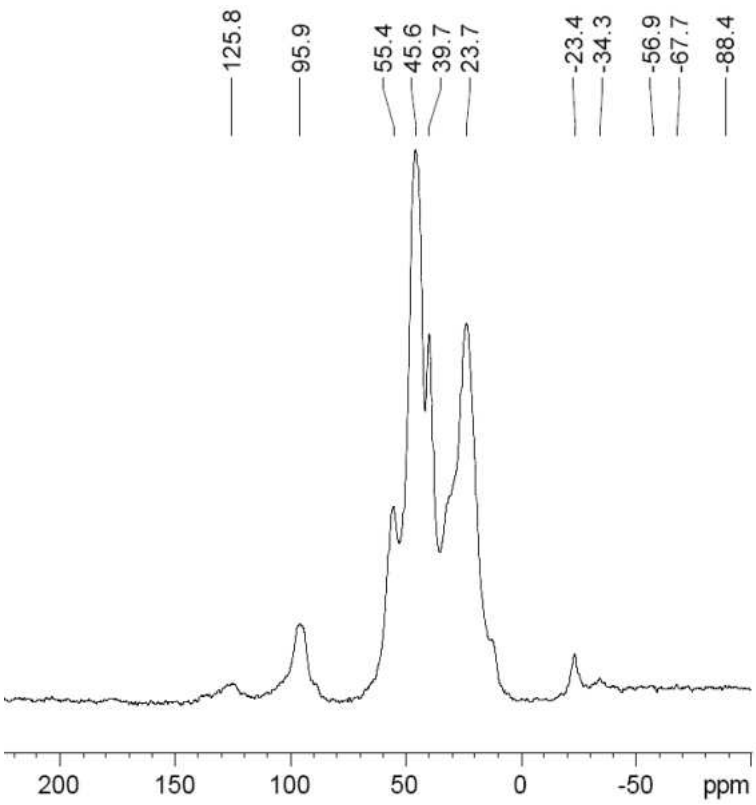

Figure 6.5. ^{13}C-MAS solid state NMR spectrum of $CpMo(CO)_3{}^{13}CH_3$ on $\gamma\text{-}Al_2O_{3\text{-}(500)}$ under MAS of 10 kHz, pulse angle of 45°.The number of scan was 34596 and the recycle delay was set to 2 sec

spectral resolution, the ^{13}C labeled complex $CpMo(CO)_3{}^{13}CH_3$ was synthesized and grafted on alumina, under the same conditions applied for the unlabeled compound. The recorded ^{13}C MAS solid state NMR revealed three new peaks not observed in the NMR spectrum of the unlabeled compound (Figure 6.5).

The signal at 45.6 ppm, which is not present in the ^{13}C solution spectrum of $CpMo(CO)_3CH_3$, coresponds to the acyl species **I** formed on the alumina, as expected considering the results of the IR and ^{1}H-NMR spectroscopy. Furthermore, the signal is identical to the signal observed for the acyl group of $CpFe(CO)_2CH_3$ immobilized on alumina (45.2 ppm).[187] The two satellites of this signal at 55.4 and 39.7 ppm can be assigned to $CpMo(CO)_3CH_3$ coordinating on different Lewis acid sites of alumina through its acyl group.

The signal at 23.7 ppm coresponds to the active [Mo−CH_2−Al] species (**II**) on $\gamma\text{-}Al_2O_{3\text{-}(500)}$. Although, these methylidene complexes usually have signals in the downfield NMR region, there are enough examples in the literature showing exceptions of this rule.[188] The signal at -23.4 is assigned to the methyl group of the physisorbed complex.

To find the corresponding ^{1}H-NMR peaks, to these new appeared signals, the 2D-HETCOR

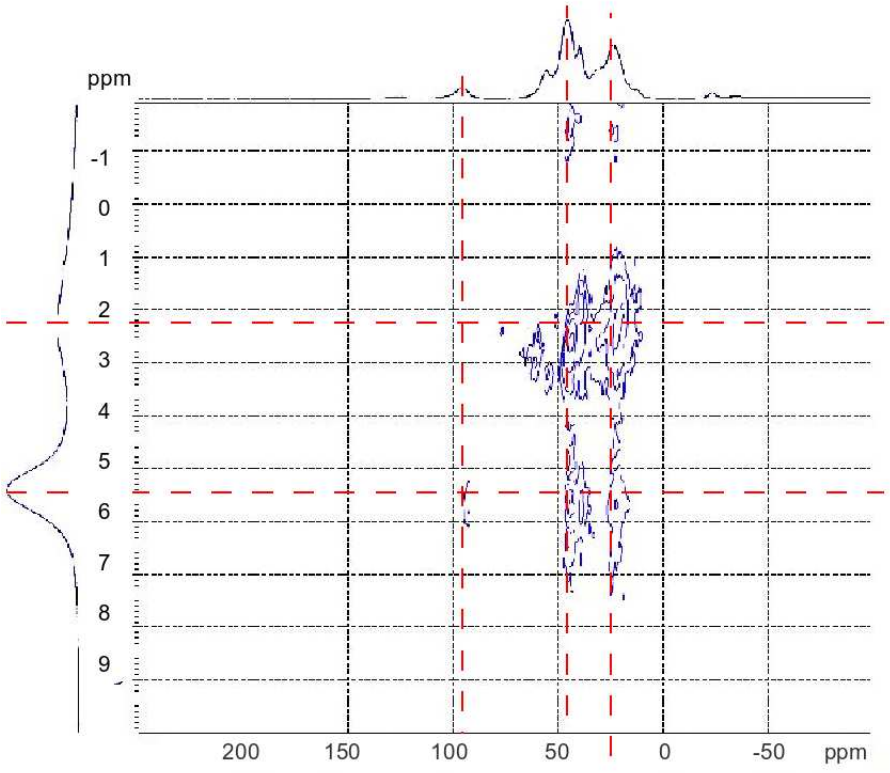

Figure 6.6. 2D-HETCOR solid state NMR spectrum of $CpMo(CO)_3{}^{13}CH_3$ on $\gamma\text{-}Al_2O_{3\text{-}(500)}$. The number of scan was 1024 and the recycle delay was set to 2 sec

NMR was recorded (Figure 6.6). As assumed, the signal at 5.5 ppm clearly corresponds to the one at 84 ppm as a signal for the cyclopentadienyl ligand. The two signals at 23.7 and 45.6 ppm are clearly in relation with the broad signal at around 2 ppm. Unfortunately, the bad resolution in the ^{1}H-solid state NMR spectrum hinders further characterization of these surface species.

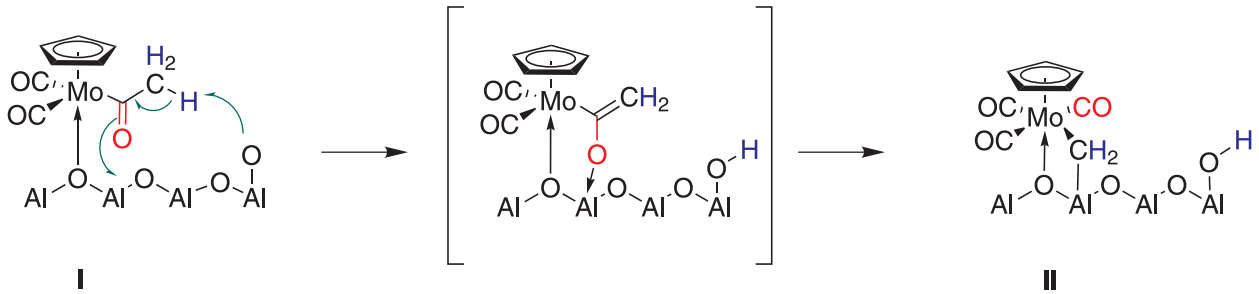

Scheme 6.2. Possible reaction of the surface species **I** with alumina surface, based on the ^{13}C-MAS solid state spectra

In order to gain more information and diversity about the $CpMo(CO)_3{}^{13}CH_3$ -compound on $\gamma\text{-}Al_2O_{3\text{-}(500)}$ ^{13}C-MAS NMR spectrum of the same, was measured again, five months after the

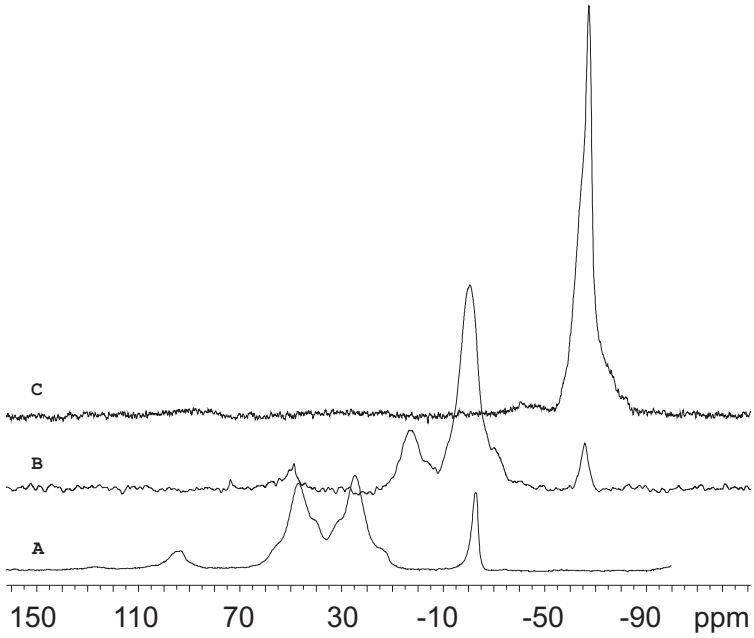

Figure 6.7. ^{13}C-MAS solid state NMR spectrum of $CpMo(CO)_3{}^{13}CH_3$ on $\gamma\text{-}Al_2O_{3\text{-}(500)}$. (**A**) The initial ^{13}C-MAS-NMR spectrum, recorded shortly after the grafting procedure; (**B**) ^{13}C-MAS-NMR spectrum recorded 5 months after the grafting under MAS of 12 kHz. The number of scan was 40951 and the recycle delay was set to 2 sec; (**C**) ^{13}C-MAS solid state NMR spectrum recorded 12 months after the grafting under MAS of 12 kHz, 40951 scans and recycle delay of 2 sec

grafting was performed. A slow disappearance of the signal at 45.6 ppm, accompanied with an increase in signal intensity at 23.7 ppm were the main changes in the spectra. This surface rearrangement was followed continuously and finished with a complete disappearance of the signal at 45.6 ppm one year after the grafting of $CpMo(CO)_3{}^{13}CH_3$ on $\gamma\text{-}Al_2O_{3\text{-}(500)}$.

This slow transformation of complex **I** to **II** is probably initiated, with a deprotonation of the methyl group[Mo−$COCH_3$] by the aluminum surface shown in Scheme 6.2. The newly formed double bond further reacted with the Lewis acidic centers of alumina, building the [Mo−CH_2−Al] moiety and reversing the CO - insertion.

6.3. Propene metathesis with $CpMo(CO)_3CH_3$ on $\gamma\text{-}Al_2O_{3\text{-}(500)}$

$CpMo(CO)_3CH_3$ on $\gamma\text{-}Al_2O_{3\text{-}(500)}$, converts 257 equivalents of propene per mmol Mo to a mixture of ethene and but-2-ene in two days. This is the first example of a molybdenum catalyst

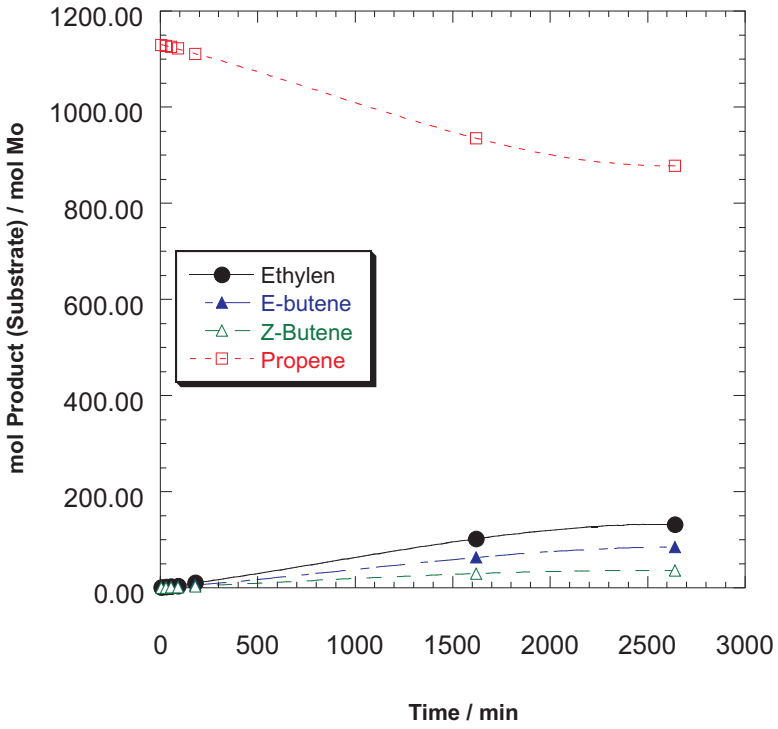

Figure 6.8. The amount of converted propene and produced olefin respectively, pro mMol of molybdenum, as a function of time. Reaction using 50 mg of $CpMo(CO)_3CH_3$ on $\gamma\text{-}Al_2O_{3\text{-}(500)}$ and 0.01 mol of propene

immobilized on alumina displaying an activity in the olefin metathesis at room temperature without any preactivation.

A closer examination of the reaction course in the first 200 min (see Figure 6.9), revealed considerable differences in the reaction rate. The first 100 min were characterized by a very dull reaction progress that abruptly changed in the following hour. The new reaction rate was than maintained without any significant changes, for the next 24 h. This reaction behavior can be associated with a rearrangement of the structure of the immobilized complex, or formation of another, more active species during the reaction.

After the first 24 h the reactor was evacuated and the same amount of propene was introduced to the catalyst again. Exactly the same reaction progress, as in the first cycle, was observed (see Figure 6.9). These catalytic results can be taken as evidence for a short lived active species, formed at the beginning of the catalysis, which is active as long as an olefin is available. After the reaction is completed, the catalyst rearranges back in its initial resting state, that can be reactivated by further addition of the olefin.

In the first 10 min of the reaction, ethane was the main metathesis product with a selectivity

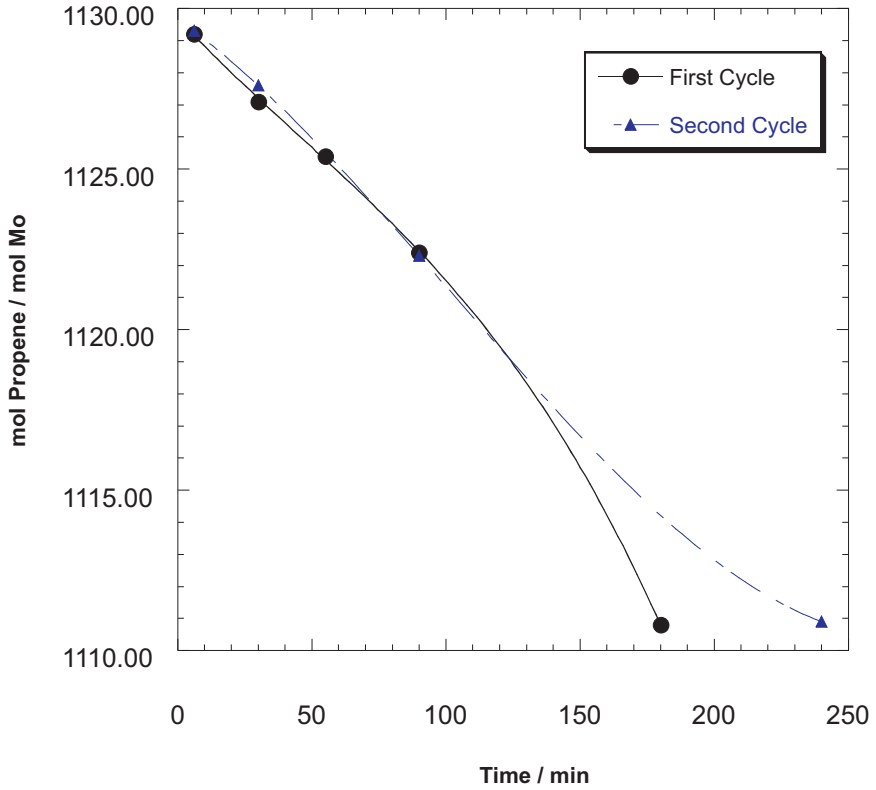

Figure 6.9. The amount of converted propene per Mol of molybdenum as a function of time, in the first 240 min of the catalysis in the first and second cycle, respectively

of 81.5 % (Figure 6.11). With the mechanism of the olefin metathesis kept in mind, the catalytic species active at the beginning of the reaction, should have a molybdenum alkylidene group as a promoter of the reaction. This is a unique structural feature which allows ethene formation at the beginning of the metathesis, before longer chain alkenes can be produced. As the reaction proceeded, E- and Z-Butene are detected as well, but neither in the thermodynamic ratio of (3:1) nor in the statistical one (1:1). Instead, a E/Z selectivity of 1.7 is found (Figure 6.11), which could correspond to the true selectivity of the catalyst. The E to Z ratio slowly reaches the thermodynamic equilibrium by the end of the reaction due to isomerization reactions on the surface and on the active site (unproductive metathesis).

Experiments for the application of $CpMo(CO)_3CH_3$ on $\gamma\text{-}Al_2O_{3\text{-}(500)}$ as a catalyst in the olefin metathesis of functionalized olefins were conducted as well, in a batch reactor with ethyloleate, as a typical substrate for this type of reactions. No metathesis products were observed even after several days of reaction. This is consistent with previous results on molybdenum systems, which are very efficient catalysts for the metathesis of olefins without functional groups, but show a dramatic decline in activity when functional groups are present in the system.

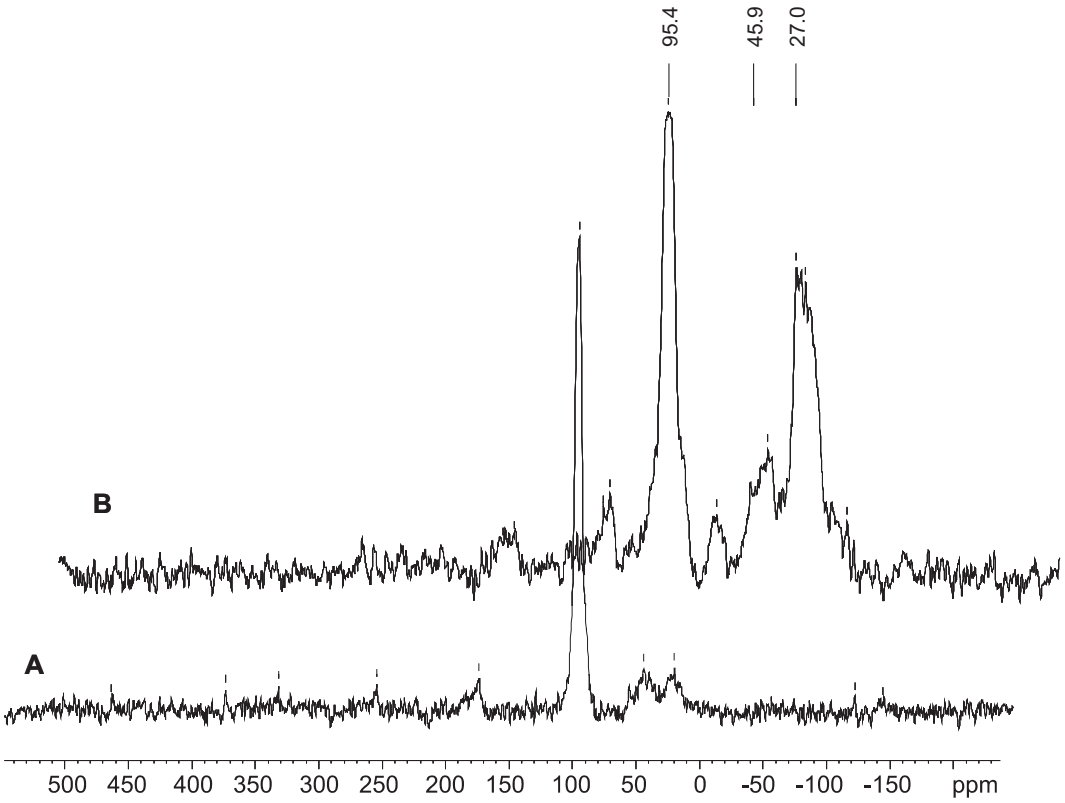

Figure 6.10. ^{13}C-MAS solid state NMR spectrum of $CpMo(CO)_3CH_3$ on $\gamma\text{-}Al_2O_{3\text{-}(500)}$ [**A**] before the metathesis of di-labeled ethene and [**B**] after metathesis of di-labeled ethene. MAS of 10 kHz and a pulse angle of 45° were used. The number of scans was 36664 and the recycle delay was set to 2 sec

6.3.1. Metathesis of ^{13}C-di-labeled ethene with $CpMo(CO)_3CH_3$ on $\gamma\text{-}Al_2O_{3\text{-}(500)}$

The metathesis reaction was also conducted with ^{13}C-di-labeled ethene (0.012 mmol per Mo) as a substrate using the unlabeled complex as a catalyst. After 24 h of reaction, a part of the catalyst was taken out of the reactor and analyzed by ^{13}C-MAS solid state NMR spectroscopy.

This used catalyst displays two major signals that were already present in the previous spectra with the labeled compound (see Figure 6.5 and Figure 6.7). The signal at 95.4 ppm previously assigned to the Cp ring of the grafted complex, and a broad signal at 27 ppm assigned to the molybdenum methyliden species **II**. The signal assigned to the acyl compound at 45.9 ppm is also present but it has a very low intensity. Knowing, that only the surface species active in metathesis can be labeled with ^{13}C - atoms originating from the substrate, **II** is as expected the active site of the $CpMo(CO)_3CH_3$ - $\gamma\text{-}Al_2O_{3\text{-}(500)}$.

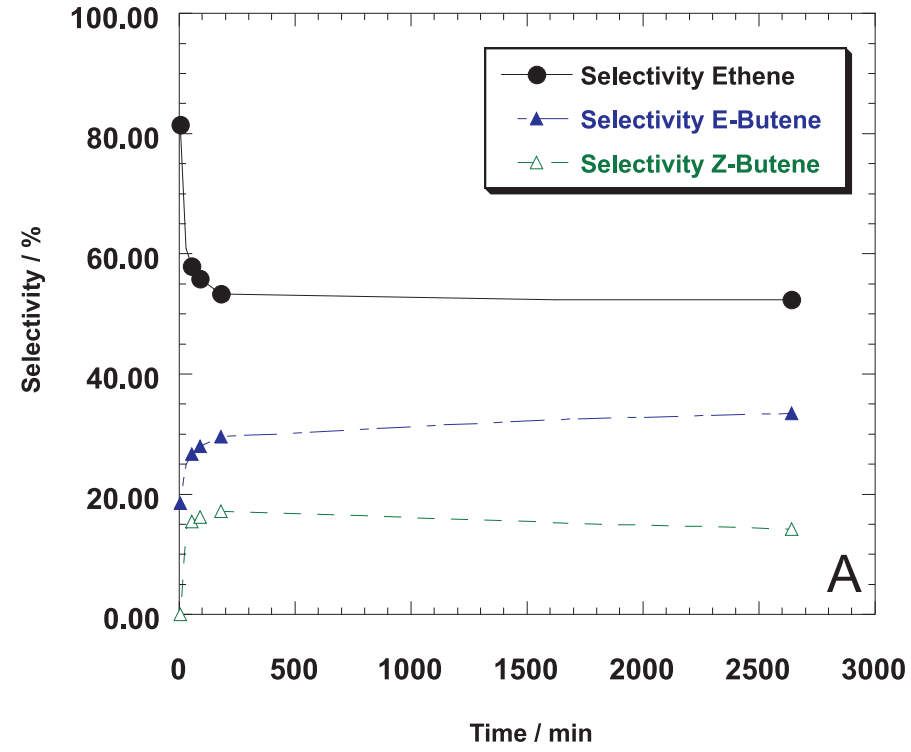

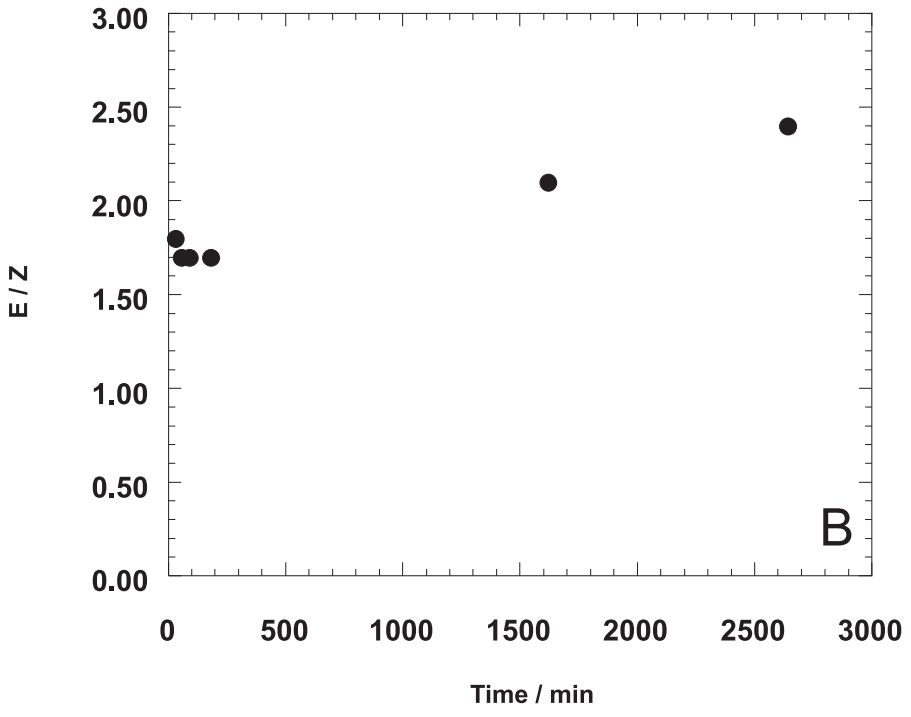

Figure 6.11. Propene metathesis in a batch reactor. Reaction using 50 mg of $CpMo(CO)_3{}^{13}CH_3$ on $\gamma\text{-}Al_2O_{3\text{-}(500)}$ and 0.01 mol of propene. **A** Selectivity as a function of time. **B** E/Z ratio as a function of time

7. Synthesis and characterization of $(CH_3)_3ReO_2$ on γ-$Al_2O_{3\text{-}(500)}$, a new heterogeneous catalyst for the olefin metathesis

Soon after the importance of MTO on γ-$Al_2O_{3\text{-}(500)}$ as a catalyst in olefin metathesis (see Section 5.2.2) was realized, a quest for alternative Rhenium complexes started. The biggest disadvantage of the MTO - γ-$Al_2O_{3\text{-}(500)}$ system to cope with, was its rapid deactivation. As previously discussed, in Section 5.2.2 and Scheme 5.17, the deactivation is induced by a coordination of ethene to the metal center and its insertion in the metal - metylidene bond. The so-formed, unstable, propyliden species is not able to propagate the metathesis further, and the active site is destroyed.

Inert to structural changes, $(CH_3)_3ReO_2$ could provide an alternative Rhenium source on alumina, minimizing the ethene coordination and rearrangement reaction, respectively. On the other hand, the methyl groups should be acidic enough to be deprotonated and could give rise to an active catalyst on γ-$Al_2O_{3\text{-}(500)}$.

7.1. Spectroscopic characterization of $(CH_3)_3ReO_2$ on γ-$Al_2O_{3\text{-}(500)}$

7.1.1. IR spectroscopy

in situ - IR spectroscopy was performed on a $(CH_3)_3ReO_2$ sublimed on γ-$Al_2O_{3\text{-}(500)}$ pellet at 25 °C. The IR spectrum of the surface, before and after immobilization are shown in Figure 7.1.

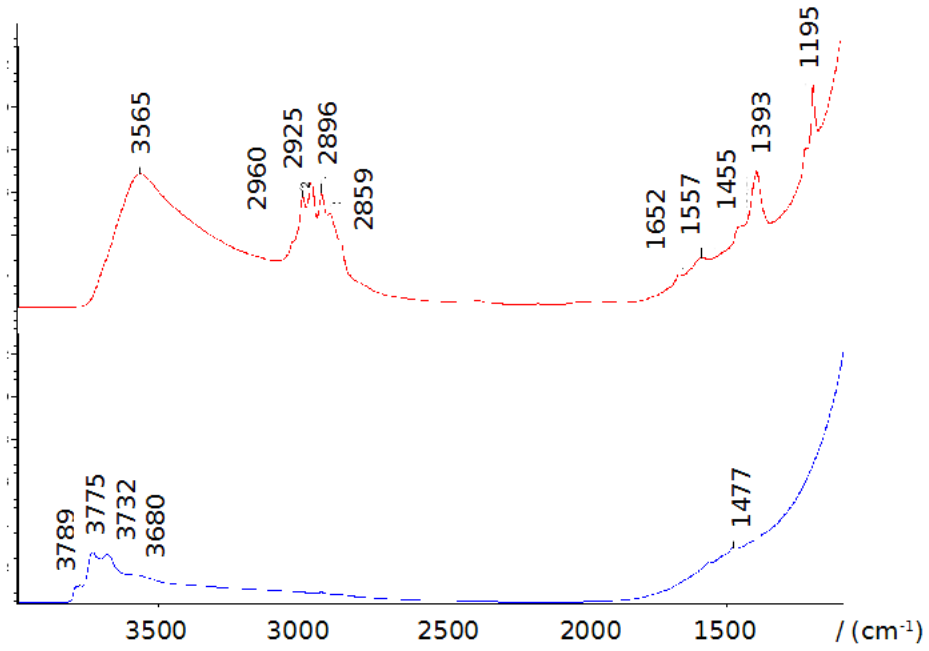

Figure 7.1. *in situ* IR-spectroscopy of the grafting of $(CH_3)_3ReO_2$ on γ-$Al_2O_{3\text{-}(500)}$. The spectrum on the bottom shows γ-$Al_2O_{3\text{-}(500)}$ after calcination and treatment at 500 °C under vacuum (10^{-5} mbar. The top one shows the aluminum surface after $(CH_3)_3ReO_2$ was grafted and the physisorbed complex was removed by reverse sublimation

The characteristic signals between 3680 - 3789 cm^{-1} showing the five different hydroxyl groups on the surface of γ-$Al_2O_{3\text{-}(500)}$ disappeared after the grafting, and a new, broad signal at 3565 cm^{-1} appeared. This signal derives from the surface hydroxyl groups interacting with the newly immobilized complex.

The multiplet that appeared in the region of 2960 - 2859 cm^{-1} is representative for the asymmetric C-H vibration of the methyl groups of $(CH_3)_3ReO_2$ immobilized on γ-$Al_2O_{3\text{-}(500)}$.[189] The deformation vibrations are to be found in the signals at 1453 and 1393 cm^{-1}.

7.1.2. Mass balance analysis

The elemental analysis reveals a Re content of a 1.6 wt% which corresponds to 0.51 Re/nm^2, much lower than the hydroxyl group coverage of the γ-$Al_2O_{3\text{-}(500)}$ (approx. 4 OH/nm^2). The analysis of the gas phase, performed during the grafting procedure, showed no presence of methane, proving that no bond breaking of the [M−CH_3] bonds occurred.

7.1.3. NMR spectroscopy

The grafted complex was analyzed only by ^{1}H - solid state NMR spectroscopy that showed four different signals. Two of them, at 0.3 and 2.4 ppm, are representative for the methyl groups of $(CH_3)_3ReO_2$ coming at the same position as the signals in the solution spectra. The two other observed signals shifted downfield to 8.3 and 7.0 ppm respectively, are not existing in the solution NMR and a probably related to the rhenium species formed on the γ-$Al_2O_{3\text{-}(500)}$ (see Scheme 16.1). The existence of a carbene Species on the surface must be taken in to the account, considering the downfield shift of these signals, especially the one at 8.3 ppm.

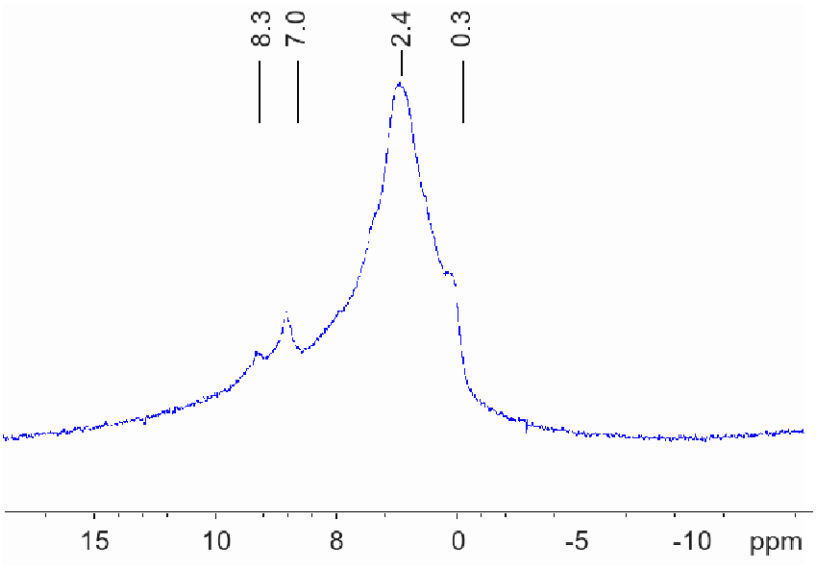

Figure 7.2. ^{1}H-NMR spectra of $(CH_3)_3ReO_2$ on γ-$Al_2O_{3\text{-}(500)}$

7.2. Propene metathesis with $(CH_3)_3ReO_2$ on γ-$Al_2O_{3\text{-}(500)}$

The $(CH_3)_3ReO_2$ on γ-$Al_2O_{3\text{-}(500)}$ catalyst converts 250 (mol Propene)/(mol Re) in a batch reactor in 31 h, producing a mixture of ethene and 2-butene. The initial TOF is 2.6 mol of

Propene permol Re per min (Figure 7.3).

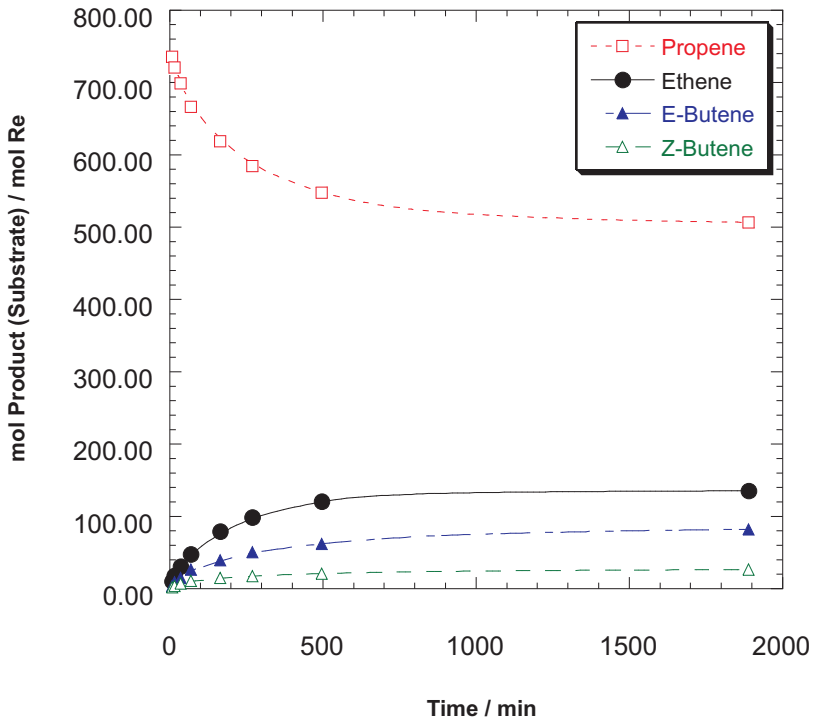

Figure 7.3. The amount of converted propene and produced olefin respectively, pro mol of Rhenium, as a function of time. Reaction using 80 mg of $(CH_3)_3ReO_2$ on γ-$Al_2O_{3\text{-}(500)}$ and 0.01 mol of propene

Ethene was the main product at the beginning of the reaction with 63 % product share, a behavior observed with catalysts, containing [M=CH_2] bond as an initial catalytic species. As the reaction proceeded E and Z - butene were produced as well, with an initial E/Z ratio of 2.4 (see Figure 7.4). Secondary isomerization steps occurring on the alumina surface and in the gas phase induced further changes in the initial ratio, driving it to 3.1 by the end of the reaction.

7.3. Propene metathesis with $(CH_3)_3ReO_2$ on γ-$Al_2O_{3\text{-}(500)}$ in a flow reactor

$(CH_3)_3ReO_2$ on γ-$Al_2O_{3\text{-}(500)}$ was also used as a catalyst in a flow reactor at 30 °C and a flow rate of 400 ml/min (2507 mol/mol Re · min) see Figure 7.5. Under these conditions the catalysts made 120 turnovers in the first 6 min of the reaction which yields TOF of 20 mol(Propene) per mol of Re per min. All calculations were performed taking into account the overall Re coverage on the surface. Assuming that the actual active site made up only around 10 % of the total

amount of metal on the surface, the initial activity of a single active site should be 10 times greater than the calculated value. This fact emphasized $(CH_3)_3ReO_2$ on γ-$Al_2O_{3\text{-}(500)}$ as one of the most active catalyst for olefin metathesis on rhenium basis (see Table 7.1 for comparison).

Table 7.1: Comparison of the rhenium based heterogeneous catalysts for the olefin metathesis[190,181]

Catalyst	Converted propene / equiv.	TOF / min^{-1}
Re_2O_7/Al_2O_3	163	-
$(CH_3)_3ReO_2/\gamma$-$Al_2O_{3\text{-}(500)}$	250	2.6
MTO/γ-$Al_2O_{3\text{-}(500)}$	500	11

Over 1600 min the catalyst converts 5366 mol of Propene per mol of Re while the conversion decreases from 1.6 to 0.03 % by the end of the reaction, showing a rapid catalyst deactivation. Following the conversion as a function of time (Figure 7.6), an exponential decay can be observed, with highest conversion decrease of 60 % in the first 50 min of the reaction. Similar behavior was observed for the MTO on γ-$Al_2O_{3\text{-}(500)}$ catalyst as well, showing similarities between these two Rhenium systems.

Another feature common to the two catalytic systems is the selectivity (Figure 7.7 and Section 5.2.2). In both cases, the E/Z value decreases with decrease in the conversion, reaching 0.38 at a conversion of 0.03 % in the case of $(CH_3)_3ReO_2$ on γ-$Al_2O_{3\text{-}(500)}$. Considering the detailed observation of the MTO-γ-$Al_2O_{3\text{-}(500)}$ system by Coperet et al., this value can represent the intrinsic selectivity of the active site.[183] The need of calculating this intrinsic selectivity at low conversions, is due to the strong adsorption of olefins on the aluminum surface. The adsorbed olefins undergo an isomerization reaction, on the Lewis acidic alumina support and on the catalyst (secondary process) respectively. The isomerization rate due to the secondary, unproductive metathesis reactions is 15 times faster than the isomerization on the support, making the activity of the catalyst responsible for the isomerization reactions.[183] Being able to desorb the products immediately after the [2+2] - cycloreversion is done, can lead to less secondary processes and probably a higher catalytic activity (this has been already demonstrated by Coperet et al. on the MTO - γ-$Al_2O_{3\text{-}(500)}$ system.[182]).

Although the E product is the favored isomer by the metathesis of terminal olefins, Basset

et al. showed that this is not always the case with catalysts on alumina surfaces, were the Z isomer was preferred.[191] An explanation of this behavior can be found in the olefin approach to the catalyst, were the substituents are showing away from the sterically demanding surface.

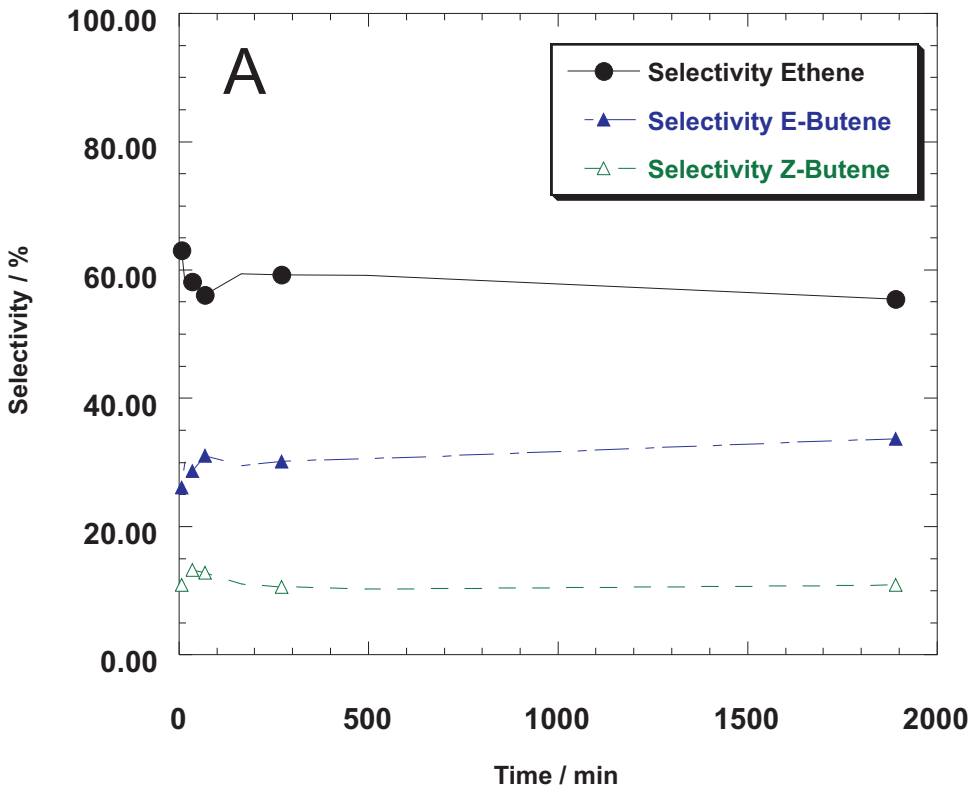

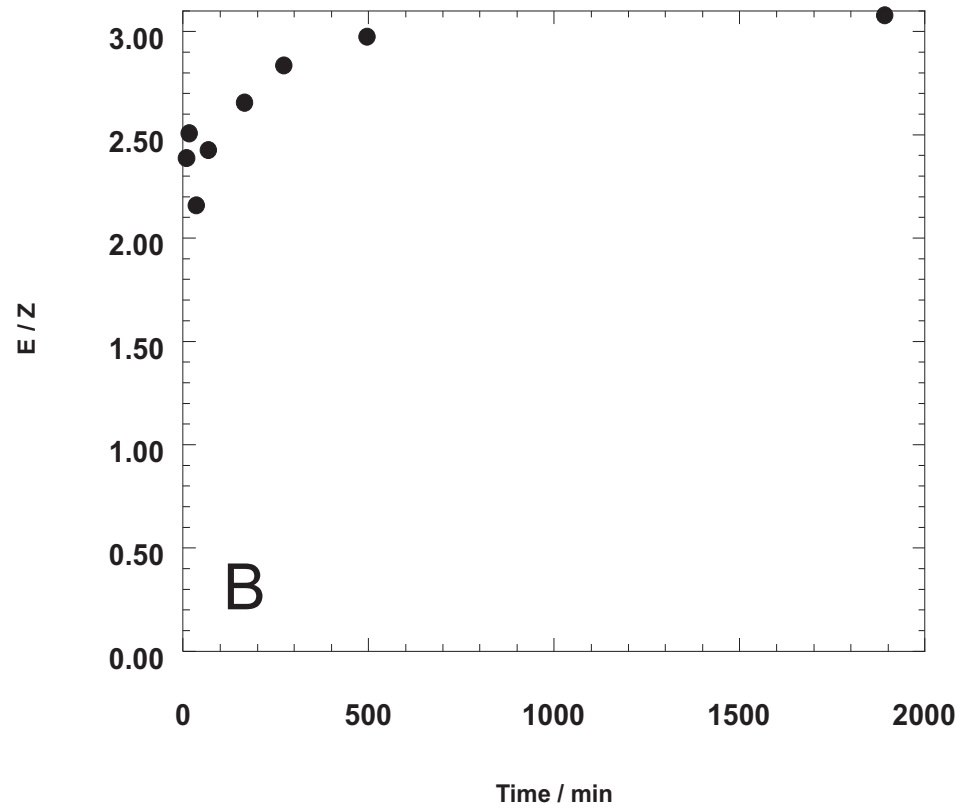

Figure 7.4. Selectivity as a function of time. Reaction using 80 mg of $(CH_3)_3ReO_2$ on γ-$Al_2O_{3\text{-}(500)}$ and 0.01 mol of propene. **A** Selectivity as a function of time. **B** E/Z ratio as a function of time

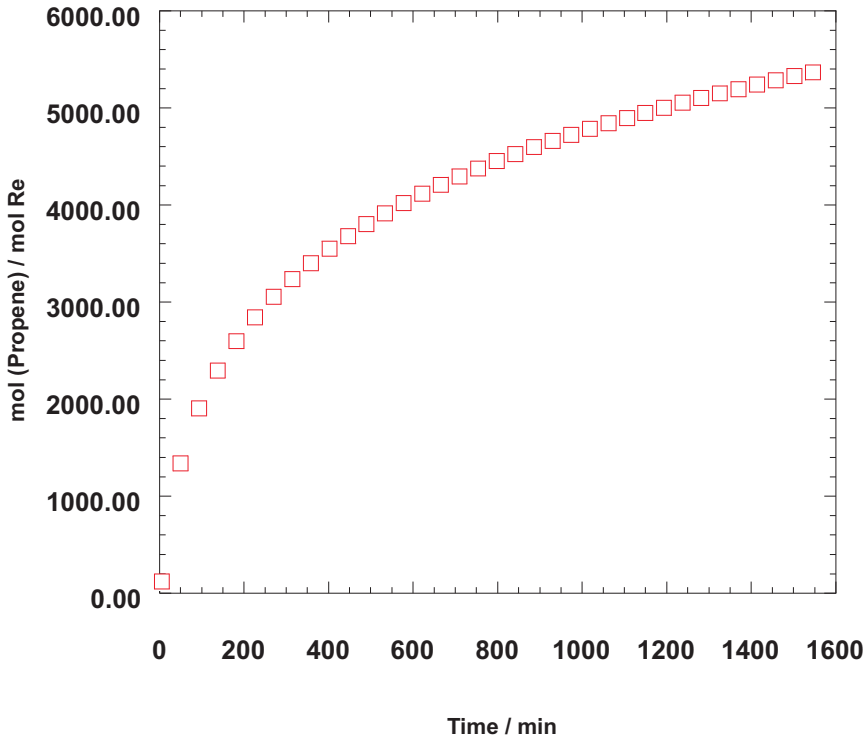

Figure 7.5. Propene metathesis in a flow reactor. 400 ml/min Propene (2507 mol (propene)/(mol of Re) · min, 1 atm. pressure, and 70 mg of $(CH_3)_3ReO_2$ on γ-$Al_2O_{3\text{-}(500)}$. Conversion of Propene per mol of Re with time

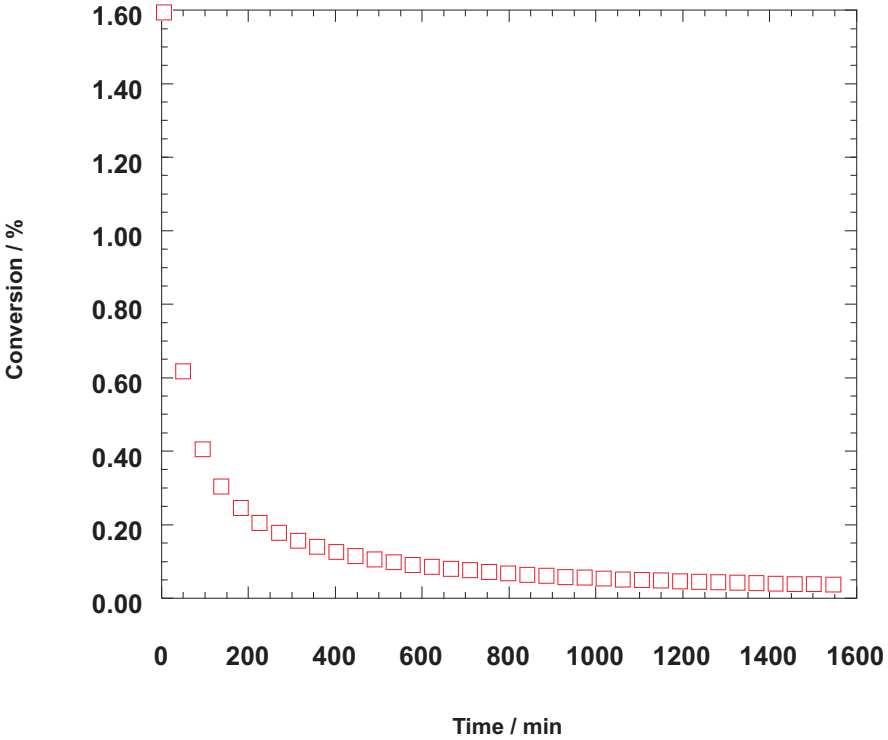

Figure 7.6. Propene conversion as a function of time in a flow reactor. 400 ml/min Propene (2507 mol (propene)/(mol of Re) · min, 1 atm. pressure, and 70 mg of $(CH_3)_3ReO_2$ on γ-$Al_2O_{3\text{-}(500)}$

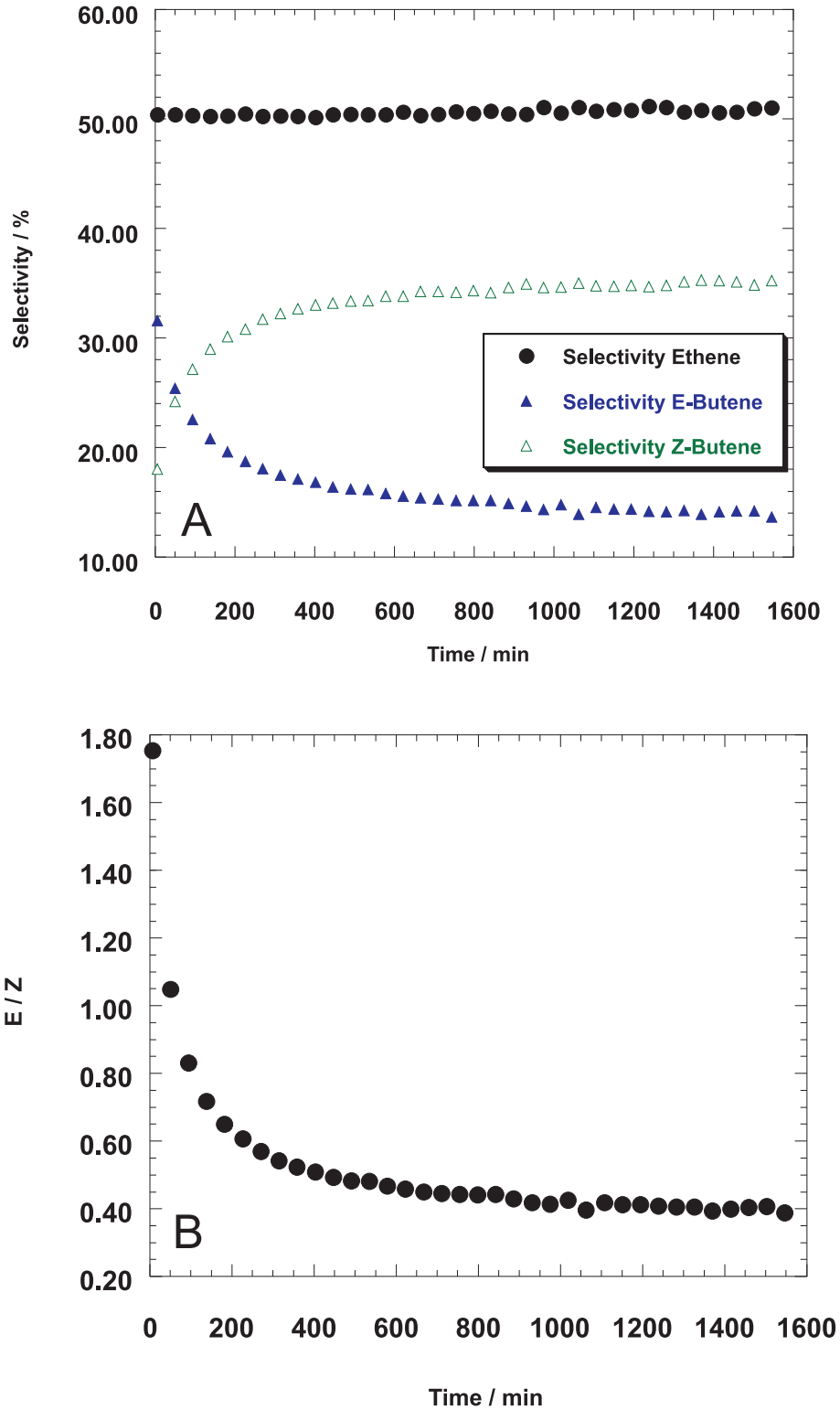

Figure 7.7. Selectivity as a function of time. Propene metathesis in a flow reactor 400 ml/min Propene (2507 mol (propene)/(mol of Re) · min, 1 atm. pressure, and 70 mg of $(CH_3)_3ReO_2$ on γ-$Al_2O_{3\text{-}(500)}$. **A** Selectivity as a function of time. **B** E/Z ratio as a function of time

Part III.

Experimental procedures

8. General procedures

All experiments were conducted under strict inert atmosphere using standard Schlenk technique. All solvents, with exception of THF that was purified by standard procedures and distilled prior to use, were derived from MBraun solvent purification system. Cyclooctene and β-methoxystyrene (Aldrich) were used as received without further purification. TBHP (Aldrich, 5.0-6.0 M solution in decane) was used after drying over molecular sieves to remove the residual water (< 4 % when received). Acylperrhenate was always synthesized new, prior to use, as already described in literature.[45] The $CpMo(CO)_3CH_3$ was synthesized and purified using a slightly modified literature method.[115,92] Elemental analysis were performed both, at the CNRS Central Analysis Service of Solaize (Re) and at the Mikroanalytisches Labor of the Technische Universität München (Mo). Gas phase analysis was performed on a Hewlett-Packard 5890 series II gas chromatograph equipped with a flame ionization detector and an KCl/Al_2O_3 on fused silica column (50 m X 0.32 mm). UV-VIS spectra were measured on JASCO UV-Vis V-550 Spectrophotometer. Transmission electron microscopy (TEM) data were recorded on a JEOL JEM2010 operating at 120 kV.

8.1. IR spectroscopy

The Infrared measurements of the complexes grafted on Alumina, were carried on a Nicolet 550-FT spectrometer by using an infrared cell equiped with CaF_2 windows, allowing *in situ* studies. Typically 16 scans were accumulated for each spectrum (resolution 2 cm^{-1}). The Infrared spectra of the Molybdenum and Rhenium complexes in solution were recorded on JASCO FT-IR-460Plus spectrometer in a NaCl fluid cell. 32 scans were accumulated for each spectrum.

8.2. NMR spectroscopy

Solution NMR spectra were measured applying JEOL 400, 270 and Brücker Avance DPX-400 spectrometers. All solid-state NMR spectra were recorded under MAS (ν_R=10 KHz) on a Brüker Avance 500 spectrometer equipped with a standard 4 mm double-bearing probe head and operating at 500.13, 125.73 MHz for ^{1}H and ^{13}C, respectively. The samples were introduced in the 4 mm zirconia rotor in a glove box and tightly closed. Compressed air was used for both bearing and driving the rotors. Chemical shifts are reported in ppm downfield from $SiMe_4$ ($\pm$ 0.1 and 1 ppm for ^{1}H and ^{13}C spectra, respectively). The typical cross - polarization sequence was used for the ^{13}C CP MAS NMR spectra: 90° proton pulse, cross - polarization step to carbon spins and detection of the carbon magnetization under proton decoupling TPPM - 15. For the CP step, a ramp radio frequency (rf) field centered at ν^{CP}=60 KHz was applied on protons, while the carbon rf field was matched to obtain optimal signal. The contact time for CP was set to 2 ms. An exponential line broadening of 80 Hz was applied before Fourier transform. All other details are given in the caption of figures.

8.3. The power X-ray diffraction

Power XRD data were collected using a Philips X'pert diffractometer applying Cu Kα radiation. Nitrogen adsorption - desorption measurements were carried out at 77 K, using a gravimetric adsorption apparatus equipped with a CI electronic MK2-M5 microbalance and an Edwards Barocel pressure sensor. Prior to analysis, parent and grafted samples were degassed at 723 K overnight resulting in a residual pressure of ca. 10 - 24 mbar.

8.4. The low temperature N_2 adsorption/desorption isotherms

The specific surface area (SBET) was determined by the BET method.The total pore volume (VP) was estimated from the N2 uptake at p/p0 = 0.95, using a liquid nitrogen density of 0.8081 g/cm^3. The pore size distribution curves (PSD, the differential volume adsorbed with respect to the differential pore size per unit mass as a function of pore width) were computed

from the desorption branch of the experimental isotherms, using a method based on the area of the pore walls.

9. The synthesis of the catalyst precursors

9.1. Preparation of $CpMo(O)_2OCH_3$

$CpMo(CO)_3CH_3$ (1 mmol, 260 mg) was mixed with 10 eq TBHP (10 mmol) in 40 ml dichloromethane at room temperature. The oxidation continued for 3 hours, and then MnO_2 was added to quench the reaction. After another 1 h stirring, the solution was filtrated to removed MnO_2 and the solvent evaporated under vacuum at 0 °C. The pale yellow solid was washed three times with hexane (3 x 5 mL) and dried under vacuum.

Yield 140 mg (63 %).

Elemental analysis (C, 32.06; H, 3.76) is in agreement with the calculated values for $C_6H_8O_3Mo$ (224.06): C, 32.17; H, 3.60. The spectral data of the pure compound are in agreement with those reported for the Mo-oxoperoxo compound, $CpMo(O)(O_2)CH_3$, prepared previously by the method of Legzdins.[81] IR (KBr, ν in cm^{-1}): 3102s (Cp), 3064w, 2987w, 2943w, 2895w, 1633bw, 1454w, 1420m, 1169m, 1067m, 1029m, 1002m, 951vs; ν(Mo=O), 931s, 877vs ν(O-O), 849s, 831s, 774w, 748w, 575s, 565s ν(Mo-O); ^{1}H-NMR ($CDCl_3$, 400 MHz, ppm): 6.29 (5H, s, Cp), 2.12 (3H, s, CH3), ^{13}C-NMR (C_6D_6, 100.28 MHz, ppm): 109.3, 24.7; ^{95}Mo-NMR (C_6D_6, 26.07 MHz, ppm): -609 ppm; ^{17}O NMR ($CDCl_3$, 54.26 MHz, ppm): 869 (oxo), 359 ,336 (peroxo).

9.2. Single crystal determination of $CpMo(O_2)OCH_3$

Crystal data and details of the structure determination are presented in Table 9.1 and 4. Suitable single crystals for the X-ray diffraction study were grown from diethyl ether. A clear yellow fragment was stored under perfluorinated ether, transferred in a Lindemann capillary, fixed, and sealed. Preliminary examination and data collection were carried out on a kappa-CCD device (Nonius Mach3) with an Oxford Cryosystems cooling device at the window of a rotating an-

ode (Nonius Fr591) with graphite monochromated Mo-K_α radiation ($\lambda = 0.71073$ Å). Data collection was performed at 173 K within the Θ range of $3.45° < \Theta < 27.81°$. A total of 5660 reflections were integrated, corrected for Lorentz polarization, and, arising from the scaling procedure, corrected for latent decay and absorption effects. After merging ($R_{int} = 0.019$), 1711 [$1662 : I_0 > 2\sigma(I_0)$] independent reflections remained and all were used to refine 94 parameters. The structure was solved by a combination of direct methods and difference-Fourier syntheses. All non-hydrogen atoms were refined with anisotropic displacement parameters. Methyl hydrogen atoms were calculated as a part of rigid rotating groups, with $d_{C\text{-}H} = 0.98$ Å and $U_{iso(H)} = 1.5U_{eq(C)}$. Aromatic hydrogen atoms were placed in ideal positions and refined using a riding model with $d_{C\text{-}H}$ = of 0.95 Å and $U_{iso(H)} = 1.2U_{eq(C)}$. Small extinction effects were corrected with the SHELXL-97 procedure [$\varepsilon = 0.013(2)$]. Full-matrix least-squares refinements were carried out by minimizing $\Sigma w(F_o^2 - F_c^2)^2$ with the Shelxl-97 weighting scheme and converged with $R_1 = 0.0384[I_o > 2\sigma(I_o)]$, wR2 = 0.0989 [all data], GOF = 1.094, and shift/error < 0.001. The final difference-Fourier map shows clearly a disorder, which could not be resolved and modeled without some remaining doubts. This fact is obvious, too, in the unusual high thermal displacement parameters and the positions of the two highest difference-Fourier peaks. As can be seen by Flack's Parameter $\varepsilon = 0.51(15)$ the crystal is twinned and the refinements were completed with the Twin / Basf option. All calculations were performed with the WinGX system, including the programs Diamond, Platon, Shelxl-97, and Sir92

9.3. Preparation of $CpMo(^{13}CO)_3CH_3$

$[Bu_4N][Mo(CO)_5I]$ (1 g, 1.65 mmol) was put in a 100 ml flask under vacuum (10^{-2} mbar). Subsequently, the flask was filled with ^{13}CO (Cambridge Isotope Laboratories, Inc.; ^{13}C, 99 % and <2 % ^{18}O). 40 ml dichloromethane was added, and the yellow solution was stirred for 40 h on 25 °C. After the reaction was over, the solvent was evaporated under vacuum and a small part of the yellow solid won, was analyzed with IR and NMR spectroscopy.

The remaining labeled substance was soluted in 10 ml THF and mixed with a THF solution (10 ml) of NaCp (0.2 g, 2.2 mmol). The mixture was refluxed at 65 °C for 18 h. After it was cooled down freshly distilled methyl iodide (0.33 ml, 5.3 mmol) was added and the mixture was stirred at 25 °C for 4 h. The solvent was than evaporated under vacuum and the product was

purified by sublimation (50 °C, 10^{-2} mbar).

Yield 75 %

IR (in chloroform) ν(C=O): 2018.6, 2008, 1972.8, 1929.4, 1911.5, 1895.2. ^{13}C-NMR ($CDCl_3$, 400 MHz, ppm): 239.7 (t), 226.6 (t), 92.4 (s), -22.2 (s)

9.4. Preparation of $CpMo(CO)_3{}^{13}CH_3$

The preparation of $CpMo(CO)_3{}^{13}CH_3$ follows the same literature procedure as for non labeled compound using only ^{13}C labeled CH_3I as a reagent.

9.5. Preparation of trimethylsilyl perrhenate

Re_2O_7 (2.6 g, 5.4 mmol) was dissolved in acetonitrile, and to this light yellow solution, acetic anhydride (0.56 g, 5.4 mmol) was added dropwise. Acylperrhenate was formed 30 min after the addition and it was used without further purification. Trimethylsilanol (1 g, 10.8 mmol), synthesized from trimetylchlorsilane applying the two-phase hydrolysis,[192] was slowly added to this acylperrhenate solution and the reaction mixture was left stirring for 24 h at 25 °C. The product was purified by crystallization at - 30 °C. See literature for the spectroscopic data.[44,110,111]

Yield: 62.5 %

9.6. Preparation of $(CH_3)_3ReO_2$

$AgReO_4$ (500 mg, 1.5 mmol) was soluted in 10 ml acetonitrille and freshly distilled acetyl chloride (0.09 ml, 1.3 mmol) was added. After stirring the mixture for 10 min the AgCl precipitate was filtered out, and the acetonitrille solution containing the acetyl perrhenate was cool down to -30 °C. Dimethylzinc (0.35 ml, 3.6 mmol), prepared according to the literature procedure,[193] was added dropwise and the reaction solution turned red. This solution was kept for 30 min on -30 °C, and than slowly brought up to 80 °C were it was stirred under reflux for 1 h. The reaction mixture was cooled down again to 25 °C and the product was extracted with pentane (5 X 10 ml).

The oxidation was done in the pentane solution with $(CH_3)_3NO$ (300 mg, 3.5 mmol) as an oxidant. The change of color from deep red to yellow showed the completion of the reaction. The solvent was cooled down to 0 °C and evaporated (10^{-2} mbar). The $(CH_3)_3ReO_2$ as a red oil stayed behind and was purified by two consecutive sublimations. 210.2 mg, 0.8 mmol of pure $(CH_3)_3ReO_2$ could be isolated.

53.3 % Yield.

IR (in pentane) ν(Re=O): 1001s, 963vs. ^{1}H NMR ($CDCl_3$, 270 MHz, ppm): 2.48 (6H, s), 2.04 (3H, s). ^{13}C NMR ($CDCl_3$, 100.28 MHz, ppm): 29.68, 26.74. CI-MS: 264.7 (M^+).

Table 9.1: Crystallographic Data for $CpMo(O_2)OCH_3$

	$CpMo(O_2)OCH_3$
Formula	$C_6H_8MoO_3$
fw	224.06
color / habit	yellow / fragment
cryst. dimensions (mm^3)	0.10 x 0.18 x 0.46
cryst. syst	Orthorombic
space group	$P2_12_12_1$ (no. 19)
a, $\AA$	6.5225(5)
b, $\AA$	7.9532(5)
c, $\AA$	13.9632(7)
V, $\AA^3$	724.34(8)
Z,	4
T, K	173
D_{calcd}, gcm^{-3}	2.055
μ, mm^{-1}	1.751
F(000)	440
θ range, deg	3.45 - 27.81
Index ranges (h, k, l)	±8, ±10, -10: 18
no. of rflns collected	5660
no. of indep rflns / R_{int}	1711 / 0.019
no. of obsd rflns ($I > 2\sigma(I)$)	1662
no. of data / restraints / params	1711 / 0 / 94
R1 / $wR2(I > 2\sigma(I))$[a]	0.0384 / 0.0984
R1 / $wR2$ (all data)[a]	0.0391 / 0.0389
GOF (on F^2)[a]	1.094
Largest diff peak and hole (e $\AA^{-3}$)	+1.23 / -0.72

[a] $R1 = \Sigma(||F_o| - |F_c||)/\Sigma|F_o|$;
$wR2 = \{\Sigma[w(F_o^2 - F_c^2)^2]/\Sigma[w(F_o^2)^2]\}^{1/2}$;
$GOF = \{\Sigma[w(F_o^2 - F_c^2)^2]/(n-p)\}^{1/2}$

10. The grafting procedures

10.1. Preparation of mesoporous molecular sives

Mesoporous molecular sieves were synthesized following the procedures described earlier[105,107,113,114] with molar gel compositions of 1.0 SiO_2 : 0.2 NaOH : 0.27 TMAOH : 0.27 CtABR : 60 H_2O : x Al_2O_3 (x = 0 for MCM-41 and x = 0.005 Al-MCM-41); and 5.0 SiO_2 : 0.85 CTABr : 0.15 Brij 30 : 2.46 NaOH : 400 H_2O : x Al_2O_3 (x = 0 for MCM-48 and x = 0.025 for Al-MCM-48).

10.2. Preparation of γ-$Al_2O_{3\text{-}(500)}$

γ-Al_2O_3 from Degussa was calcined at 500 °C in dry air for 18 h and than treated at 500 °C under vacuum ($0.13 \cdot 10^{-5}$ mbar) for 18 h to give γ-$Al_2O_{3\text{-}(500)}$ (105 m^2/g)

10.3. Preparation of acylperrhenate supported on mesoporous molecular sives

The procedures began with pre-activation of the mesoporous materials at 200 °C under vacuum (10^{-3} bar) for 4 h to remove the physisorbed water. After cooling the materials to 25 °C 2 mmol of acylperrhenate dissolved in 30 ml acetonitrile were added. After 24 h at 25 °C the grafting process was completed. The substrate was filtered off and washed several times with acetonitrile until the physisorbed complex was removed from the surface. The obtained, slightly brown, solid material was dried carefully under oil pump vacuum at 25 °C.

10.4. Preparation of $CpMo(CO)_3CH_3$ supported on γ-$Al_2O_{3-(500)}$

1 g of γ-$Al_2O_{3-(500)}$ was contacted, wile stirring, with 85.8 mg (2 Molek. of complex / 1 nm-surface) of $CpMo(CO)_3CH_3$ at 25 °C under vakuum. The reaction proceded for 3 h and the unreacted complex was carried out by reverse sublimation. The resulting solid was treated under vacuum ($0.13 \cdot 10^{-5}$ mbar) for 1.5 h at 90 °C. Elemental analysis 1.6 % Mo.

10.5. Preparation of $(CH_3)_3ReO_2$ supported on γ-$Al_2O_{3-(500)}$

1 g of γ-$Al_2O_{3-(500)}$ was contacted, wile stirring, with 86 mg of $(CH_3)_3ReO_2$ at 25 °C under vakuum. The reaction proceded for 3 h and the unreacted complex was carried out by reverse sublimation. The resulting solid was treated under vacuum ($0.13 \cdot 10^{-5}$ mbar) for 1.5 h at 25 °C. Elemental analysis 1.67 % Re.

11. The catalytic reactions

11.1. Epoxidation catalysis using acylperrhenate on mesoporouse molecular sieves

The catalytic reactions were performed without moisture and oxygen precautions. The anhydrous hydrogen peroxide in ethyl acetate was prepared from 30 % hydrogen peroxide under Dean-Stark conditions.

Cyclooctene (770 mg, 7 mmol), 23.8 % hydrogen peroxide in ethyl acetate (236 mg, 7 mmol), mesitylene (1 g, 8.3 mmol, internal Standard) and 7 ml of ethylacetate as a solvent were first stirred at 80 °C for one hour. After cooling down to 50 °, the catalytic reactions were started by adding 0.014 mmol catalyst (based on the rhenium content). The reactions were monitored with a Hewlett Packard 5890 Series II - gas chromatograph equipped with a Supelco Aplha DexTM 120 column and using a FID detector. Samples were taken every 30 min in the period of 2 h and each hour for the following 3 h. The reaction was terminated after 24 h.

11.2. Reactivity of $CpMo(CO)_3CH_3$ on γ-$Al_2O_{3\text{-}(500)}$ with propene

In a 22 ml batch reactor $CpMo(CO)_3CH_3$ on γ-$Al_2O_{3\text{-}(500)}$ was introduced under Ar (50 mg, 8.3 μmol Mo). The Ar was evacuated and 533 mbar of propene was added. The gas phase was analysed by GC for 24 h.

11.3. Reactivity of $CpMo(CO)_3CH_3$ on γ-$Al_2O_{3\text{-}(500)}$ and ^{13}C di - labeled ethene

The procedure is same as above. In a 22 ml batch reactor $CpMo(CO)_3CH_3$ on γ-$Al_2O_{3\text{-}(500)}$ was introduced under Ar (100 mg, 16.6 μmol Mo). The Ar was evacuated and 10 mbar of ^{13}C di-labeled ethene was added. The catalysis proceeded for 24 h and the ethene was evacuated from the reactor under high vacuum ($0.13 \cdot 10^{-5}$ mbar). The residual catalyst was applied as a sample for the following NMR experiments.

11.4. Reactivity of $(CH_3)_3ReO_2$ on γ-$Al_2O_{3\text{-}(500)}$ with propene

In a 22 ml batch reactor $(CH_3)_3ReO_2$ on γ-$Al_2O_{3\text{-}(500)}$ was introduced under Ar (80 mg, 7.2 μmol Re). The Ar was evacuated and 540 mbar of propene was added. The gas phase was analysed by GC for 24 h.

11.5. Reactivity of $(CH_3)_3ReO_2$ on γ-$Al_2O_{3\text{-}(500)}$ with propene in flow reactor

The catalyst was first loaded in a reaction chamber in glove box (70 mg, 6.6 μmol Re). The reaction chamber was than connected to the reactor system and the propene flow was set to 1 atm and 400 ml/min and the inlet valve was opened. The temperature was set to 30 °C. The outlet gas flow was analyzed with online GC.

12. The kinetic studies

Kinetic data were collected by using ^{1}H NMR and UV methods. The epoxidation of cyclooctene was monitored by NMR, and the epoxidation of β - methoxystyrene was followed by UV spectrophotometric technique. In every case the temperature was controlled at 20 °C.

The reactions studied by ^{1}H NMR were carried out in $CDCl_3$ in a total volume of 0.5-1.0 mL. The relative amounts of TBHP, the catalyst and cyclooctene were chosen with a concern for the requirements of the kinetic analysis which was carried out by a first-order or initial rate kinetic. The ^{1}H-NMR spectra were recorded at 2 - 20 min increments over the 2 - 5 h reaction time. Under pseudo - first - order conditions, the changes in the intensity (I) of the cyclooctene signal(s) and/or the cyclooctene oxide with time were fit to a single exponential decay: $I_t = I_\infty + (I_0 - I_\infty)exp(-k_\psi t)$.

In the spectrophotometric (UV) method, the reaction mixtures were prepared in the reaction cuvette (optical path = 1.0 cm, VT = 3.0 mL) with the last component added being TBHP or the olefin. Some experiments were carried out in cuvettes with short optical paths (0.1-0.2 cm) to allow direct measurement of the absorbance changes during the reaction when the catalyst or β - methoxystyrene were varied, because both have high molar absorptivities and contribute a large absorbance background at the wavelengths used. The data were obtained by following the loss of the β - methoxystyrene (or trans - β - methylstyrene) absorption in the range between 260 - 270 nm. Initial rate and pseudo-first-order conditions applied in different protocols. In the latter case, the pseudo-first-order rate constants were evaluated by nonlinear least-squares fitting of the absorbance-time curves to a single exponential equation, $A_t = A_\infty + (A_0 - A_\infty)exp(-k_\psi t)$.

12.1. H-D exchange in $CpMo(CO)_3CH_3$

All experiments were performed on a 25 °C in NMR tube. First, $CpMo(CO)_3CH_3$ (10 mg, 0.038 mmol) was disolved in 0.4 ml DMSO (d^6). To this solution CD_3OD (0.008 ml, 0.19 mmol) was added and after vigourus stirring the base (0.038 mmol) was added as well. The reaction progress was followed by ^2H NMR.

Part IV.

Conclusions and perspectives

13. Immobilization of Acylperrhenate on mesoporouse silica materials

Acylperrhenate was successfully grafted on the surface of MCM-48, MCM-41, Al-MCM-48 and Al-MCM-41 molecular sieves. Experiments where trimethylsilanol was used as a model for the MCM surface confirmed that a [≡Si-O-Re] bond was formed on the surface and [≡-SiOReO_3] was the precursor for the catalytic active species in the epoxidation reaction. The grafted samples were found to be active and highly selective catalysts for the cyclooctene epoxidation with H_2O_2 as oxidizing agent. Catalyst deactivation and leaching, however, presented a problem for most of the grafted catalyst systems studied.

The MCM-41 surface proved to be the best carrier material for the acylperrhenate, when used in combination with H_2O_2 as an oxidant, achieving 86 % selectivity to the epoxide, and the highest conversion rate. Although no leaching was observed in this system, the deactivation of the catalyst due to the water formation was inevitable. This deactivation pathway is completely suppress using TBHP as an oxidant. Unfortunately, TBHP and ^{t}BuOH adsorb easily on the surface, blocking the surface pores and making the diffusion to and away from the active site considerably more difficult. Accordingly, using the TBHP systems only low conversions and low selectivities were achieved.

Improvements of these systems can be made both, in the Rhenium complex and in the silica surface. Using a mesoporouse material with broad channels such as SBA-15 (Santa Barbara Amorphous - 15) in combination with TBHP as an oxidant gives a catalytic systems with prolonged activity. The blocking of the pores with the adsorption of TBHP and ^{t}BuOH molecules on the surface play a minor role with these materials, due to their pore size, which is almost three times the size of MCM mesoporouse sieves.

The stability of the catalyst can be improved by using an alternative anchoring method for

the Rhenium complex. It is known that complexes bearing [Re-O-Si] are quit unstable due to hydrolysis. This hydrolysis is most likely the reason why deactivation occurs in the hydrogen peroxide systems. Synthesizing complexes that have a ligand bearing a linker that can easily be attached to the surface, would produce a hydrolysis stable complex to surface connection, and minimize the surface influence on the metal center. Considering the high Lewis acidity of these surfaces, tuning the distance to the metal center could be an important alternation to the design motif, influencing the reactivity of these systems.

14. Kinetic studies of the epoxidation reaction with $CpMo(CO)_3CH_3$

Based on kinetic studies the mechanism shown in Scheme 14.1 has been proposed for the catalytic olefin epoxidation promoted by the precursor $CpMo(CO)_3CH_3$. In the presence of excess alkyl hydroperoxide (TBHP), $CpMoO_2CH_3$ and $CpMo(O_2)OCH_3$ are formed, and both act as catalysts. Whereas the isolated compound $CpMo(O_2)OCH_3$ is inactive for stoichiometric epoxidation of cyclooctene, and styrenes, epoxidation with $CpMo(O_2)OCH_3$ does proceed in the presence of TBHP, with formation of a reactive species **I**, similar to the active intermediate originating from $CpMoO_2CH_3$ and described for other Mo(VI) systems of formula $MoX_2O_2L_2$.[103,117,56,98] In these active intermediates, the [OOR] group is bound end-on to molybdenum, with the α-oxygen involved in a hydrogen bond with the neighboring OH. The β-oxygen is probably transferred to the olefin during the catalytic reaction in a seven member ring transition state. Proposed intermediates are given in Figure 14.2. DFT Calculations were initiated in our group to confirm this hypothesis. The kinetic results on the variation of the rate with the alkyl hydroperoxide are consistent with the formation of the intermediate species **I**.

In the presence of excess olefin, the catalytic system is stable and the major pathway is the epoxidation reaction. The decomposition path of the catalyst becomes competitive at low olefin concentrations, and leads to an increasingly slower conversion. The formation of σ-peroxide bound species as catalysts seems to be crucial for $CpMoO_2CH_3$ complexes to be active in olefin epoxidation, as had been reported previously for $MoO_2(X)_2(L)$ (X = halide, methyl; L = bidentate nitrogen ligand) systems.

The results gathered with this kinetic survey showed once again the stability of the Cp- and the methyl- ligand in this type of complexes. This feature encourages the grafting of these Molybdenum complexes using linkers that are bound to the Cp ligand as already performed by

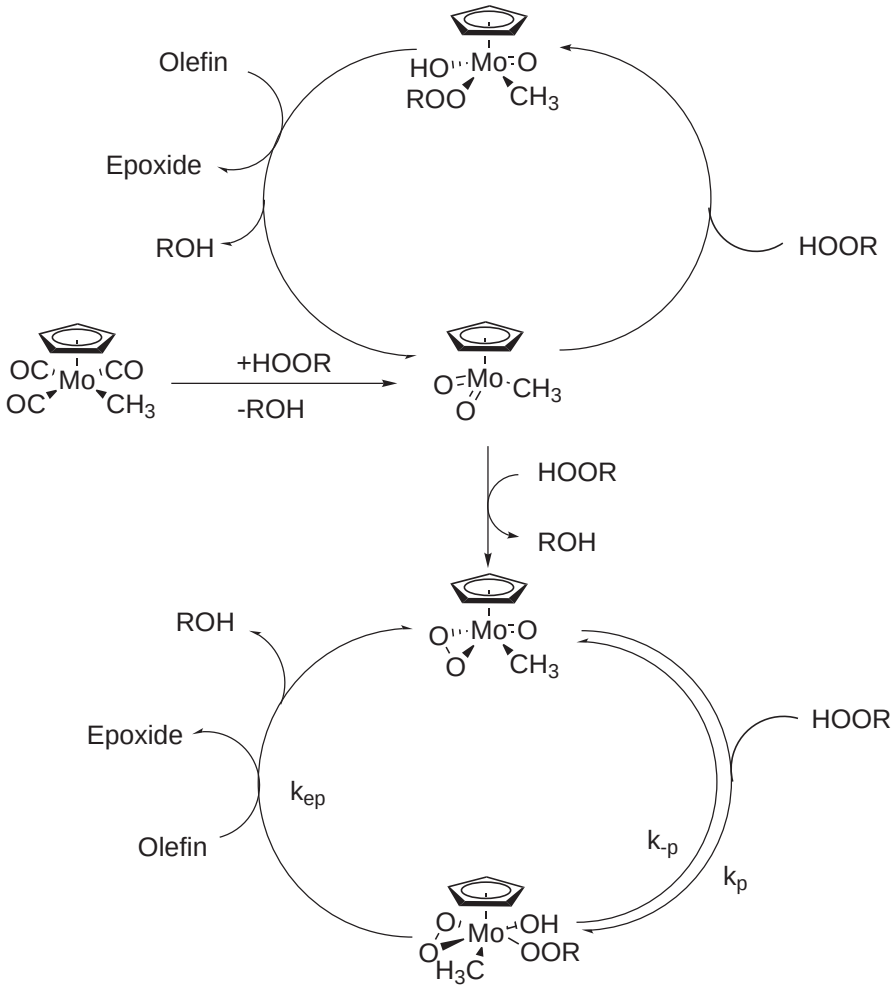

Scheme 14.1. General mechanism for the oxidation of $CpMo(CO)_3CH_3$ and catalytic activity of the resulting complexes in the presence of TBHP

Kühn et. al.[92,114] The methyl group has already been can be used as an anchor as well, already performed in this work (see Chapter 6)

Kühn et al. used the knowledge of the stability of the Cp and the alkyl ligands in these molybdenum systems to develop slightly different homogeneous systems - the *ansa* molybdenum complexes (Figure 14.1). The preliminary catalytic tests performed on these novel catalysts, are already showing very promising results considering their activity and their stability under the catalysis conditions applied (25 °C, TBHP as oxidant).[194] The most important feature of these *ansa* systems is the opportunity to add functional groups to the *ansa* bridge. This feature will provide additional possibility for anchoring these complexes to solid surfaces and their application in the heterogeneous catalysis. Furthermore, the anchoring of a chiral center on the *ansa* bridge is also possible, introducing the chirality very near to the metal center.

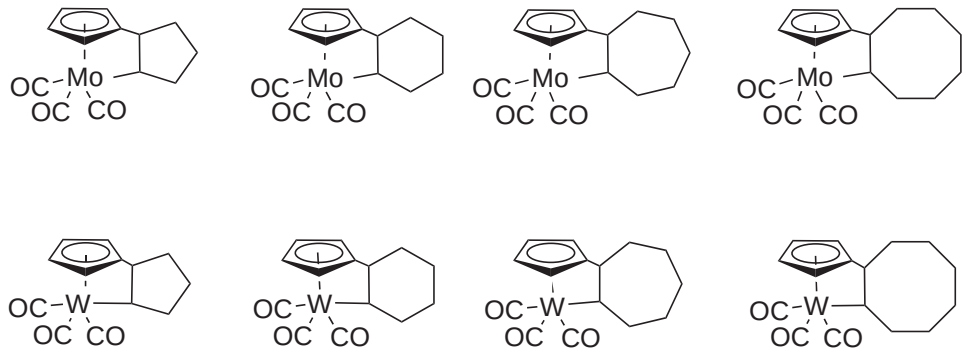

Figure 14.1. Newly synthesized *ansa* molybdenum carbonyls by Kühn et al.

Performing a chiral epoxidation under catalytic conditions is very rare and this *ansa* bridge systems may be the first group of chiral catalysts for the epoxidation reaction.

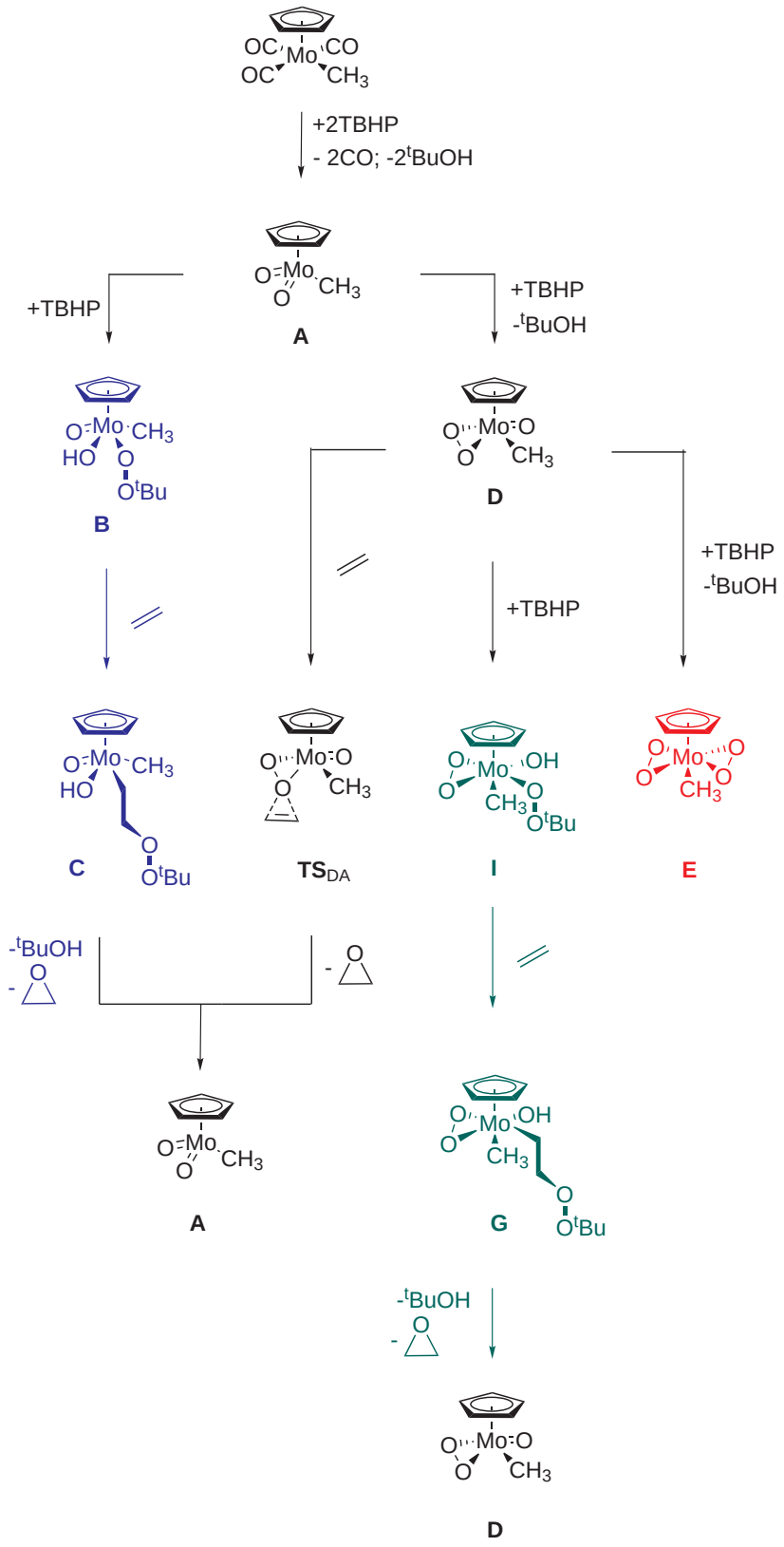

Figure 14.2. Summary of the proposed reaction pathways during the catalytic epoxidation with $CpMo(CO)_3CH_3$

15. $CpMo(CO)_3CH_3$ on γ-$Al_2O_{3\text{-}(500)}$ as a catalyst for olefin metathesis

The $CpMo(CO)_3CH_3$ complex was successfully grafted on γ-$Al_2O_{3\text{-}(500)}$. Using it as a heterogeneous catalyst for the propene metathesis in a batch reactor, 257 mol of propene per mol of Mo were converted in 24 h. This is the first Molybdenum carbonyl catalyst, active in olefin metathesis without any preactivations. The catalyst is not deactivated like the similar catalysts on Rhenium basis (see Chapter 5 and 7) and activity in two consecutive catalytic runs without significant loss in activity is observed.

This new heterogeneous system was characterized in detail using IR and solid-state NMR spectroscopy, revealing at least two different molybdenum surface species. The first molybdenum acyl compound (**I**) - was formed by a CO insertion in to the [Mo−CH_3] bond, catalyzed by the Lewis acidic centers of the alumina surface. Similar acyl complexes in homogeneous systems are found in equilibrium with the acyl complexes with the Lewis acid bound to the acyl oxygen atom (**III**), and the enolic form of this species (**IV**) sketched in Scheme 15.1.

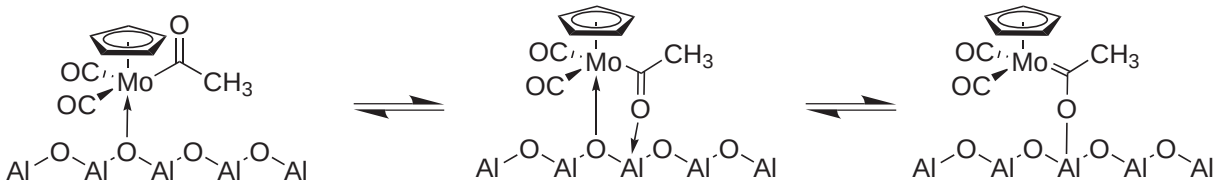

Scheme 15.1. Possible variations of the Molybdenum acyl surface species.

Analyzing the spectra of the ^{13}C - labeled, $CpMo(CO)_3CH_3$, compound, only **I** could be detected. The other two possible formations, bear an electronically poor methyl group, and would exhibit methyl signals shifted downfield in the NMR region (50 - 80 ppm), not observed

in the NMR spectra (Figure 6.5).

The second surface species observed, was the molybdenum alkylidene complex, [Mo−CH_2−Als] formed by CH - activation of the [Mo−CH_3] group on the alumina surface. The metathesis performed with the di - labelled ethylene showed that this species is also the active one in catalysis, being the only one having a ^{13}C labeled atom after the reaction was done (Figure 6.10).

Another important fact is the evolution of the two species with time, being observed on $CpMo(CO)_3{}^{13}CH_3$ on γ-$Al_2O_{3\text{-}(500)}$ (see Figure 6.7 and Scheme 6.2). The spectra recorded on the same sample over the course of a year showed a transformation over of **I** to **II** probably induced by a deprotonation of the methyl group of **I** by [Als−O]. If the rate of this secondary reaction can be increased, then a heterogeneous catalyst with 100 % of active sites may be generated.

Further improvements of this system can be made by minimizing the secondary reactions (unproductive metathesis), by decreasing the absorption capability of the alumina surface, as already performed on the MTO - γ-$Al_2O_{3\text{-}(500)}$ system.[182] Furthermore, if the observed stability is proved again in a continuous reactor flow experiments, than new catalysts like $(CH_3)_2MoO_2$ and even $CpReO(CH_3)_2$ can provide suitable alternatives for further heterogeneous systems, having similar stability but even higher catalytic activity.

16. $(CH_3)_3ReO_2$ on γ-$Al_2O_{3\text{-}(500)}$ as a catalyst for olefin metathesis

In this work, $(CH_3)_3ReO_2$ was synthesized and successfully grafted on γ-$Al_2O_{3\text{-}(500)}$. This novel heterogeneous system was used as a catalyst for propene metathesis, converting 5366 mol of Propene per mol of Re in less than 24 h reaction time. $(CH_3)_3ReO_2$ on γ-$Al_2O_{3\text{-}(500)}$ exhibits similar catalytic behavior as the already well characterized MTO - γ-$Al_2O_{3\text{-}(500)}$ system, indicating a similar active site in both cases. Considering the previous work of Coperet et al. the active site is formed on the defect sites of alumina, with CH - bond activation of at least one of the methyl groups present in the system (see Scheme 16.1).[181] The [Als$-CH_2-ReO_2(CH_3)_2$] can form the propagating species containing a Re=CH_2 group in the presence of olefin similar to the well known Tebbes reagent (see Chapter 5). Keeping in mind the low number of defect sites on aluminum, the active species is probably only makes up for 10 - 15 % of the total rhenium content on the surface, the rest being inactive, physisorbed complex.[179b]

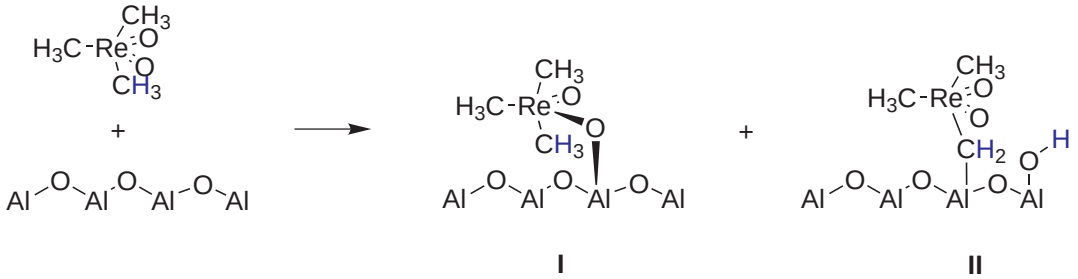

I II

Scheme 16.1. Possible surface species on γ-$Al_2O_{3\text{-}(500)}$

The catalysis results observed in the flow reactor showed two very important features of the $(CH_3)_3ReO_2$ - $\gamma Al_2O_{3\text{-}(500)}$ system already observed for MTO on γ-$Al_2O_{3\text{-}(500)}$. The selectivity of the catalyst changes drastically with the conversion, reaching 0.38 E/Z ratio by the lowest conversion, probably due to the intrinsic selectivity of the catalyst. At higher conversions,

the catalyst interacts with the products, which can not easily disorb from the surface, in the following performing continuously unproductive, isomerization reactions. The second common feature, is the rapid deactivation in both systems, probably due to ethylene insertion in to the active site, creating an unstable propylidine intermediate, that easily decomposes due to a β - H elimination (Scheme 16.2).

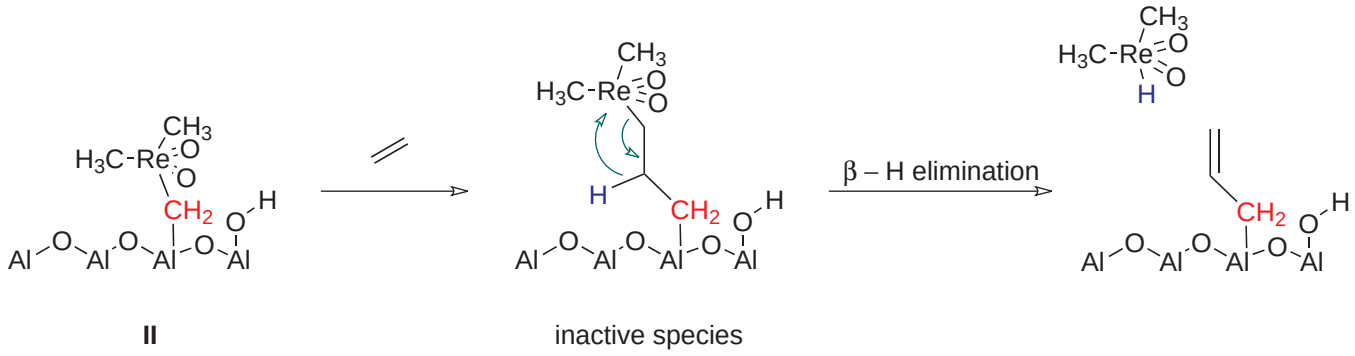

Scheme 16.2. A possible deactivation pathway of the surface active cite.

There are three main opportunities for improving this very promising catalytic system: increasing the number of active sites, hamper the deactivation, and minimizing the unproductive metathesis reaction.

The number of active sites can only be increased by performing modifications on the grafted complex itself, as there is no possibility of significantly increasing the deffects of the alumina surface. The UV experiments performed on $(CH_3)_3ReO_2$ in pentane (Figure 16.1), show a homolytic cleavage of a Re$-$CH$_3$ bond ($\lambda = 278$ nm) forming methyl and Re radicals analogous to MTO.[195,48] In solution these radicals rapidly react with the solvent molecules forming Methane and Rhenium hydride or Rhenium alkyl species, both unstable and both leading to catalyst decomposition.

On the surface however, the lack of solvent makes the neighboring methyl group the nearest reaction partner for the formed methyl radical (Scheme 16.3). This reaction can lead to Methane elimination and a surface immobilized [Re=CH$_2$] containing species which is the propagating species for the olefin metathesis reaction.

Minimizing of the deactivation process and the unproductive metathesis reaction can be performed by increasing the desorption rate of the olefins from the aluminum surface. Modifying the surface with trimethylsilyl fragments leads to an improved catalytic activity as well as *Z*-selectivity of the MTO - γ-$Al_2O_{3\text{-}(500)}$ system.[182] This can be promising a step in the right

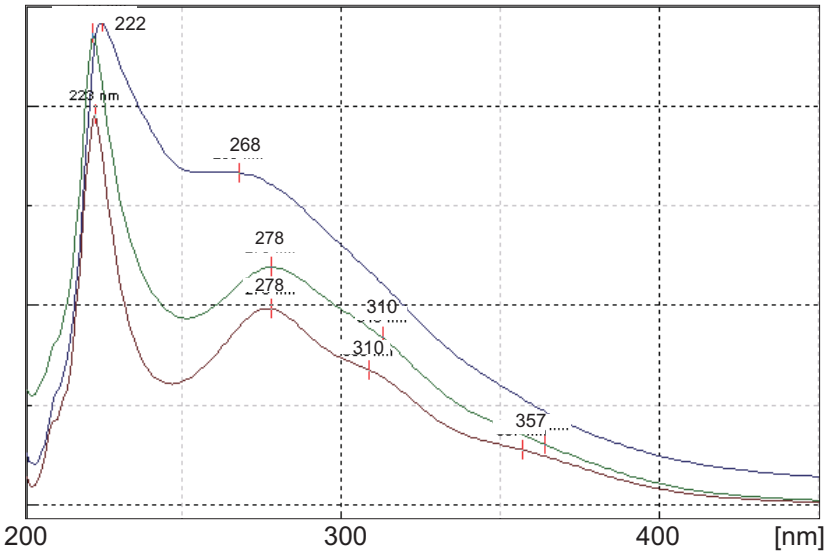

Figure 16.1. Changes in the structure of $(CH_3)_3ReO_2$ generated by UV light with time.(—) Initial UV spectra of $(CH_3)_3ReO_2$; (—) After 5 min of UV irradiation; (—) After 15 min of UV irradiation.

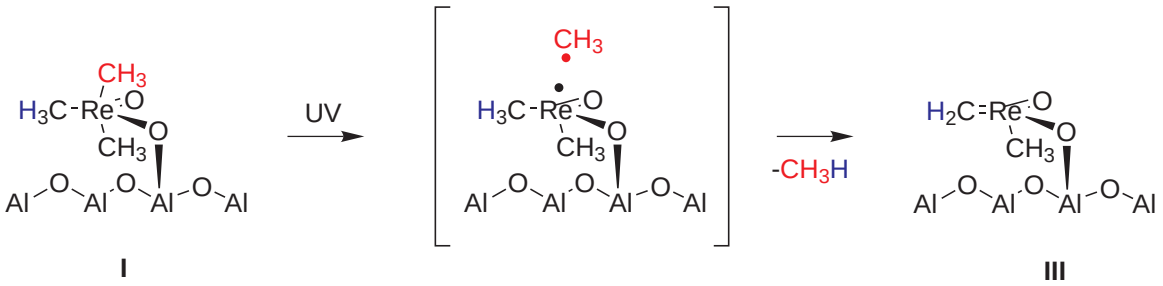

Scheme 16.3. Expected surface reaction after UV irradiation of $(CH_3)_3ReO_2$ on γ-$Al_2O_{3\text{-}(500)}$

direction for $(CH_3)_3ReO_2$ on γ-$Al_2O_{3\text{-}(500)}$ as well.

References

1. *Transition Metals for Organic Synthesis. Building Blocks and Fine Chemicals*; Beller, M., Bolm, C., Eds.; Wiley-VCH, Weinheim, 2004.

2. Laidler, K. J. *Pure And Applied Chemistry* **1996**, *68*, 149–192.

3. Muller, P. *Pure And Applied Chemistry* **1994**, *66*, 1077–1184.

4. Moss, G. P. *Pure And Applied Chemistry* **1996**, *68*, 2193–2222.

5. IUPAC, *IUPAC Gold Book*; (http://goldbook.iupac.org/), 2005-2007.

6. Wittcoff, H. A.; Reuben, B. G.; Plotkin, J. S. In *Industrial Organic Chemicals (Second Edition)*; Wiley-Interscience, 2004; pp i–xxxi.

7. Armstrong, R. W.; Beau, J. M.; Cheon, S. H.; Christ, W. J.; Fujioka, H.; Ham, W. H.; Hawkins, L. D.; Jin, H.; Kang, S. H.; et al., *J. Am. Chem. Soc* **1989**, *111*, 7530–7533.

8. (a) Trost, B. *Science* **1991**, *254*, 1471–1477; (b) Trost, B. M. *Angew. Chem. Int. Ed. Engl.* **1995**, *34*, 259–281.

9. Sheldon, R.; Arends, I.; Hanefeld, U. *Green Chemistry and Catalysis*; Wiley-VCH, 2007.

10. Lancaster, M. *Green Chemistry: An Introductory text*; The Royal Society of Chemistry, 2002.

11. Berzelius, J. *The Edinburgh New Philosophical Journal* **1836**, *21*, 223.

12. *Catalysts and Specialty Chemicals*; http://www.catalystgrp.com/catalystsandchemicals.html,, Ed.; The Catalyst Group, Inc, 2003.

13. *Industrial Catalysis: A Practical Approach*; Hagen, J., Ed.; Wiley-VCH Verlag GmbH, 2006.

14. Ertl, G. *Angew. Chem. Int. Ed* **2008**, *47*, 3524–3535.

15. (a) Cornils, B.; Herrmann, W.; Horvath, I.; Leitner, W.; Mecking, S.; Olivier-Bourbigou, H.; Vogt, D. *Multiphase Homogeneous Catalysis, Vols. 1 and 2*; Wiley-VCH, Weinheim, 2005; (b) Cornils, B.; Herrmann, W. *Aqueous-phase Organometallic Catalysis*; Wiley-VCH Verlag GmbH, 2004.

16. Hagen, J.; Hopp, V. *Chemische Reaktionstechnik-Eine Einführung mit Übungen*; Weinheim: VCH Verlagsgesellschaft, 1992.

17. McCoy, M.; Reisch, M. S.; Tullo, A. H.; Short, P. L.; Tremblay, J.-F.; Storck, W. J.; Voith, M. *Chemical and Engineering News* **2008**, *86*, 35.

18. Weissermel, K.; Arpe, H.-J. *Industrial organic chemistry*; Wiley-VCH: Weinheim, 2003.

19. Kilty, P. A.; Sachtler, W. M. *Catalysis Reviews-Science And Engineering* **1974**, *10*, 1–16.

20. McClellan, P. P. *Industrial & Engineering Chemistry* **1950**, *42*, 2402–2407.

21. Baeckvall, J.-E. *Modern oxidation methods*; Wiley-VCH: Weinheim; [Great Britain], 2004; pp –.

22. Halcon, *US Patent* **3350422**, *Oct. 31*, 1967.

23. ARCO, *GB Patent* **1136923**, *1968*, 18 Dec.

24. *Applied Homogenous Catalysis with organometllic Compounds*; Boy Cornils, W. A. H., Ed.; Wiley-VCH Verlag GmbH, 2002; Vol. 1, p 412.

25. Schindler, G.-P.; Walsdorff, C.; Koerner, R.; Goebbel, H.-G. *WO2007000396* **2007**.

26. (a) Notari, B. *Catal. Today* **1993**, *18*, 163–172; (b) Notari, B. Microporous Crystalline Titanium Silicates. In *Advances in Catalysis*; D.D. Eley, W. O. H., Gates, B., Eds.; Academic Press, 1996; Vol. Volume 41, pp 253–334.

27. Joergensen, K. A. *Chem. Rev.* **1989**, *89*, 431–458.

28. (a) Herrmann, W. A.; Kuchler, J. G.; Felixberger, J. K.; Herdtweck, E.; Wagner, W. *Angew. Chem. Int. Ed. Engl.* **1988**, *27*, 394–396; (b) Herrmann, W. A.; Wang, M. *Angew. Chem. Int. Ed. Engl.* **1991**, *30*, 1641–1643; (c) Herrmann, W. A.; Wagner, W.; Flessner, U. N.; Volkhardt, U.; Komber, H. *Angew. Chem. Int. Ed. Engl.* **1991**, *30*, 1636–1638.

29. Herrmann, W. A.; Fischer, R. W.; Marz, D. W. *Angew. Chem. Int. Ed. Engl.* **1991**, *30*, 1638–1641.

30. (a) Krebs, B. *Angew. Chem. Int. Ed. Engl.* **1968**, *7*, 308; (b) Krebs, B.; Muller, A.; Beyer, H. *Chemical Communications* **1968**, 263.

31. Herrmann, W. A.; Roesky, P. W.; Kühn, F. E.; Elison, M.; Artus, G.; Scherer, W.; Romão, C. C.; Lopes, A.; Basset, J.-M. *Inorg. Chem.* **1995**, *34*, 4701–4707.

32. Herrmann, W. A.; Fischer, R. W.; Rauch, M. U.; Scherer, W. *J. Mol. Catal* **1994**, *86*, 243–266.

33. Schmidbaur, H.; Koth, D. *Chem.-Ztg* **1976**, *100*, 290.

34. Herrmann, W. A.; Serrano, R.; Bock, H. *Angew. Chem. Int. Ed. Engl.* **1984**, *23*, 383–385.

35. Herrmann, W. A.; Taillefer, M.; De Meric de Bellefon, C.; Behm, J. *Inorg. Chem.* **1991**, *30*, 3247–3248.

36. Herrmann, W. A.; Ladwig, M.; Kiprof, P.; Riede, J. *J. Organomet. Chem.* **1989**, *371*, C13–C17.

37. Herrmann, W. A.; Khn, F. E.; Romo, C. C.; Huy, H. T.; Wang, M.; Fischer, R. W.; Kiprof, P.; Scherer, W. *Chem. Ber.* **1993**, *126*, 45–50.

38. Merrifield, J. H.; Lin, G. Y.; Kiel, W. A.; Gladysz, J. A. *J. Am. Chem. Soc* **1983**, *105*, 5811–5819.

39. Herrmann, W. A.; Floeel, M.; Kulpe, J.; Felixberger, J. K.; Herdtweck, E. *J. Organomet. Chem.* **1988**, *355*, 297–313.

40. Herrmann, W. A.; Felixberger, J. K.; Anwander, R.; Herdtweck, E.; Kiprof, P.; Riede, J. *Organometallics* **1990**, *9*, 1434–1443.

41. Felixberger, J. K.; Kiprof, P.; Herdtweck, E.; Herrmann, W. A.; Jakobi, R.; Goetlich, P. *Angew. Chem. Int. Ed. Engl.* **1989**, *28*, 334–337.

42. Hieber, W.; Braun, G. *Z. Naturforsch.* **1959**, *14b*, 132.

43. Hieber, W.; Braun, G.; Beck, W. *Chem. Ber.* **1960**, *93*, 901–908.

44. Edwards P, W. G. *J. Chem. Soc. Dalton. Trans.* **1984**, 2695.

45. Herrmann, W. A.; Thiel, W. R.; Kühn, F. E.; Fischer, R. W.; Kleine, M.; Herdtweck, E.; Scherer, W.; Mink, J. *Inorg. Chem.* **1993**, *32*, 5188–5194.

46. Mitterpleininger, J. K. M.; Szesni, N.; Sturm, S.; Fischer, R. W.; Kühn, F. E. *European Journal of Inorganic Chemistry* **2008**, *2008*, 3929–3934.

47. Hoegerl, M.; Kühn, F. E. *Zeitschrift fuer anorganische und allgemeine Chemie* **2008**, *634*, 1444–1447.

48. (a) Kühn, F. E.; Scherbaum, A.; Herrmann, W. A. *J. Organomet. Chem.* **2004**, *689*, 4149–4164; (b) Romão, C. C.; Kühn, F. E.; Herrmann, W. A. *Chem. Rev.* **1997**, *97*, 3197–3246.

49. Beattie, I. R.; Jones, P. J. *Inorg. Chem.* **1979**, *18*, 2318–2319.

50. (a) Mol, J. C.; Woerlee, E. F. G. *Journal Of The Chemical Society-Chemical Communications* **1979**, 330–331; (b) Mol, J. C. *J. Mol. Catal* **1982**, *15*, 35–45; (c) Vandenaardweg, G. C. N.; Bosma, R. H. A.; Mol, J. C. *Journal Of The Chemical Society-Chemical Communications* **1983**, 262–263; (d) Mol J. C., A. A. *J. Mol. Catal* **1988**, *46*, 151.

51. (a) Stavropoulos, P.; Edwards, P. G.; Wilkinson, G.; Motevalli, M.; Malik, K. M. A.; Hursthouse, M. B. *Journal Of The Chemical Society-Dalton Transactions* **1985**, 2167–2175; (b) Stavropoulos, P.; Edwards, P. G.; Behling, T.; Wilkinson, G.; Motevalli, M.; Hursthouse, M. B. *Journal Of The Chemical Society-Dalton Transactions* **1987**, 169–175; (c) Longley, C. J.; Savage, P. D.; Wilkinson, G.; Hussain, B.; Hursthouse, M. B. *Polyhedron* **1988**, *7*, 1079–1088.

52. (a) Herrmann, W. A.; Kühn, F. E.; Romão, C. C. *J. Organomet. Chem.* **1995**, *495*, 209–213; (b) Herrmann, W. A.; Kühn, F. E.; Romão, C. C. *J. Organomet. Chem.* **1995**, *489*, C56–C59; (c) Herrmann, W. A.; Kühn, F. E.; Romão, C. C.; Huy, H. T. *J. Organomet. Chem.* **1994**, *481*, 227–234.

53. (a) Herrmann, W. A.; Kratzer, R. M.; Fischer, R. W. *Angew. Chem. Int. Ed. Engl.* **1997**, *36*, 2652–2654; (b) Herrmann, W. A.; Kühn, F. E.; Fischer, R. W.; Thiel, W. R.; Romão, C. C. *Inorg. Chem.* **1992**, *31*, 4431–4432.

54. (a) Herrmann, W.; Rost, A.; Mitterpleininger, J.; Szesni, N.; Sturm, S.; Fischer, R.; Khn, F. *Angew. Chem. Int. Ed* **2007**, *46*, 7301–7303; (b) Tosh, E.; Mitterpleininger, J. K. M.; Rost, A. M. J.; Veljanovski, D.; Herrmann, W. A.; Kühn, F. E. *Green Chemistry* **2007**, *9*, 1296–1298.

55. Herrmann, W. A.; Fischer, R. W.; Scherer, W.; Rauch, M. U. *Angew. Chem. Int. Ed. Engl.* **1993**, *32*, 1157–1160.

56. (a) Al-Ajlouni, A. M.; Espenson, J. H. *J. Am. Chem. Soc* **1995**, *117*, 9243–9250; (b) Al-Ajlouni, A.; Espenson, J. *J. Org. Chem.* **1996**, *61*, 3969–3976.

57. Herrmann, W. A.; Correia, J. D. G.; Artus, G. R. J.; Fischer, R. W.; Romão, C. C. *J. Organomet. Chem.* **1996**, *520*, 139–142.

58. (a) Gisdakis, P.; Antonczak, S.; Kostlmeier, S.; Herrmann, W. A.; Rosch, N. *Angew. Chem. Int. Ed* **1998**, *37*, 2211; (b) Kühn, F. E.; Santos, A. M.; Rösky, P. W.; Herdtweck, E.; Scherer, W.; Gisdakis, P.; Yudanov, I. V.; Di Valentin, C.; Rosch, N. *Chemistry-A European Journal* **1999**, *5*, 3603–3615; (c) Deubel, D.; Frenking, G.; Gisdakis, P.; Herrmann, W.; Rosch, N.; Sundermeyer, J. *Acc. Chem. Res.* **2004**, *37*, 645–652.

59. (a) Sharpless, K. B.; Townsend, J. M.; Williams, D. R. *J. Am. Chem. Soc* **1972**, *94*, 295–296; (b) Chong, A. O.; Sharpless, K. B. *J. Org. Chem.* **1977**, *42*, 1587–1590.

60. (a) Rudolph, J.; Reddy, K. L.; Chiang, J. P.; Sharpless, K. B. *J. Am. Chem. Soc* **1997**, *119*, 6189–6190; (b) Adolfsson, H.; Converso, A.; Sharpless, K. B. *Tetrahedron Lett.* **1999**, *40*, 3991–3994.

61. (a) Coperet, C.; Adolfsson, H.; Sharpless, K. B. *Chemical Communications* **1997**, 1565–1566; (b) Adolfsson, H.; Coperet, C.; Chiang, J. P.; Yudin, A. K. *Journal Of Organic Chemistry* **2000**, *65*, 8651–8658.

62. (a) Herrmann, W. A.; Ding, H.; Kratzer, R. M.; Kühn, F. E.; Haider, J. J.; Fischer, R. W. *J. Organomet. Chem.* **1997**, *549*, 319–322; (b) Herrmann, W. A.; Kühn, F. E.; Mattner, M. R.; Artus, G. R. J.; Geisberger, M. R.; Correia, J. D. G. *J. Organomet. Chem.* **1997**, *538*, 203–209.

63. (a) Malek, A.; Ozin, G. *Adv. Mat.* **1995**, *7*, 160–163; (b) Bein, T.; Huber, C.; Moller, K.; Wu, C.-G.; Xu, L. *Chem. Mater.* **1997**, *9*, 2252–2254.

64. Adam, W.; Saha-Moller, C.; Weichold, O. *J. Org. Chem.* **2000**, *65*, 2897–2899.

65. Herrmann, W. A.; Fritz-Meyer-Weg, D. M.; Wagner, M.; Kuchler, J. G.; Weichselbaumer, G.; Fischer, R. *US Patent* **5155247**, *October 13*, 1992.

66. (a) Saladino, R.; Neri, V.; Pelliccia, A. R.; Mincione, E. *Tetrahedron* **2003**, *59*, 7403–7408; (b) Lazzaro, F.; Crucianelli, M.; De Angelis, F.; Neri, V.; Saladino, R. *Tetrahedron Lett.* **2004**, *45*, 9237–9240; (c) Saladino, R.; Mincione, E.; Attanasi, O. A.; Filippone, P. *Pure And Applied Chemistry* **2003**, *75*, 265–272; (d) Saladino, R.; Neri, V.; Cardona, F.; Goti, A. *Adv. Syn. Catal.* **2004**, *346*, 639–647.

67. (a) Bernini, R.; Coratti, A.; Provenzano, G.; Fabrizi, G.; Tofani, D. *Tetrahedron* **2005**, *61*, 1821–1825; (b) Bernini, R.; Coratti, A.; Fabrizi, G.; Goggiamani, A. *Tetrahedron Lett.* **2003**, *44*, 8991–8994; (c) Abu-Omar, O. S., Mahdi M. *Chem. Commun.* **2000**, 1165.

68. (a) Kühn, F.; Santos, A.; Abrantes, M. *Chem. Rev.* **2006**, *106*, 2455–2475; (b) Kühn, F. E.; Santos, A. M.; Herrmann, W. A. *Dalton Transactions* **2005**, 2483–2491; (c) Bottomley, F.; Sutin, L. *Advances In Organometallic Chemistry* **1988**, *28*, 339–396; (d) Roesky, H. W.; Haiduc, I.; Hosmane, N. S. *Chem. Rev.* **2003**, *103*, 2579–2595.

69. (a) Freund, C.; Abrantes, M.; Kühn, F. E. *J. Organomet. Chem.* **2006**, *691*, 3718–3729; (b) Bottomley, F. *Polyhedron* **1992**, *11*, 1707–1731.

70. Kühn, F. E.; Herdtweck, E.; Haider, J. J.; Herrmann, W. A.; Gonçalves, I. S.; Lopes, A. D.; Romão, C. C. *J. Organomet. Chem.* **1999**, *583*, 3–10.

71. Heyn, B.; Hoffmann, R. *Z. Chem.* **1976**, *16*, 195.

72. da Costa, A. P.; Reis, P. M.; Gamelas, C.; Romão, C. C.; Royo, B. *Innorg. Chim. Acta* **2008**, *361*, 1915–1921.

73. Schrauzer, G. N.; Moorehead, E. L.; Grate, J. H.; Hughes, L. A. *J. Am. Chem. Soc* **1978**, *100*, 4760–4765.

74. (a) Schrauzer, G. N.; Hughes, L. A.; Strampach, N. *Zeitschrift Fur Naturforschung Section B-A Journal Of Chemical Sciences* **1982**, *37*, 380–385; (b) Schrauzer, G. N.; Hughes, L. A.; Strampach, N.; Robinson, P. R.; Schlemper, E. O. *Organometallics* **1982**, *1*, 44–47.

75. (a) Schrauzer, G. N.; Hughes, L. A.; Schlemper, E. O.; Ross, F.; Ross, D. *Organometallics* **1983**, *2*, 1163–1166; (b) Schrauzer, G. N.; Hughes, L. A.; Strampach, N.; Ross, F.; Ross, D.; Schlemper, E. O. *Organometallics* **1983**, *2*, 481–485; (c) Hughes, L. A.; Hui, L. N.; Schrauzer, G. N. *Organometallics* **1983**, *2*, 486–489.

76. (a) Kühn, F. E.; Lopes, A. D.; Santos, A. M.; Herdtweck, E.; Haider, J. J.; Romão, C. C.; Santos, A. G. *Journal Of Molecular Catalysis A-Chemical* **2000**, *151*, 147–160; (b) Santos, A. M.; Kühn, F. E.; Bruus-Jensen, K.; Lucas, I.; Romão, C. C.; Herdtweck, E. *Journal Of The Chemical Society-Dalton Transactions* **2001**, 1332–1337; (c) Kühn, F. E.; Santos, A. M.; Gonçalves, I. S.; Romão, C. C.; Lopes, A. D. *Applied Organometallic Chemistry* **2001**, *15*, 43–50; (d) Kühn, F. E.; Groarke, M.; Bencze, E.; Herdtweck, E.; Prazeres, A.; Santos, A. M.; Calhorda, M. J.; Romão, C. C.; Gonçalves, I. S.; Lopes, A. D.; Pillinger, M. *Chemistry-A European Journal* **2002**, *8*, 2370–2383.

77. (a) Jain, K. R.; Kühn, F. E. *Dalton Transactions* **2008**, 2221–2227; (b) Valente, A. A.; Petrovski, Z.; Branco, L. C.; Afonso, C. A. M.; Pillinger, M.; Lopes, A. D.; Romão, C. C.; Nunes, C. D.; Gonçalves, I. S. *Journal Of Molecular Catalysis A-Chemical* **2004**, *218*, 5–11.

78. Cousins M., G. M. L. H. *J. Chem. Soc.* **1963**, 889.

79. (a) Segal, J. A.; Green, M. L. H.; Daran, J. C.; Prout, K. J. *Journal Of The Chemical Society-Chemical Communications* **1976**, 766–768; (b) Cousins, M.; Green, M. L. H. *Journal Of The Chemical Society A -Inorganic Physical Theoretical* **1969**, 16–&.

80. Herrmann, W. A. *Angew. Chem. Int. Ed. Engl.* **1988**, *27*, 1297–1313.

81. Legzdins, P.; Phillips, E. C.; Sanchez, L. *Organometallics* **1989**, *8*, 940–949.

82. (a) Legzdins, P.; Phillips, E. C.; Rettig, S. J.; Sanchez, L.; Trotter, J.; Yee, V. C. *Organometallics* **1988**, *7*, 1877–1878; (b) Hoyano J. K., P., Legzdins; T., M. J. *Inorg. Synth.* **1978**, *18*, 126.

83. Elcesser, W. L.; Sorlie, M.; Hubbard, J. L. *Organometallics* **1996**, *15*, 2534–2542.

84. Faller, J. W.; Ma, Y. *J. Organomet. Chem.* **1988**, *340*, 59–69.

85. Faller, J. W.; Ma, Y. *Organometallics* **1988**, *7*, 559–561.

86. Bottomley, F.; Boyle, P. D.; Chen, J. *Organometallics* **1994**, *13*, 370–373.

87. Trost, M. K.; Bergman, R. G. *Organometallics* **1991**, *10*, 1172–1178.

88. (a) Abrantes, M.; Santos, A.; Mink, J.; Kühn, F.; Romão, C. *Organometallics* **2003**, *22*, 2112–2118; (b) Martins, A.; Romão, C.; Abrantes, M.; Azevedo, M.; Cui, J.; Dias, A.; Duarte, M.; Lemos, M.; Lourenco, T.; Poli, R. *Organometallics* **2005**, *24*, 2582–2589.

89. Rau, M. S.; Kretz, C. M.; Geoffroy, G. L.; Rheingold, A. L. *Organometallics* **1993**, *12*, 3447–3460.

90. Chakraborty, D.; Bhattacharjee, M.; Kratzner, R.; Siefken, R.; Roesky, H.; Uson, I.; Schmidt, H.-G. *Organometallics* **1999**, *18*, 106–108.

91. Abrantes, M.; Valente, A. A.; Pillinger, M.; Gonçalves, I. S.; Rocha, J.; Romão, C. C. *Inorg. Chem. Comm.* **2002**, *5*, 1069–1072.

92. Abrantes, M.; Gago, S.; Valente, A.; Pillinger, M.; Gonalves, I.; Santos, T.; Rocha, J.; Romo, C. *Eur. J. Inorg. Chem.* **2004**, *2004*, 4914–4920.

93. Zhao, J.; Santos, A. M.; Herdtweck, E.; Kühn, F. E. *J. Mol. Catal. A: Chem.* **2004**, *222*, 265–271.

94. Minelli, M.; Enemark, J. H.; Brownlee, R. T. C.; Oconnor, M. J.; Wedd, A. G. *Coordination Chemistry Reviews* **1985**, *68*, 169–278.

95. Masters, A. F.; Brownlee, R. T. C.; O'Connor, M. J.; Wedd, A. G. *Inorg. Chem.* **1981**, *20*, 4183–4186.

96. van Vliet, M. C. A.; Arends, I. W. C. E.; Sheldon, R. A. *Chemical Communications* **1999**, 821–822.

97. (a) Mimoun, H.; Seree de Roch, I.; Sajus, L. *Tetrahedron* **1970**, *26*, 37–50; (b) Chaumette, P.; Mimoun, H.; Saussine, L.; Fischer, J.; Mitschler, A. *J. Organomet. Chem.* **1983**, *250*, 291–310.

98. (a) Veiros, L. F.; Prazeres, A.; Costa, P. J.; Romão, C. C.; Kühn, F. E.; Calhorda, M. J. *Dalton Trans.* **2006**, *11*, 1383; (b) Kühn, F. E.; Groarke, M.; Bencze, E.; Herdtweck, E.; Prazeres, A.; Santos, A. M.; Calhorda, M. J.; Romão, C. C.; Gonçalves, I. S.; Lopes, A. D.; Pillinger, M. *Chem. Eur. J.* **2002**, *8*, 2370–2383.

99. Mimoun, H. *Angew. Chem. Int. Ed. Engl.* **1982**, *21*, 734–750.

100. (a) M. N. Sheng, J. G. Z. *ACS Advan. Chem. Ser.* **1968**, *76*, 418; (b) Sheng, M. N.; Zajacek, J. G. *J. Org. Chem.* **1970**, *35*, 1839–1843.

101. Sheldon, R. A.; Van Doorn, J. A. *J. Catal.* **1973**, *31*, 427–437.

102. Thiel, W. R. *J. Mol. Catal. A: Chem.* **1997**, *117*, 449–454.

103. Hroch, A.; Gemmecker, G.; Thiel, W. *Eur. J. Inorg. Chem.* **2000**, *2000*, 1107–1114.

104. Kresge, C. T.; Leonowicz, M. E.; Roth, W. J.; Vartuli, J. C.; Beck, J. S. *Nature* **1992**, *359*, 710–712.

105. (a) Sakthivel, A.; Selvam, P. *J. Catal.* **2002**, *211*, 134–143; (b) Sakthivel, A.; Dapurkar, S. E.; Selvam, P. *Appl. Catal. A.* **2003**, *246*, 283–293; (c) Sakthivel, A.; Selvam, P. *Catal. Lett.* **2002**, *84*, 37–43.

106. Zhao, X.; Lu, G.; Millar, G. *Industrial and Engineeting Chemistry Research* **1996**, *35*, 2075.

107. (a) Corma, A.; Garcia, H. *Chem. Rev.* **2002**, *102*, 3837–3892; (b) Cunha-Silva, L.; Gonçalves, I. S.; Pillinger, M.; Xue, W.-M.; Rocha, J.; Teixeira-Dias, J. J. C.; Kühn, F. E.

J. Organomet. Chem. **2002**, *656*, 281–287; (c) Jia, M.; Seifert, A.; Berger, M.; Giegengack, H.; Schulze, S.; Thiel, W. *Chem. Mater.* **2004**, *16*, 877–882; (d) Sakthivel, A.; Zhao, J.; Raudaschl-Sieber, G.; Hanzlik, M.; Chiang, A. S.; Kühn, F. E. *Appl. Catal. A.* **2005**, *281*, 267–273.

108. Sing, K. S. W.; Everett, D. H.; Haul, R. A. W.; L., M.; A., P. R.; T., R.; Siemienewska, T. *Pure Appl. Chem.* **1985**, *57*, 603.

109. (a) Calabro, D. C.; Valyocsik, E. W.; X., R. F. *Microporous Materials* **1996**, *7*, 243; (b) Holmes, S. M.; Zholobenko, V. L.; Thursfield, A.; Plaisted, R. J.; Cundy, C. S.; Dwyer, J. *J. Chem. Soc., Faraday Trans.* **1998**, *94*, 2025.

110. Schmidbaur H., S. M. *Innorg. Synth.* **1967**, *9*, 149.

111. M., S. G.; S., S. W. *Journal Of The Chemical Society A -Inorganic Physical Theoretical* **1969**, 2160.

112. Bouh, A. O.; Espenson, J. H. *J. Mol. Catal. A: Chem.* **2003**, *200*, 43–47.

113. (a) Sakthivel, A.; Zhao, J.; Hanzlik, M.; Khn, F. *Dalton. Trans.* **2004**, 3338; (b) Sakthivel, A.; Zhao, J.; Kühn, F. *Microporous and Mesoporous Materials* **2005**, *86*, 341–348; (c) Sakthivel, A.; Zhao, J.; Raudaschl-Sieber, G.; Kühn, F. *J. Organomet. Chem.* **2005**, *690*, 5105–5112.

114. (a) Zhao, J.; Sakthivel, A.; Santos, A. M.; Kühn, F. E. *Innorg. Chim. Acta* **2005**, *358*, 4201–4207; (b) Sakthivel, A.; Zhao, J.; Hanzlik, M.; Chiang, A.; Herrmann, W.; Khn, F. *Adv. Syn. Catal.* **2005**, *347*, 473–483.

115. (a) Burgmayer, S. J. N.; Templeton, J. L. *Inorg. Chem.* **1985**, *24*, 2224–2230; (b) King, R. B.; Bisnette, M. B. *J. Organomet. Chem.* **1967**, *8*, 287–297.

116. (a) Wahl, G.; Kleinhenz, D.; Schorm, A.; Sundermeyer, J.; Stowasser, R.; Rummey, C.; Bringmann, G.; Fickert, C.; Kiefer, W. *Chem. Eur. J.* **1999**, *5*, 3237–3251; (b) Poli, R. *Chem. Eur. J.* **2004**, *10*, 332–341.

117. (a) Al-Ajlouni, A.; Valente, A. A.; Nunes, C. D.; Pillinger, M.; Santos, A. M.; Zhao, J.; Romo, C. C.; Gonalves, I. S.; Khn, F. E. *Eur. J. Inorg. Chem.* **2005**, *2005*, 1716–1723; (b) Espenson, J. H. *Chem. Commun.* **1999**, *6*, 479.

118. (a) Zhao, J.; Herdtweck, E.; Kühn, F. E. *J. Organomet. Chem.* **2006**, *691*, 2199–2206; (b) Zhao, J.; Jain, K. R.; Herdtweck, E.; Kühn, F. E. *Dalton Trans.* **2007**, *47*, 5567.

119. Astruc, D. *New Journal Of Chemistry* **2005**, *29*, 42–56.

120. Casey, C. P. *Journal Of Chemical Education* **2006**, *83*, 192–195.

121. Banks, R. L.; Bailey, G. C. *Industrial & Engineering Chemistry Product Research And Development* **1964**, *3*, 170.

122. (a) Calderon, N.; Chen, H. Y.; Scott, K. W. *Tetrahedron Lett.* **1967**, 3327; (b) Calderon, N.; Ofstead, E. A.; Judy, W. A. *Journal Of Polymer Science Part A-1-Polymer Chemistry* **1967**, *5*, 2209; (c) Calderon, N.; Ofstead, E. A.; Ward, J. P.; Judy, W. A.; Scott, K. W. *J. Am. Chem. Soc* **1968**, *90*, 4133.

123. Grubbs, R. *Handbook of metathesis*; Wiley-VCH, 2003.

124. Khosravi, E.; Szymanska-Buzar, T. *Ring Opening Metathesis Polymerisation and Related Chemistry: State of the Art and Visions for the New Century*; Kluwer Academic Publishers, 2002.

125. *http://www.materia-inc.com*; 2008.

126. *http://plastics.inwiki.org/Reaction_injection_molding*; 2007.

127. Rouhi, A. M. *Chemical and Engineering News* **2002**, *80*, 29.

128. Mol, J. C. *J. Mol. Catal. A: Chem.* **2004**, *213*, 39–45.

129. Giardello, M. A.; Cruce, C. J.; Haar, M.; Lasch, J. G.; Macleod, J. G. *WO0046255* **2000**.

130. Frenzel, U.; Nuyken, O. *Journal of Polymer Science Part A: Polymer Chemistry* **2002**, *40*, 2895–2916.

131. Lewandos, G. S.; Pettit, R. *J. Am. Chem. Soc* **1971**, *93*, 7087.

132. Hérisson, P. J.-L.; Chauvin, Y. *Die Makromolekulare Chemie* **1971**, *141*, 161–176.

133. Elschenbroich, C. *Organometallchemie*; Teubner, 2005.

134. Casey, C. P.; Burkhard, T. J. *J. Am. Chem. Soc* **1974**, *96*, 7808–7809.

135. Katz, T. J.; McGinnis, J. *J. Am. Chem. Soc* **1975**, *97*, 1592–1594.

136. McGinnis, J.; Katz, T. J.; Hurwitz, S. *J. Am. Chem. Soc* **1976**, *98*, 605–606.

137. Tebbe, F. N.; Parshall, G. W.; Reddy, G. S. *J. Am. Chem. Soc* **1978**, *100*, 3611–3613.

138. Howard, T. R.; Lee, J. B.; Grubbs, R. H. *J. Am. Chem. Soc* **1980**, *102*, 6876–6878.

139. Schrock, R. R. *J. Organomet. Chem.* **1976**, *122*, 209–225.

140. Schrock, R. *J. Am. Chem. Soc* **1974**, *96*, 6796–6797.

141. Schrock, R. *J. Am. Chem. Soc* **1976**, *98*, 5399–5400.

142. Guggenberger, L. J.; Schrock, R. *J. Am. Chem. Soc* **1975**, *97*, 6578–6579.

143. Schrock, R. *by A. Fuerstner, Springer, Berlin* **1998**, *1*, –.

144. Wood, C. D.; McLain, S. J.; Schrock, R. *J. Am. Chem. Soc* **1979**, *101*, 3210–3222.

145. Rocklage, S. M.; Fellmann, J. D.; Ruprecht, G. A.; Messerle, L. W.; Schrock, R. *J. Am. Chem. Soc* **1981**, *103*, 1440–1447.

146. (a) Wengrovius, J. H.; Schrock, R.; Churchill, M. R.; Missert, J. R.; Youngs, W. J. *J. Am. Chem. Soc* **1980**, *102*, 4515–4516; (b) Churchill, M. R.; Rheingold, A. L.; Youngs, W. J.; Schrock, R.; Wengrovius, J. H. *J. Organomet. Chem.* **1981**, *204*, C17–C20.

147. Wengrovius, J. H.; Schrock, R. *Organometallics* **1982**, *1*, 148–155.

148. (a) Kress, J.; Russell, M. J. M.; Wesolek, M.; Osborn, J. A. *Journal Of The Chemical Society-Chemical Communications* **1980**, 431–432; (b) Kress, J.; Wesolek, M.; Leny, J. P.; Osborn, J. A. *Journal Of The Chemical Society-Chemical Communications* **1981**, 1039–1040; (c) Kress, J.; Wesolek, M.; Osborn, J. A. *Journal Of The Chemical Society-Chemical Communications* **1982**, 514–516; (d) Youinou, M. T.; Kress, J.; Fischer, J.; Aguero, A.; Osborn, J. A. *J. Am. Chem. Soc* **1988**, *110*, 1488–1493.

149. (a) Schaverien, C. J.; Dewan, J. C.; Schrock, R. *J. Am. Chem. Soc* **1986**, *108*, 2771–2773; (b) Schrock, R.; Depue, R. T.; Feldman, J.; Schaverien, C. J.; Dewan, J. C.; Liu, A. H. *J. Am. Chem. Soc* **1988**, *110*, 1423–1435.

150. (a) Schrock, R. R.; Murdzek, J. S.; Bazan, G. C.; Robbins, J.; Dimare, M.; Oregan, M. *J. Am. Chem. Soc* **1990**, *112*, 3875–3886; (b) Oskam, J. H.; Fox, H. H.; Yap, K. B.; McConville, D. H.; Odell, R.; Lichtenstein, B. J.; Schrock, R. R. *J. Organomet. Chem.* **1993**, *459*, 185–198.

151. Solans-Monfort, X.; Clot, E.; Coperet, C.; Eisenstein, O. *J. Am. Chem. Soc* **2005**, *127*, 14015–14025.

152. Poater, A.; Solans-Monfort, X.; Clot, E.; Coperet, C.; Eisenstein, O. *J. Am. Chem. Soc* **2007**, *129*, 8207–8216.

153. (a) Novak, B. M.; Grubbs, R. H. *J. Am. Chem. Soc* **1988**, *110*, 7542–7543; (b) Novak, B. M.; Grubbs, R. H. *J. Am. Chem. Soc* **1988**, *110*, 960–961.

154. McGrath, D. V.; Grubbs, R. H.; Ziller, J. W. *J. Am. Chem. Soc* **1991**, *113*, 3611–3613.

155. (a) Bohle, D. S.; Clark, G. R.; Rickard, C. E. F.; Roper, W. R.; Shepard, W. E. B.; Wright, L. J. *Journal Of The Chemical Society-Chemical Communications* **1987**, 563–565; (b) Hill, A. F.; Roper, W. R.; Waters, J. M.; Wright, A. H. *J. Am. Chem. Soc* **1983**, *105*, 5939–5940.

156. Nguyen, S. T.; Johnson, L. K.; Grubbs, R. H.; Ziller, J. W. *J. Am. Chem. Soc* **1992**, *114*, 3974–3975.

157. Johnson, L. K.; Grubbs, R. H.; Ziller, J. W. *J. Am. Chem. Soc* **1993**, *115*, 8130–8145.

158. (a) Schwab, P.; Grubbs, R. H.; Ziller, J. W. *J. Am. Chem. Soc* **1996**, *118*, 100–110; (b) Schwab, P.; France, M. B.; Ziller, J. W.; Grubbs, R. H. *Angew. Chem. Int. Ed. Engl.* **1995**, *34*, 2039; (c) Nolan, S. P.; Belderrain, T. R.; Grubbs, R. H. *Organometallics* **1997**, *16*, 5569–5571.

159. (a) Nguyen, S. T.; Grubbs, R. H.; Ziller, J. W. *J. Am. Chem. Soc* **1993**, *115*, 9858–9859; (b) Fu, G. C.; Nguyen, S. T.; Grubbs, R. H. *J. Am. Chem. Soc* **1993**, *115*, 9856–9857.

160. Dias, E. L.; Nguyen, S. T.; Grubbs, R. H. *J. Am. Chem. Soc* **1997**, *119*, 3887–3897.

161. (a) Hinderling, C.; Adlhart, C.; Chen, P. *Angew. Chem. Int. Ed* **1998**, *37*, 2685; (b) Adlhart, C.; Hinderling, C.; Baumann, H.; Chen, P. *J. Am. Chem. Soc* **2000**, *122*, 8204–8214; (c) Adlhart, C.; Volland, M. A. O.; Hofmann, P.; Chen, P. *Helvetica Chimica Acta* **2000**, *83*, 3306–3311.

162. Sanford, M. S.; Love, J. A.; Grubbs, R. H. *J. Am. Chem. Soc* **2001**, *123*, 6543–6554.

163. Weskamp, T.; Schattenmann, W. C.; Spiegler, M.; Herrmann, W. A. *Angew. Chem. Int. Ed* **1998**, *37*, 2490.

164. (a) Weskamp, T.; Kohl, F. J.; Hieringer, W.; Gleich, D.; Herrmann, W. A. *Angew. Chem. Int. Ed* **1999**, *38*, 2416; (b) Weskamp, T.; Kohl, F. J.; Herrmann, W. A. *J. Organomet. Chem.* **1999**, *582*, 362–365; (c) Weskamp, T.; Bohm, V. P. W.; Herrmann, W. A. *J. Organomet. Chem.* **1999**, *585*, 348–352; (d) Ackermann, L.; Furstner, A.; Weskamp, T.; Kohl, F. J.; Herrmann, W. A. *Tetrahedron Lett.* **1999**, *40*, 4787–4790; (e) Huang, J. K.; Stevens, E. D.; Nolan, S. P.; Petersen, J. L. *J. Am. Chem. Soc* **1999**, *121*, 2674–2678; (f) Scholl, M.; Trnka, T. M.; Morgan, J. P.; Grubbs, R. H. *Tetrahedron Lett.* **1999**, *40*, 2247–2250; (g) Scholl, M.; Ding, S.; Lee, C. W.; Grubbs, R. H. *Organic Letters* **1999**, *1*, 953–956.

165. Love, J. A.; Sanford, M. S.; Day, M. W.; Grubbs, R. H. *J. Am. Chem. Soc* **2003**, *125*, 10103–10109.

166. (a) Coperet, C.; Chabanas, M.; Saint-Arroman, R. P.; Basset, J.-M. *Angew. Chem. Int. Ed* **2003**, *42*, 156–181; (b) Coperet, C. *New J. Chem.* **2004**, *28*, 1; (c) Blanc, F.; Coperet, C.; Lesage, A.; Emsley, L. *Chem. Soc. Rev.* **2008**, *37*, 518.

167. Dufaud, V.; Niccolai, G. P.; Thivolle-Cazat, J.; Basset, J. M. *J. Am. Chem. Soc* **1995**, *117*, 4288–4294.

168. Lefort, L.; Chabanas, M.; Maury, O.; Meunier, D.; Coperet, C.; Thivolle-Cazat, J.; Basset, J. M. *J. Organomet. Chem.* **2000**, *593*, 96–100.

169. Chabanas, M.; Quadrelli, E. A.; Fenet, B.; Coperet, C.; Thivolle-Cazat, J.; Basset, J. M.; Lesage, A.; Emsley, L. *Angew. Chem. Int. Ed* **2001**, *40*, 4493.

170. (a) Chabanas, M.; Baudouin, A.; Coperet, C.; Basset, J. M. *J. Am. Chem. Soc* **2001**, *123*, 2062–2063; (b) Lesage, A.; Emsley, L.; Chabanas, M.; Coperet, C.; Basset, J.-M. *Angew. Chem. Int. Ed* **2002**, *41*, 4535–4538; (c) Chabanas, M.; Baudouin, A.; Coperet, C.; Basset, J. M.; Lukens, W.; Lesage, A.; Hediger, S.; Emsley, L. *J. Am. Chem. Soc* **2003**, *125*, 492–504.

171. (a) Herrmann, W. A.; Stumpf, A. W.; Priermeier, T.; Bogdanovic, S.; Dufaud, V.; Basset, J. M. *Angew. Chem. Int. Ed. Engl.* **1996**, *35*, 2803; (b) Yang, Q. H.; Coperet, C.; Li, C.; Basset, J. M. *New Journal Of Chemistry* **2003**, *27*, 319–323.

172. (a) Blanc, F.; Coperet, C.; Thivolle-Cazat, J.; Basset, J.-M. *Angew. Chem. Int. Ed* **2006**, *45*, 6201–6203; (b) Blanc, F.; Coperet, C.; Thivolle-Cazat, J.; Basset, J.-M.; Lesage, A.; Emsley, L.; Sinha, A.; Schrock, R. R. *Angew. Chem. Int. Ed* **2006**, *45*, 1216–1220.

173. (a) Blanc, F.; Thivolle-Cazat, J.; Basset, J.-M.; Coperet, C.; Hock, A.; Tonzetich, Z.; Schrock, R. *J. Am. Chem. Soc* **2007**, *129*, 1044–1045; (b) Blanc, F.; Berthoud, R.; Salameh, A.; Basset, J. M.; Coperet, C.; Singh, R.; Schrock, R. R. *J. Am. Chem. Soc* **2007**, *129*, 8434–+; (c) Blanc, F.; Thivolle-Cazat, J.; Basset, J. M.; Coperet, C.; Hock, A. S.; Tonzetich, Z. J.; Schrock, R. R. *J. Am. Chem. Soc* **2007**, *129*, 1044–1045; (d) Blanc, F.; Berthoud, R.; Coperet, C.; Lesage, A.; Emsley, L.; Singh, R.; Kreickmann, T.; Schrock, R. R. *Proceedings of the National Academy of Sciences* **2008**, *105*, 12123–12127.

174. Poater, A.; Solans-Monfort, X.; Clot, E.; Coperet, C.; Eisenstein, O. *Dalton Trans.* **2006**, *25*, 3077.

175. (a) Blanc, F.; Rendon, N.; Berthoud, R.; Basset, J. M.; Coperet, C.; Tonzetich, Z. J.; Schrock, R. R. *Dalton Transactions* **2008**, 3156–3158; (b) Wampler, K. M.; Schrock, R. R.; Hock, A. S. *Organometallics* **2007**, *26*, 6674–6680; (c) Kreickmann, T.; Arndt, S.; Schrock, R. R.; Muller, P. *Organometallics* **2007**, *26*, 6684–6684; (d) Singh, R.; Schrock, R. R.; Muller, P.; Hoveyda, A. H. *J. Am. Chem. Soc* **2007**, *129*, 16278–16278.

176. (a) Buffon, R.; Choplin, A.; Leconte, M.; Basset, J. M.; Touroude, R.; Herrmann, W. A. *J. Mol. Catal* **1992**, *72*, L7–L10; (b) Rost, A. M.; Schneider, H.; Zoller, J. P.; Herrmann, W. A.; Kühn, F. E. *J. Organomet. Chem.* **2005**, *690*, 4712–4718; (c) Moses, A.;

Ramsahye, N.; Raab, C.; Leifeste, H.; Chattopadhyay, S.; Chmelka, B.; Eckert, J.; Scott, S. *Organometallics* **2006**, *25*, 2157–2165.

177. Ertl, G.; Knozinger, H.; Weitkamp, J. *JohnWiley& Sons* **1999**.

178. (a) Knözinger, H.; Ratnasamy, P. *Catal. Rev.* **1978**, *17*, 31–70; (b) Digne, M.; Sautet, P.; Raybaud, P.; Euzen, P.; Toulhoat, H. *J. Catal.* **2002**, *211*, 1–5; (c) Digne, M.; Sautet, P.; Raybaud, P.; Euzen, P.; Toulhoat, H. *J. Catal.* **2004**, *226*, 54–68.

179. (a) Joubert, J.; Delbecq, F.; Sautet, P.; Roux, E.; Taoufik, M.; Thieuleux, C.; Blanc, F.; Coperet, C.; Thivolle-Cazat, J.; Basset, J.-M. *J. Am. Chem. Soc* **2006**, *128*, 9157–9169; (b) Joubert, J.; Salameh, A.; Krakoviack, V.; Delbecq, F.; Sautet, P.; Coperet, C.; Basset, J. M. *J. Phys.Chem. B.* **2006**, *110*, 23944–23950.

180. (a) Parry, E. P. *J. Catal.* **1963**, *2*, 371–379; (b) Schekler-Nahama, F.; Clause, O.; Commereuc, D.; Saussey, J. *Appl. Catal. A.* **1998**, *167*, 237–245.

181. Salameh, A.; Joubert, J.; Baudouin, A.; Lukens, W.; Delbecq, F.; Sautet, P.; Basset, J. M.; Coperet, C. *Angew. Chem. Int. Ed* **2007**, *46*, 3870.

182. Salameh, A.; Baudouin, A.; Basset, J. M.; Coperet, C. *Angew. Chem. Int. Ed* **2008**, *47*, 2117.

183. Salameh, A.; Baudouin, A.; Soulivong, D.; Boehm, V.; Roeper, M.; Basset, J. M.; Coperet, C. *J. Catal.* **2008**, *253*, 180–190.

184. Herrmann, W.; Kühn, F. *Acc. Chem. Res.* **1997**, *30*, 169–180.

185. (a) Liewellyn, S.; Green, M.; Cowley, A. *Dalton Transactions* **2006**, *2006*, 1776–1783; (b) Butts, S. B.; Holt, E. M.; Strauss, S. H.; Alcock, N. W.; Stimson, R. E.; Shriver, D. F. *J. Am. Chem. Soc* **1979**, *101*, 5864–5866.

186. (a) Butts, S.; Strauss, S.; Holt, E.; Stimson, R.; Alcock, N.; Shriver, D. *J. Am. Chem. Soc* **1980**, *102*, 5093–5100; (b) Kotz, J.; Turnipseed, C. *Journal of the Chemical Society D: Chemical Communications* **1970**, *1970*, 41–42.

187. Toscano, P. J.; Marks, T. J. *Organometallics* **1986**, *5*, 400–402.

188. Herrmann, W. A. *Advances in Organometallic Chemistry* **1982**, 159.

189. Downs, A.; Dierker, G.; Green, J.; Greene, T.; McGrady, G.; Morris, L.; Scherer, W.; Sirsch, P. *Journal of the Chemical Society, Dalton Transactions* **2002**, *2002*, 3349–3360.

190. Salameh, A.; Coperet, C.; Basset, J.-M.; Böhm, V. P.; Röper, M. *Adv. Syn. Catal.* **2007**, *349*, 238–242.

191. (a) Basset, J. M.; Bilhou, J. L.; Mutin, R.; Theolier, A. *J. Am. Chem. Soc* **1975**, *97*, 7376–7377; (b) Bilhou, J. L.; Basset, J. M.; Mutin, R.; Graydon, W. F. *J. Am. Chem. Soc* **1977**, *99*, 4083–4090.

192. (a) Cella, J. A.; Carpenter, J. C. *J. Organomet. Chem.* **1994**, *480*, 23–26; (b) Marciniec B., K. M., Blazejewska-Chadyniak P. *Can. J. Chem.* **2003**, *81*, 1292; (c) Popowski, E.; Holst, N.; Kelling, H. *Z. Anorg. Allg. Chem.* **1982**, *494*, 166–178.

193. Galyer, L.; Wilkinson, G. *Inorganic Syntheses* **1979**, *19*, 253.

194. Capape, A.; Raith, A.; Kühn, F. E. *Advanced Synthesis and Catalysis* **2009**, in press.

195. Herrmann, W. A.; Kühn, F. E.; Fiedler, D. A.; Mattner, M. R.; Geisberger, M. R.; Kunkely, H.; Vogler, A.; Steenken, S. *Organometallics* **1995**, *14*, 5377–5381.